

**Motion Tracking Based Lower Limb Musculoskeletal Imbalance
Identification Mechanism Using Kinematic Analysis of Human Gait Cycle**

Tennakoon Rallage Kashmila Hiranthi
(13020218)

Charitha Paranamana
(13020341)

University of Colombo
School of Computing

2017

Declaration

I, T. R. K. Hiranthi (2013/IS/021) hereby certify that this dissertation entitled Motion Tracking Based Lower Limb Musculoskeletal Imbalance Identification Mechanism Using Kinematic Analysis of Human Gait Cycle by motion tracking is entirely my own work and it has never been submitted nor is currently been submitted for any other degree.

.....

Date

.....

Student's Signature

I, C. Paranamana (2013/IS/034) hereby certify that this dissertation entitled Motion Tracking Based Lower Limb Musculoskeletal Imbalance Identification Mechanism Using Kinematic Analysis of Human Gait Cycle by motion tracking is entirely my own work and it has never been submitted nor is currently been submitted for any other degree.

.....

Date

.....

Student's Signature

I, Dr. K. D. Sandaruwan, certify that I supervised this dissertation entitled Motion Tracking Based Lower Limb Musculoskeletal Imbalance Identification Mechanism Using Kinematic Analysis of Human Gait Cycle by motion tracking conducted by T. R. K. Hiranthi and C, Paranamana in partial fulfillment of the requirements for the degree of Bachelor of Science Honours in Information Systems.

.....

Date

.....

Supervisor's Signature

Acknowledgement

This research study is a result of many people who have made commitments in terms of time, effort, guidance and inspiration. This space is dedicated to extend our sincere gratitude towards them.

Firstly, we would like to express our enormous gratitude to our research supervisor, Dr. K. D. Sandaruwan and research evaluators, Dr. Chamath Kappatiyagama and Dr. Hiran Ekanayaka. We also thank for the domain knowledge and the resources provided by the research advisors, Ms. Maheshya Weerasinghe of University of Colombo School of Computing and Dr. Kalpani Mahindaratne of General Hospital, Peradeniya without whose admonition and counsel this research project could have been an unsuccessful.

We express our appreciation to Dr. Deepthika Chandrasekara and all the staff of General Hospital, Peradeniya for their immense support in providing us the research sample and helping us in conducting the data gathering aspects of the research.

We also thank the staff of the Score Lab and Modelling and Simulation Group of University of Colombo School of Computing for the immense support provided. We also hereby show our courtesy to the staff of Department of Statistics of University of Colombo and Mr. Umesh Jayasinghe of University of Colombo School of Computing for their support in the areas of statistics and model building.

We convey our gratefulness to all the lecturers, assistant lecturers, instructors of the University of Colombo School of Computing and our families and friends who always supported and motivated us in times of desperate.

Abstract

According to biomedical researches, repetitive usage of one body muscle sector than the other, incorrect postures a human body takes and practices on a regular basis may cause muscle imbalances in the skeletal system. A muscle imbalance should be paid adequate attention since both neurological and physical performances can be severely affected due to imbalances as time progresses. Current clinical practices of imbalance identification as in gait and posture analysis, movement analysis, joint range of motion analysis and muscle length analysis require and depend on domain expertise and experience. Technical methods of imbalance identification as in X-Rays and CT scans also require the assistance of domain experts to interpret results and cost and time an individual has to bear for this is excessive.

To overcome cost, time and domain expertise constraints, this research proposes a mechanism for an individual to self-identify body imbalances and track their progress with treatments. This research considers tracking human gait cycle as the technique for muscle imbalance identification and address the area of physiotherapy. Kinect motion capturing device which is able to track human skeleton, its joints and body movements within its sensory range is used for the gait cycle tracking purposes of this research.

Dot product is used in the proposed research as a mathematical operation in order to calculate joint angles applying joint information obtained via the Kinect. Gait cycle patterns of a healthy person are defined by performing several calculations using the proposed mechanism and the skeletal imbalance of a person is defined by differentiating the deviation against the defined healthy gait cycle patterns.

A quantifiable final result is produced by this research study pertaining to the status of the skeletal imbalance. The final outcome of the study can be further used to decide the pathology of the imbalance. A satisfactory end result is derived by this research study and followed by further development of the concept, the proposed method can be used in sports and games, clinical and physical fitness domains as a self-identification musculoskeletal imbalance mechanism.

Table of Contents

Declaration	i
Acknowledgement	ii
Abstract	iii
Table of Contents	iv
List of Figures	vii
List of Tables.....	x
1. Introduction	1
1.1. Problem definition	1
1.2. Causes of musculoskeletal imbalances and relative effects	3
1.3. Contribution.....	5
1.3.1. Goals and objectives.....	5
1.3.2. Research questions	5
Research question 01 - How to build a generic human gait cycle for a selected age range of using the captured data parameters?	5
Research question 02 - How the gait cycle of an imbalanced person is differentiated from the generic gait cycle?.....	5
1.3.3. Research scope	6
1.4. Muscle imbalance identification techniques.....	6
1.4.1. Gait cycle analysis.....	6
1.4.2. Movement analysis.....	7
1.4.3. Joint range of motion analysis.....	8
1.4.4. Muscle length analysis.....	9
1.4.5. Electromyography	10
1.4.6. X-ray and CT scan.....	10
1.5. Issues with current techniques.....	11
1.6. Thesis outline.....	12
2. Background.....	14
2.1. Study review of muscle imbalances	14
2.2. Study review of utilization of tracking devices in human movement capturing	14
2.3. Study review of motion tracking in gait cycle applications	25
2.4. Study review of Kinect motion tracking device	26
2.5. Generic gait cycle graphs in medical domain.....	29
2.6. Summary.....	31

3.	Design and methodology	33
3.1.	Research design	33
3.1.1.	Sampling mechanism.....	34
3.1.1.1.	Sampling mechanism for healthy subjects	34
3.1.1.2.	Sampling mechanism for imbalanced subjects.....	35
3.1.2.	Data capturing via Kinect	35
3.1.3.	Mathematical operation for joint angle calculation	36
3.1.4.	.csv file generation.....	39
3.1.5.	Modelling the gait cycle graph	39
3.1.5.1.	Hip gait cycle graph.....	40
3.1.5.2.	Knee gait cycle graph	40
3.1.5.3.	Ankle gait cycle graph.....	40
3.1.6.	Generation of generic gait cycle graph.....	40
3.1.7.	Comparison of graphs.....	42
3.2.	Research methodology	44
3.2.1.	Environmental setup	44
3.2.2.	Data collection.....	45
3.2.3.	Data cleansing and preparation.....	48
4.	Implementation.....	52
4.1.	Capturing human gesturing via Vitruvius library	52
4.2.	Obtaining joint positions via Vitruvius library	52
4.3.	Application interfaces.....	55
5.	Evaluation and results.....	58
5.1.	Evaluation.....	58
5.1.1.	Generic graph generation.....	58
5.1.2.	Male generic graph generation	59
5.1.2.1.	Male hip generic graph generation	59
5.1.2.2.	Male knee generic graph generation.....	62
5.1.2.3.	Male ankle generic graph generation.....	65
5.1.3.	Female generic graph generation.....	67
5.1.3.1.	Female hip generic graph generation.....	68
5.1.3.2.	Female knee generic graph generation	70
5.1.3.3.	Female ankle generic graph generation	73
5.2.	Quantitative evaluation.....	75

5.2.1.	Data evaluation of healthy subjects	75
5.2.2.	Data evaluation of imbalanced subjects	79
5.2.2.1.	Hip gait cycle graph of imbalanced subjects	79
5.2.2.2.	Knee gait cycle graph of imbalanced subjects.....	83
5.2.2.3.	Ankle gait cycle graph of imbalanced subjects	85
5.3.	Qualitative evaluation.....	91
5.4.	Comparison of evaluation methods	92
5.5.	Confusion matrix	94
6.	Discussion and conclusion	96
6.1.	Contribution.....	100
7.	Future directions.....	102
	Bibliography	104
	Appendices	108

List of Figures

Figure 1 - Ideal alignment (side view).....	2
Figure 2 - Ideal alignment (posterior view).....	2
Figure 3 - Kyphosislordosis.....	2
Figure 4 - Sway-back posture.....	3
Figure 5 - Flat-back posture	3
Figure 6 - Dynamic lengthening characteristics of pectoralis major and dorsi during pitching.....	4
Figure 7 - Gait cycle phases	7
Figure 8 - Motion captured from inertial.....	15
Figure 9 - Sensor to segment alignment	15
Figure 10 - Relation of segment with global frame.....	16
Figure 11 - Phases of sensor signals.....	17
Figure 12 - Modeling of LPM/ Inertial motion capture.....	18
Figure 13 - Mismatch of capture dimension.....	19
Figure 14 - MVN modelling	20
Figure 15 - MVN modelling	20
Figure 16 - MVN modelling.....	20
Figure 17 - Plot of movements	22
Figure 18 - Comparison of Kinect and Vicon captures	23
Figure 19 - Application of marker based sensor.....	23
Figure 20 - Hand modelling process	28
Figure 21 - Joints considered to generate generic gait cycle graphs in medical domain.....	29
Figure 22 - Ankle gait cycle graph	30
Figure 23 - Knee gait cycle graph	30
Figure 24 - Hip gait cycle graph.....	31
Figure 25 - Research design	33
Figure 26 - Human joints captured by Kinect	36
Figure 27 - Joint angle calculation in 3D space.....	37
Figure 28 - Generic graph generation process.....	42
Figure 29 - Gait cycle comparison	43
Figure 30 - Defined walkway	44
Figure 31 - Data collection of imbalanced test subject	46
Figure 32 - Boxplot outlier identification 1.....	49
Figure 33 - Boxplot for outlier identification 2	50

Figure 34 - Boxplot for outlier identification 3	50
Figure 35 - Boxplot for outlier identification 4	51
Figure 36 - Initial user interface of the application	56
Figure 37 - Side view of the tracked user skeleton.....	57
Figure 38 - Front view of the tracked user skeleton	57
Figure 39 - Generation of generic gait cycle for male hip.....	60
Figure 40 - Generic gait cycle for male hip (initial step)	60
Figure 41 - Generic gait cycle for male hip (secondary step).....	61
Figure 42 - Generation of generic gait cycle for male knee	62
Figure 43 - Generic gait cycle for male knee (initial step).....	63
Figure 44 - Generic gait cycle for male knee (secondary step)	64
Figure 45 - Generation of generic gait cycle for male ankle	65
Figure 46 - Generic gait cycle for male ankle (initial step).....	66
Figure 47 - Generic gait cycle for male ankle (secondary step)	67
Figure 48 - Generation of generic gait cycle for female hip.....	68
Figure 49 - Generic gait cycle for female hip (initial step)	69
Figure 50 - Generic gait cycle for female hip (secondary step)	70
Figure 51 - Generation of generic gait cycle for female knee	71
Figure 52 - Generic gait cycle for female knee (initial step).....	71
Figure 53 - Generic gait cycle for female knee (secondary step)	72
Figure 54 - Generation of generic gait cycle for female ankle	73
Figure 55 - Generic gait cycle for female ankle (initial step).....	74
Figure 56 - Generic gait cycle for female ankle (secondary step).....	75
Figure 57 - Hip gait cycle graph of subject 2	77
Figure 58 - Knee gait cycle graph of subject 2.....	78
Figure 59 - Ankle gait cycle graph of subject 2	78
Figure 60 - Imbalanced hip graph of subject 10 (initial step).....	80
Figure 61 - Imbalanced hip graph of subject 10 (secondary step).....	80
Figure 62 - Imbalanced hip graph of subject 14 (initial step).....	81
Figure 63 - Imbalanced hip graph of subject 14 (secondary step).....	81
Figure 64 - Imbalanced hip graph of subject 15 (secondary step).....	82
Figure 65 - Imbalanced hip graph of subject 18 (initial step).....	82
Figure 66 - Imbalanced knee graph of subject 14 (secondary step)	83
Figure 67 - Imbalanced knee graph of subject 17 (secondary step)	84
Figure 68 - Imbalanced knee graph of subject 18 (initial step)	84

Figure 69 - Imbalanced ankle graph of subject 11 (initial step)	85
Figure 70 - Imbalanced ankle graph of subject 11 (secondary step)	86
Figure 71 - Imbalanced ankle graph of subject 12 (initial step)	86
Figure 72 - Imbalanced ankle graph of subject 11 (secondary step)	87
Figure 73 - Imbalanced ankle graph of subject 14 (initial step)	88
Figure 74 - Imbalanced ankle graph of subject 14 (secondary step)	88
Figure 75 - Imbalanced ankle graph of subject 15 (secondary step)	89
Figure 76 - Qualitative Evaluation Process	91
Figure 77 - Systematic approach followed in the research.....	97
Figure 78 - Knee gait cycle graph of subject 14 (initial step)	99
Figure 79 - Knee gait cycle graph of subject 13 (initial step)	100
Figure 80 - Generic ankle gait cycle graph (2nd order).....	109
Figure 81 - Generic ankle gait cycle graph (3rd order)	110
Figure 82 - Generic ankle gait cycle graph (4th order)	111
Figure 83 - Generic ankle gait cycle graph (5th order)	111
Figure 84 - Imbalanced sample subject a	112
Figure 85 - Imbalanced sample subject b	112
Figure 86 - Imbalanced sample subject c	113

List of Tables

Table 1 - Faulty movements	8
Table 2 - Captured data of a healthy subject	47
Table 3 - Captured data of an imbalanced subject.....	48
Table 4 - Gender distribution of the research sample.....	58
Table 5 - Quantitative evaluation results	90
Table 6 - Qualitative evaluation results	92
Table 7 - Qualitative and quantitative result comparison	93
Table 8 - Confusion matrix for the results obtained.....	94

Chapter 1

1. Introduction

1.1. Problem definition

To function properly as individuals, it is important to maintain a healthy and a strong body. In order to provide the body with shape, protection and internal structure, human skeleton is a necessary component and should be handled with care. For the human skeleton to function, support of skeleton muscles is crucial. Since human skeleton cannot be accessed directly like skin, hair or nails and a daily care routine cannot be carried out on the surface level, professional consultancy to identify 'what could go wrongs' pertaining to the skeletal system have to be gained and address the issues diagnosed should be addressed in a proper manner for its wellbeing.

A muscle imbalance can cause severe damages to the musculoskeletal system and affect the bearer both physically and mentally. In human body structure, most of the muscles and bones come in pairs. A muscle consists with agonist and antagonist muscles where agonist is the working muscle and the antagonist is the muscle at rest. A muscle imbalance can be defined as one of the muscles from the pair getting stronger, longer and stiffer than the other muscle [1]. For proper utilization of muscles, muscle balance is a vital concern. Repetitive usage of muscles and everyday excessive routine activities, taking an incorrect body posture for long hours and emotional stress can lead to imbalances. Final results of a muscle imbalance are known as severe physical injuries, lower back pain, shoulder impingement, neck pain, trapped nerves, sports injuries, hamstring tears, anterior knee pain and nerve damages of a person [1] [2]. Disorders related to the musculoskeletal system are distressing health problems to the general public considering sickness absence, work disability and health care cost. According to the American Journal of Sports Medicine, there have been 2123 muscle injuries documented in the major lower extremity muscle groups: adductors (n = 523), hamstrings (n = 900), quadriceps (n = 394), and calf (n = 306). Injuries to the adductors (56%; $P = .015$) and quadriceps (63%; $P < .001$) were more frequent in the kicking leg of a soccer player [3]. Since Human movements and functions require a balance of muscle length and strength between opposing muscles surrounding a joint, normal amounts of opposing force between muscles are necessary to keep the bones centered

in the joint during a motion [3] . When a muscle imbalance pulls one of the joints out of position, a strain on that joint is left. When that strain stresses nerves around the joint, it causes pain. If the body re-adjusts itself to ease the pain, other sets of muscles can become imbalanced and the cycle continues. A small, local problem in some muscles can become a neuro muscular skeletal that affects distant parts of the human body [4]. In the course of time, muscle imbalances can lead to severe sicknesses as in arthritis, lower back tightness [6], hamstring strains and nerve damages [4] [49]. To individuals like professional athletes, gymnists as well to ordinary men, it is important to identify muscle imbalances in order to address them with appropriate cures for the purpose of living a healthy life. A skeletal imbalance is not visible to the eye hence a proper identification methodology should be there to identify the problematic situation associated. Figure 1 – Figure 5 illustrate the ideal and imbalanced postures of a person.

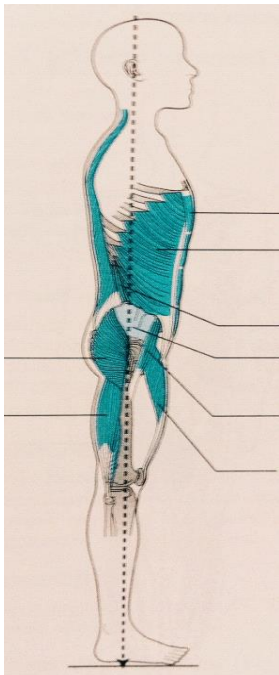


Figure 1 - Ideal alignment (side view)

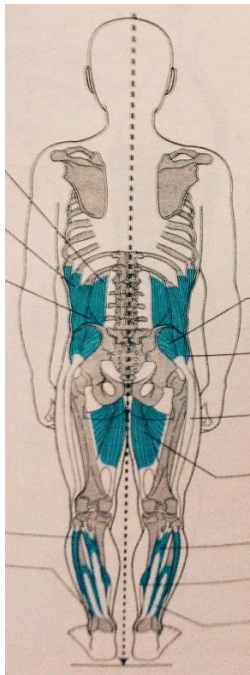


Figure 2 - Ideal alignment (posterior view)

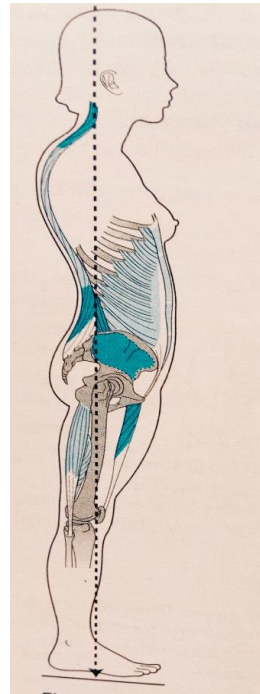


Figure 3 – Kyphosis/lordosis

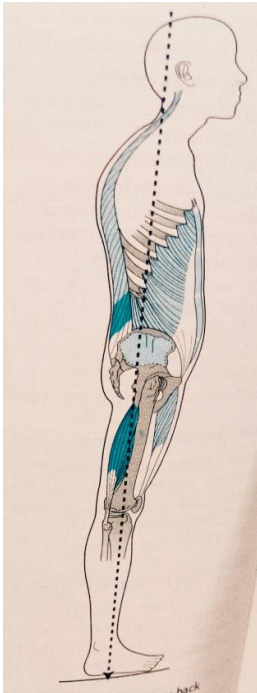


Figure 4 - Sway-back posture

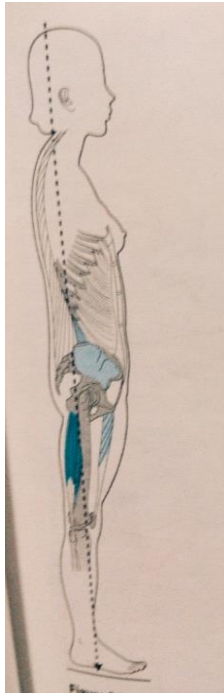


Figure 5 - Flat-back posture

1.2. Causes of musculoskeletal imbalances and relative effects

In human musculoskeletal system, joints seize a slight floppiness in joint orientation and positioning [3] [5]. Hence human body and joints cannot be modeled as a pure kinematic chain with well-defined joints such as hinge joints and ball and socket joints. Hence more than three degrees of freedom is required as given by an orientation measurement to track the human joints and non-rigid body segments accurately. When it comes to identifying feet motion which occurs during running and jumping motions of a human body, it is not possible to analyze the motion with only orientation driven motion capturing.

Negative results of long term repetitive training, muscle usage and overuse can lead to muscle injuries as well. There are mainly two categories under muscle injuries rise from physical activities; impact injuries where the physiological limits of the individual are surpassed and repetitive stress injuries where the accumulation of micro injury from physical overuse surpass the individual's physiological tolerance [7]. Repetitive stress injuries can be seen in most domains as sports, dancing and instrumental music [3]. Muscle strain is a common repetitive stress injury in sports. These strains usually occur during sprinting, kicking, stretching, overhead throwing and rapid deceleration. A

previous study [3] has been conducted to identify the characteristics of range of motion characteristics and the muscle lengthening characteristics and muscle injury prevention strategies using 3D motion tracking sensor. In the mentioned study lower limb instep kicking, baseball pitching, fan kick and axe kick are tracked to reveal above stated characteristics. Lower limb instep kicking which is consisted of two phases; formation of tension arc and releasing tension arc is tracked using 3D motion tracking. Muscle injuries in latissimus dorsi and pectoralis major muscles are studied in this survey. The Figure 6 shows the lengthening capacities of latissimus dorsi and pectoralis major muscle in baseball pitching activity.

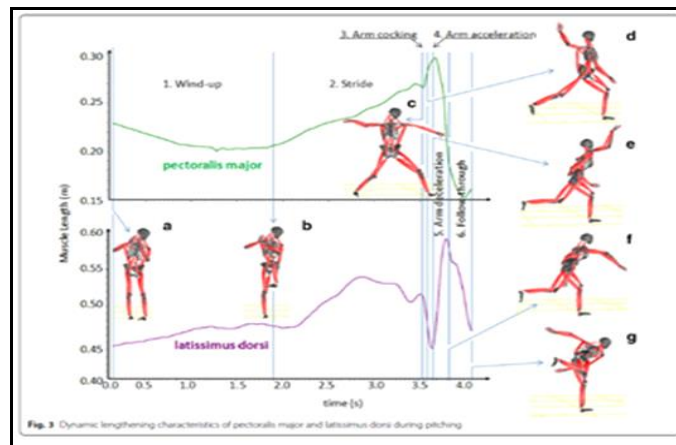


Figure 6 - Dynamic lengthening characteristics of pectoralis major and dorsi during pitching

According to a recent study, 40% of women suffers from one or more musculoskeletal system injuries [8]. Following are some statistics for lower limb muscle imbalance in athletes.

- A right knee flexor 15% stronger than the left knee flexor at 180 deg/sec.
- A right hip extensor 15% more flexible than the left hip extensor.
- A knee flexor/knee extensor ratio of less than 0.75 at 180 deg/sec.

According to the above statistics, higher injury rates are associated with knee flexor and hip extensor imbalances and is of 15% greater than the injury rate of the other side of the body. Specific strength and flexibility imbalances may be associated with athletic injuries which may manifest as differences between the right and left legs or as abnormal ratios between antagonistic muscle groups.

1.3. Contribution

1.3.1. Goals and objectives

- Identify a suitable technological device to track imbalances of a human musculoskeletal system via gait analysis
- Get body measurements of a person and derive generic joint movement variation behaviors
- Identify generic gait cycle of an average healthy person
- Identify the deviations of the generic joint movements of an average healthy person with a person holding a body imbalance via gait cycle analysis
- Output the status of the musculoskeletal system

1.3.2. Research questions

Research question 01 - How to build a generic human gait cycle for a selected age range of using the captured data parameters?

Before identify an imbalance of a person, the gait cycle behavior of a healthy person should be defined. Since the musculoskeletal system varies with different age limits and levels of a lifetime of a human being, a specific common generic for every man cannot be found within the clinical approaches [9]. Gait analysis is to be used in order to identify the generic joint movements for a particular age range. The problem is “what are the generic angular measurements in each phase of the gait cycle of an average healthy person”. The angle measurements and a systematic approach therefore should be defined.

Research question 02 - How the gait cycle of an imbalanced person is differentiated from the generic gait cycle?

If the gait cycle of an imbalanced person is considered, it naturally deviates from a generic gait cycle of an average healthy person. But that deviation can be differ from person to person. The second research question is to find the deviation of an imbalanced gait cycle from the generic gait cycle. In order to identify musculoskeletal imbalance of a subject, according to the research approach,

the gait cycle parameters have to be considered. Therefore joint angle values of an appraised joint in each phase of the gait cycle have to be considered to identify the deviation of an imbalanced person from the musculoskeletal system of a healthy person.

1.3.3. Research scope

- Sample - Male (age: 25-45) and female (age: 30-50)
- BMI value of the sample - BMI 18.5 - 23
- Approach of musculoskeletal imbalance identification - gait cycle
- Applicability of the study - lower limb musculoskeletal system joints (hip joint, knee joint and ankle joint)

1.4. Muscle imbalance identification techniques

1.4.1. Gait cycle analysis

Gait cycle primarily can be defined as the way an individual walks. The gait cycle begins when one foot makes contact with the ground and ends with the contact of the same foot with the ground again. Gait cycle can be mainly divided into two phases; stance phase and swing phase where 60% of the cycle is included in the stance phase and 40% includes in the swing phase. These two phases can then be divided into eight minor phases; initial contact, loading response, mid-stance, heel off, pre-swing, initial swing, mid-swing and terminal swing [5] [7].

Initial contact is also known as the heel strike and in this phase the individual is on double support. 300 hip flexion and full extension of the knee can be observed in this phase [10] [11]. In loading response phase (also known as the foot flat), knee flexes to 150 - 200 and the ankle flexion increases from 100-150 [10] [11]. In mid stance phase, the knee reaches its maximal extension and then extension and the body is on single support in this phase [10]. In heel off phase, the limb is lifted and there is no contact with the ground and the knee flexed to 00-50 [12]. In pre-swing phase (also known as toe off), knee flexes to 350 - 400 and the ankle flexion increases to 200 [10] [11]. In the initial swing phase, the knee flexes to 400 - 600 [13]. In mid swing phase, the knee flexes 600 and extends approximately to 300 [10] [11]. In the terminal swing phase (also known as late swing phase), the

knee is at locked extension and a neutral position of the ankle is obtained [7] [10]. The eight main phases of the gait cycle for both the limbs are represented in Figure 7.

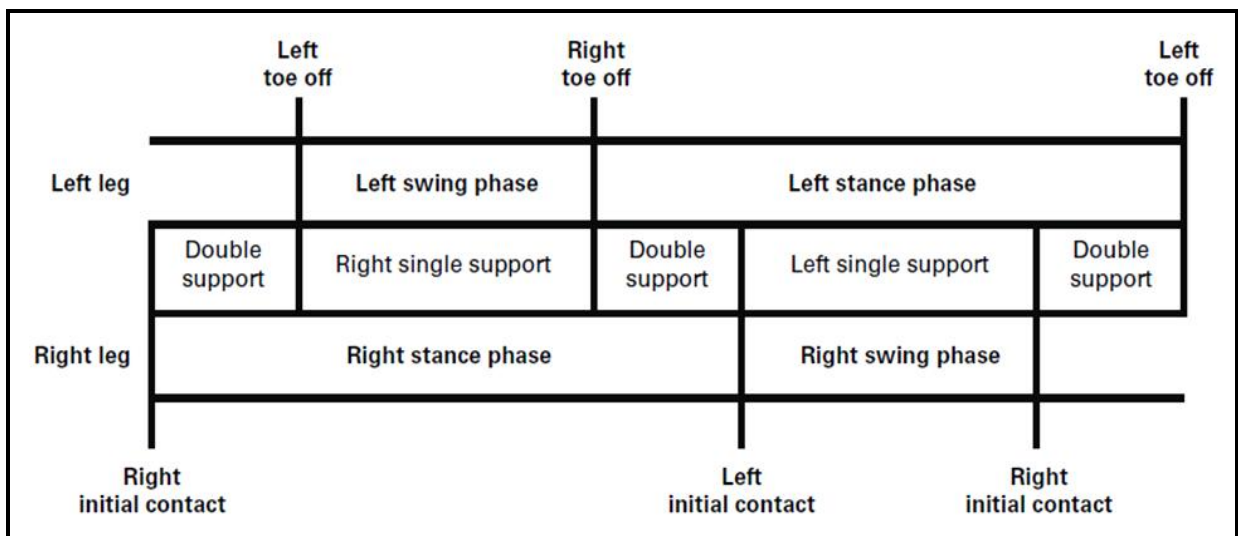

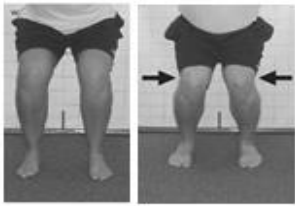
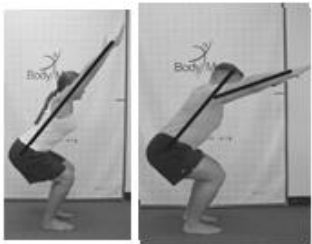




Figure 7 - Gait cycle phases

1.4.2. Movement analysis

In movement analysis, a patient is requested by the physiotherapist to perform various activities to determine whether the patient holds a musculoskeletal imbalance or not by analyzing the behaviors and stances the patient's body takes. Requested stance is highly depended on the experience and knowledge of the observer. There are three main methods of movement analysis; movement phases, free body diagrams and deterministic models [12] [14]. In movement analysis phase, analysis of preparation, execution and follow-through is analysed. In preparation phase, movement preparation by the individual to perform a particular motion is analysed and in the execution phase, movement of the patient is analysed. All the behaviors of the individual after the movement is also analysed in this phase. In free body diagram analysis, a two dimensional or three dimensional diagram of the predicted movement is created but forces on the outer body is concerned. In deterministic model, biomechanical factors which determine a movement is analysed and one primary movement is divided into several secondary factors for further analysis of a muscle imbalance. Following characteristics of movement patterns stated in Table 1 are considered in this analysis [15].

Table 1 - Faulty movements

View	Faulty Movement
Anterior	<div style="display: flex; justify-content: space-around; align-items: center;"> <div style="text-align: center;">  <p data-bbox="560 493 662 527">Toe out</p> </div> <div style="text-align: center;">  <p data-bbox="1008 493 1386 527">Knee moves inward (Valgus)</p> </div> </div>
Lateral	<div style="display: flex; justify-content: space-around; align-items: center;"> <div style="text-align: center;">  <p data-bbox="483 888 716 921">Arms fall forward</p> </div> <div style="text-align: center;">  <p data-bbox="1019 888 1398 921">Excessive forward trunk lean</p> </div> </div>
Posterior	<div style="text-align: center;">  <p data-bbox="370 1360 857 1394">Flattening of medial longitudinal arch</p> </div>

1.4.3. Joint range of motion analysis

In joint range of motion analysis, the range a human can perform his motions and movements is taken to consideration. Main considerations in this approach are: the plane of the movement occurrence, muscle used to produce the movement, function of the involved muscle: agonist [3]. There are mainly four planes a human body can be divided into:

- Sagittal plane
- Coronal plane
- Transverse plane
- Oblique plane

The three axis which are considered are:

- Frontal axis
- Sagittal/ Transverse axis
- Longitudinal axis

In this analysis method all mentioned planes and axis and both active and passive range of motion are measured [16] and with the aid of Goniometer angles between the joints are measured and compared with the generic angles defined in the clinical domain with respect to the person's age, weight and fat elements [17] [19]. A noticeable deviation of joint angles from the generics is determined as a muscle imbalance. In order to measure the range of motion of lower body joints on both right and left sides goniometer is used by physiotherapist [8] [17] [19]. These joints involves the hip flexors (hamstrings), hip extensors, hip adductors, hip external rotators, knee flexors (quadriceps) and ankle dorsiflexors (gastrocnemius and soleus). In order to measure the joint orientation, two measurements are obtained from each joint and average value from these two were taken. Hip extension flexibility was measured with the subject in the prone position, knees flexed at 90°.

The goniometer was centered on the greater trochanter with one arm on the lateral midline of the thigh and the other arm parallel to the table. The subject extended the hip while keeping the anterior superior iliac spine on the table. Body fat was obtained from skinfold measurements using the equations of Durnin and Womersley.

1.4.4. Muscle length analysis

Muscle length is analysed against the age and other physical parameters of the person which assesses the resistance to passive movement. In order to gain accurate result, muscle length should be

performed when the patient is not in acute pain in order to avoid pain inhibition and muscle guarding [18]. Goniometer or a tape can be used to do the measurements and there are four steps in performing muscle length analysis [14] [15].

- Ensure maximal lengthening of the muscle from origin to insertion
- Firmly stabilize one end (usually the origin)
- Slowly elongate the muscle
- Assess the end feel

1.4.5. Electromyography

A needle is injected to the surface level of the human body and this stimulation is used to measure the reaction and activities of muscles to the mentioned electrical stimulation. Muscle activities grasped by the electrodes are displayed in a monitor called oscilloscope and an audio amplifier is also used to listen to the muscle activities. To determine a muscle imbalance, currently consultants analyse these muscle activities and their responses to the electric stimulation [19] and a muscle imbalance is determined if found.

1.4.6. X-ray and CT scan

In Computed Tomography special X-Ray equipment is used to detect body conditions. X-ray and CT scanning produces multiple images of the inner body of a person. X-Ray beams and electronic X-Ray detectors rotate around the patient and different parts of the body absorb the produced X-ray in different degrees and it records in a special electronic recording plate [24]. These record and datasets create a two dimensional image of the body. In determining musculoskeletal imbalances, the domain experts analyse these scanned body images to conclude whether the patient is having a muscle imbalance or not.

1.5. Issues with current techniques

Issues with these current processes lie in their practicality. Identification process in physiotherapy according to the information obtained from a domain expert, is the experience and knowledge base of the physiotherapist hence it differs from which consultant an individual prefers [9]. Identification of muscle imbalances via CT scans and x-rays is time consuming, costly and sometimes may seem as a hectic process since the patient has to be there in person. The accuracy of clinical methodology totally depends on the experience and knowledge of the physiotherapist [9] hence the presence of a domain expert is a must. Since a physical pain is the only way to identify troubles in the musculoskeletal system, another issue is that it might be behindhand and in a severe stage of the imbalance when an ordinary person go for these treatments as a person will go for consultancy only when a pain or other symptoms are visible to them.

Therefore rather than paying attention to the musculoskeletal system when an issue is identified, it is vital to have an individual identification mechanism and also to analyze the progress of the treatments which have been carried out by the patients which can also overcome the issues mentioned with the current clinical and physiotherapy approaches. To propose and prove a proper mechanism to identify muscle imbalances through performing a gait analysis for the skeleton with the aid of an ICT based mechanism is the motivation behind this research project and we present a mechanism to overcome these issues by proposing an ICT oriented approach to keep track of the musculoskeletal system where a motion tracking sensor is used to sense the skeleton, calculate the angles and give an output pertaining to the body imbalances and visualize patient's own progress without having to pay visit to doctor. By fulfilling the above requirement we tend to provide an interpretation with precision to optimize the treatments in order to make the professional clinical methodologies more accurate as well as to provide a healthier lifestyle for the general public.

1.6. Thesis outline

The Introduction chapter of this thesis consists and presents an overall review of the research being carried out. Motivation behind the research project, scope, goals and objectives and the research contribution is described in this section.

A comprehensive literature review is presented throughout the Background chapter with regard to the causes and effects of musculoskeletal imbalances emphasizing the criticality of a research such as the proposed, existing mechanisms to identify musculoskeletal imbalances and their drawbacks and usage of motion tracking devices in biomechanical domains as per the related works. Furthermore, current motion capturing technologies and their reliability is addressed in this section. The purpose of the background chapter is to present the identified gaps which are not yet being addressed by the related works carried out in similar domains and to emphasize the contribution of the proposed research project to overcome the current limitation of existing mechanisms.

The Design and methodology chapter gives the reader an understanding of the proposed novel musculoskeletal imbalance identification approach, its design and the methodology followed. The proposed methodology focuses on the developing a novel and reliable mechanism of tracking down muscle imbalances in order to reduce the consequences in the clinical and technical mechanisms which are currently used in the clinical domain to identify an imbalance in the human musculoskeletal system. A comprehensive on data gathering techniques proposed to be used, sampling mechanisms, research design, data analysis and evaluation techniques and procedures which has been used in this research project are given in this section.

Implementation chapter gives the reader a comprehensive idea about the functional aspect of the research. A code review is the main concern in this section. The GUIs and the steps to be followed, how the process is carried out by the system and data that should be fed to the system is presented in this section.

The Evaluation and results chapter describes the evaluation techniques used in this research project. Quantitative and qualitative experiment results are described in detail in this chapter. Data cleansing and analysis mechanisms for both balanced and an imbalanced subjects are described.

Comparison of the evaluation methods which are been followed also is given in this section in order to validate the accuracy and applicability of the proposed concept.

The conclusion and future work section presents the reader with a brief understanding of the system procedure and the final results and the real world interpretation of the results. This section also include the future developments and enhancement methods and aspects of this research project in order for the future researchers to gain an understanding.

Chapter 2

2. Background

2.1. Study review of muscle imbalances

In recent years, clinical researches have been conducted to identify after effects of muscle imbalances and it was found that the root cause for neuro musculoskeletal damages [21], lower back tightness, repetitive stress injuries, hamstring strains, altered movement patterns and postural dysfunctions lie in muscle imbalances [11] [20] [22]. It also depicts that a large range of motions of joints would lead to several causes like muscle over lengthening and imbalances in agonist and antagonist (a muscle pair) in [11]. The previous study [11] also has concluded that frequent muscle over lengthening causes micro-trauma accumulation which can be resulted in repetitive stress injuries in long term. It is stated in a previous study [23] that faulty postures, joint malalignment and development of altered inefficient movement patterns result in strain and degeneration of joints, myofascial and ligamentous structures which lead to muscle imbalances. In another study [9] it is statistically given that there is a trend for higher injury rates to be associated with knee or hip extensor imbalances of 15% or more than on either side of the body. American journal of Sports Medicine in 2012 by conducting a research [24] on soccer players stated “there were 2123 muscle injuries documented in the major lower extremity muscle groups: adductors (n = 523), hamstrings (n = 900), quadriceps (n = 394), and calf (n = 306). Injuries to the adductors (56%; P = .015) and quadriceps (63%; P < .001) were more frequent in the kicking leg of soccer players” (n: number of injuries reported).

2.2. Study review of utilization of tracking devices in human movement capturing

Muscle imbalance is type of a muscle risk which is very important to identify and address since it can lead to muscle injuries with time. In the Information Technology domain researchers have done studies to identify muscle abnormalities using motion tracking sensors. In many studies they have considered sports domain to identify musculoskeletal issues since athletes are often having issues

related to their musculoskeletal systems. Shan and Wan [11] have done a research to achieve mainly three aims using 3D motion tracking system. The research has been conducted to identify range of motion characteristics and muscle lengthening characteristics to identify muscles at risks and to build injury prevention strategies. Soccer, baseball pitching, dancing and taekwondo were the selected physical activities/ sports to do the study. A nine-camera, 3D motion capture system to track 42 reflective markers on subject's body have been used to track body movements and to identify muscles at risk. The gray image of the subject is created as in Figure 8, cameras are represented in the numbered circles and it captures the human movement information. Using these raw 3D data it produces biomechanical modeling of the subjects. Using inertial sensor for motion analysis is a common trend nowadays [17] [25].

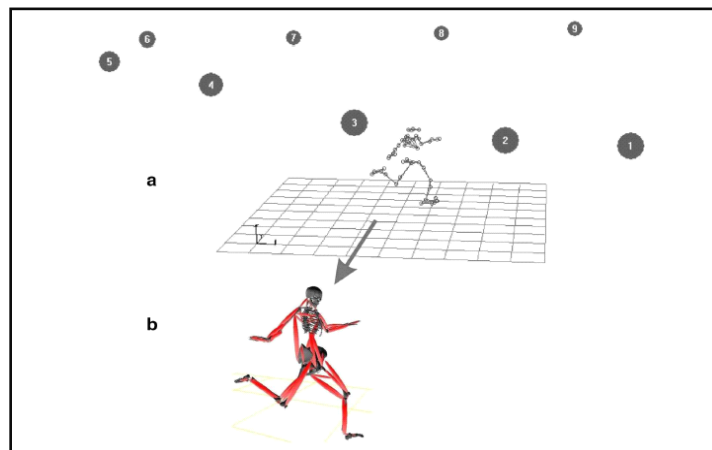


Figure 8 - Motion captured from inertial

Combining the signals from 3D gyroscopes, accelerometers, and magnetometers are used to estimate drift free orientation accurately. Integrating the gyroscope data and double integrating accelerometer data in time is facilitating the estimation of each body segment's orientation and position which provide full six-degree-of-freedom tracking of body segments with connected inertial sensor modules [23]. In order to estimate the orientation of a rigid body using the accelerometer, magnetometer, and gyroscope readings provided by an IMU sensor researchers have presented an algorithm. In a previous research [26] they have used a method somewhat similar to Complementary Quaternion Attitude Filter presented by Bachmann but have included removal of the Gauss-Newton iteration method for execution on the Atmel Mega 32 microcontroller. When calculating the human kinematics, it is required to define all joint orientation in its local frame [26]. Hence the local

orientation can be easily converted into the angular values of each joint of musculoskeletal system. In the inertial sensor, each individual sensor of the system provides orientation with respect to global frame. In a previous experiment researchers have placed two inertial sensors to capture the arm motion; one in the upper arm and the other one in the lower arm. In the mentioned study design these two sensors are working according to parent-child relationship of the sensor placement. In another experiment [11] they have used 42 reflective markers place in the subjects' body to track the each body motions.

The MVN motion capture system is consisted of body worn sensors which have a unique approach to estimate body segment orientation and position changes by integration of gyroscope and accelerometer signals [23]. These signals are continuously updated by using the biomechanical models of the human body which allows to track the human musculoskeletal system motions. This system is running real-time with maximum update rate. It is possible to observe, record and export the human muscle movements in 3D version with the MVN studio software. MVN Studio features stream output to MotionBuilder and Maya which allows real-time character animation including retargeting. MVN gives an estimate of the center of mass based on the segment positions and orientations together with a body mass distribution model. The initial pose between the sensors and body segments is unknown when attaching sensors to a body. Since the assessment of distances between body segments is difficult to estimate, calibration procedure is used to perform the alignment of the sensor to the body and to determine the body dimensions as presented in Figure 19 – Figure 11.

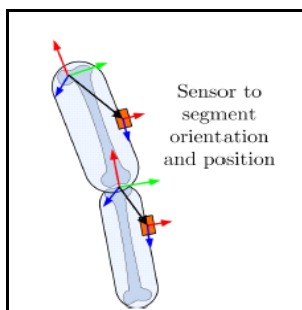


Figure 9 - Sensor to segment alignment

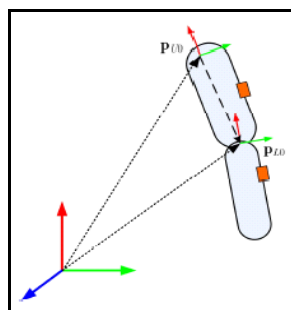


Figure 9 - Relation of segment with global frame

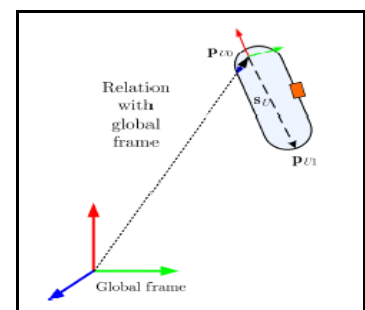


Figure 11 - Relation of two connecting segments at $t=0$

In this study it has described the sensor signal and biomechanical model in two steps sensor signals and correction [23]. In the first step, prediction, all the sensor signals are processed using inertial navigation system algorithm by the prediction step. Figure 12 shows overall mechanism followed.

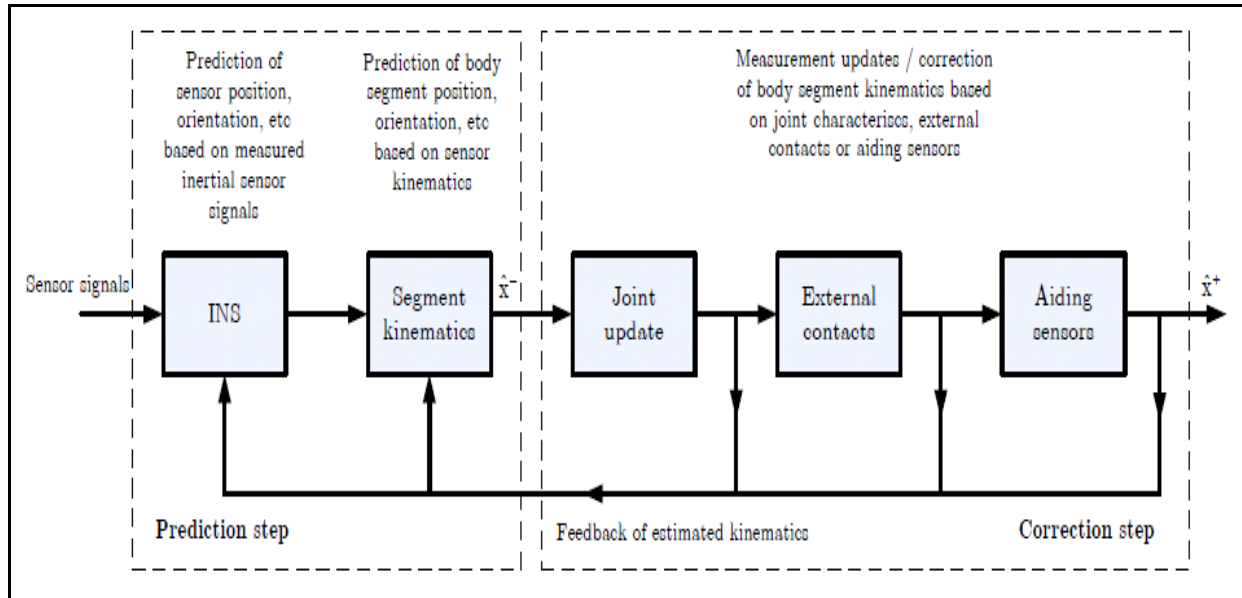


Figure 12 - Phases of sensor signals

Sensor noise, sensor signal offset, sensor orientation errors can be lead to errors in sensor data. The orientation, velocity and the position in quantified in order to correct these quantities. In the correction step, it includes updates of biomechanical characteristics of human body, notably joint detection of contact points of the body with global position and the velocity. Estimated kinematics are fed back to the INS algorithms and segment kinematic step to be used in the next time frame. Orientation of the sensor module with respect to the segment and the relative distances between joints are determined in order to express segment kinematics in the global frame in this study.

Several methods can be combined and used in order to find the sensor to segment alignment. In a previous research [23] the researchers have tracked priori known poses of subjects. By matching the orientation of the sensor in the global frame with the known orientation of each segment in particular pose, the rotation from sensor to body segment is been determined. The subject has to perform a certain movement that is assumed to correspond to a certain axis. The measured orientation and angular velocity are used to find the sensor orientation with respect to the segment's functional

axes. Several body dimensions; body height, arm span and foot size are measured to estimate joint positions of musculoskeletal system. By measuring several anatomical landmarks it is possible to refine some estimates. With each additional provided dimension, the scaling model is adjusted. Dimensions which can be entered include greater trochanter, lateral epicondyle on the femoral bone, lateral malleolus, anterior, spine and the acromion. Other dimensions are obtained by using regression equations based on anthropometric models. The sensor to segment alignment and segments lengths can be re-estimated by using medical generic values about the distance between two points in kinematics. Using biomechanical model, which assumes that a subject's body includes body segments linked by joints and that the sensors are attached to the subject's body segments, the inertial navigation system kinematics are translated to body kinematics. When calculating the joint angles, the origin values are defined in the center of the functional axes with the directions of the X, Y and Z related to functional movements. For example, flexion and extension of the knee is described by the rotation about the BY-axis of the lower leg with respect to the upper leg; abduction and adduction is the rotation about the BX-axis; and endo and exon rotation is about the BZ-axis. The sensor fusion scheme can seamlessly be integrated with various types of aiding sensors like a barometer, a camera, as well as pressure or force sensors in order to improve the accuracy of captured motion data.

MVN MotionGrid [23] is an Ultra-Wideband based tracking technology complementary to the MVN system. A local GPS system is added to the sensor fusion scheme of MotionGrid. In this technology large capture volumes of 20x20m (60x60ft) can be easily realized using the default 9-reader configuration and does not require line of sight or special lighting conditions. Local positioning system is another position aiding source. This system can be installed and used in ice arenas to measure the speed of a skater and is presented in Figure 13.



Figure 13 - Modeling of LPM/ Inertial motion capture

This application, LPM/inertial fusion makes it possible to accurately assess all the kinematics of an athlete even during high centripetal accelerations [23]. The sensor fusion scheme is capable to calculate the position, velocity, acceleration, orientation, angular velocity and angular acceleration of each body segment with respect to the global reference coordinate system. The global reference coordinate system is determined by the position system when MVN is combined with a position aiding system.

The dimensions and joints of the character (creature) may not be exactly match with the subject being captured. These errors can result in conflicting marker and joint angle data between character and subject. Retargeting means the problem which adapting recorded motions of a subject to a character. Many animation software packages have various tools to inverse kinematics retargeting. Figure 16 shows the MVN output of subject playing basketball and Figure 14 is the retargeting of the mocap data to the character. MVN studio allows the user to observe the movements of the subject in real-time and from previous recordings. Figure 15 shows screenshot of MVN Studio.

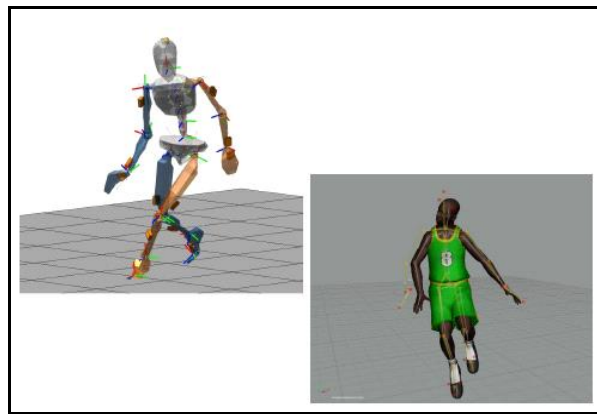


Figure 10 - Mismatch of capture dimension

The data can be stored in the native formats MVN which conserves all raw sensor data and can be used for re-processing, and the MVN Open XML format which contains all kinematic data. Studio is having an option to capture up to four actors at the same time. Also this is capable of processing real time 3D position aiding input. When tracking human using this system, it is not necessary the subject to be in a specific environment. It is possible to track the motion while they are performing their day today activities as mentioned in the study.

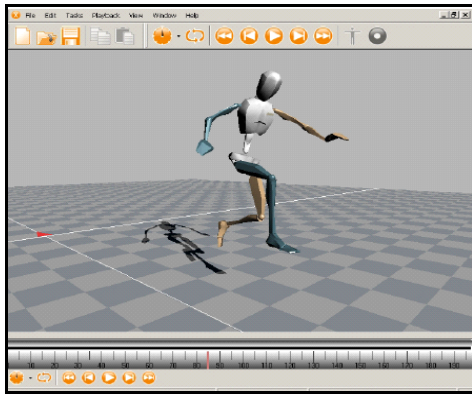


Figure 11 - MVN modelling



Figure 12 - MVN modelling



Figure 17 - MVN modelling

When tracking human motions using Kinect, it is possible to acquire images using the sensor with its accompanying depth map [27]. Skin color of the human body section can be detected followed by depth segmentation and also this is used to capture the 3D image of particular body segment. In a previous research, human hand has been tracked using Kinect sensor. In order to model each hand pose they have used 27 parameters represented as vector [27]. In order to quantify the inconsistency between hand hypotheses and the actual observation, it is possible to use graphics rendering techniques to compare skin and depth maps for a particular hand pose.

Kinect, a markerless technology made its appearance in the videogame industry is used in a recent study which was carried out to study the precision in the joint angles computation against a professional optical motion capturing device. The researches have obtained a guaranteed range of disparities to make validations on the used two devices regarding joint angles when the limbs are involved [8]. Rehabtimals; a framework which covers the physical rehabilitation cycle by making patients contribute themselves in a game series to track their progress is the ultimate outcome from this study to the biomechanical domain [8]. Findings of this study are assistive to the proposed research in the means that we intend to use Kinect technology as well and the precision of the device is one of our concerns.

By mounting a Kinect device and setting up an optical motion capture in the same motion capture laboratory, a comparison has been made. 32 cameras have been set up in the laboratory and 30 – 2000 frames are captured via these cameras per second and the capture volume is stated as 45 m². In order to track the movements, several movements are predefined as follows.

- Knee flexion and extension
- Hip flexion and extension on the sagittal plane
- Hip adduction and abduction on the coronal plane with knee extended
- Shoulder flexion and extension on the sagittal plane with elbow extended
- Shoulder adduction and abduction on the coronal plane with elbow extended
- Shoulder horizontal adduction and abduction on the transverse plane with elbow extended

The researchers have configured a calculation in order to calculate the joint positions of the markers and two markers are placed in each joint (front and back body element). Data captured from these markers are recorded in frame rate of 120 fps and OpenNI joint specification is used to capture Kinect motion data in framerate of 30 fps.

A conversion of data obtained by the optical motion capture to align with the representation of Kinect motion data has been taken place in the data processing phase of the research and the captured movements are analysed to build a grouping of the same movement in both the systems. The two systems have exchanged the axes though the orientation was the same and the research team has corrected the exchange by rotating the capture.

To make the appearance of the gathered data via the two systems, joint positions obtained from Kinect are estimated and captured from the optical markers by calculating the midpoint of the markers. Then rotational data has been computed with respect to knee, hip and shoulder rotations and the planes. Figure 18 – Figure 19 represent the comparison against the data captured by the two systems.

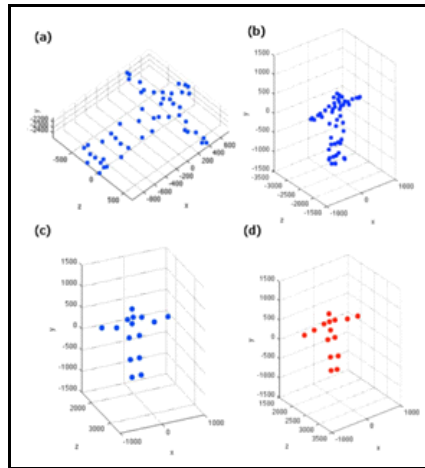


Figure 18 - Plot of movements

The research has been concluded by the comparison of joint rotational values. It is stated that Kinect, although not accurate and the precision is lower than the optical motion capture, can be used in the frame of physical rehabilitation and emphasizing the fact that it can be useful in this area.

The MVN motion tracking sensor is used to track human body movement which is consisted of 17 MTx sensors with two Xbus Masters [23]. MTx is an inertial and magnetic measurement unit and comprises 3D gyroscopes, 3D accelerometers and 3D magnetometers. The sensor modules are connected to the part called Xbus Masters which synchronizes all the sensor sampling and provides sensors with power and handles the wireless communication with the laptop. The sensors and cables are integrated in Xbus Masters for quick and convenient placement. MVN sensor modules are placed on body parts like feet, lower leg, upper leg, pelvis, shoulders, sternum, head, upper arm, forearm and hands [23].

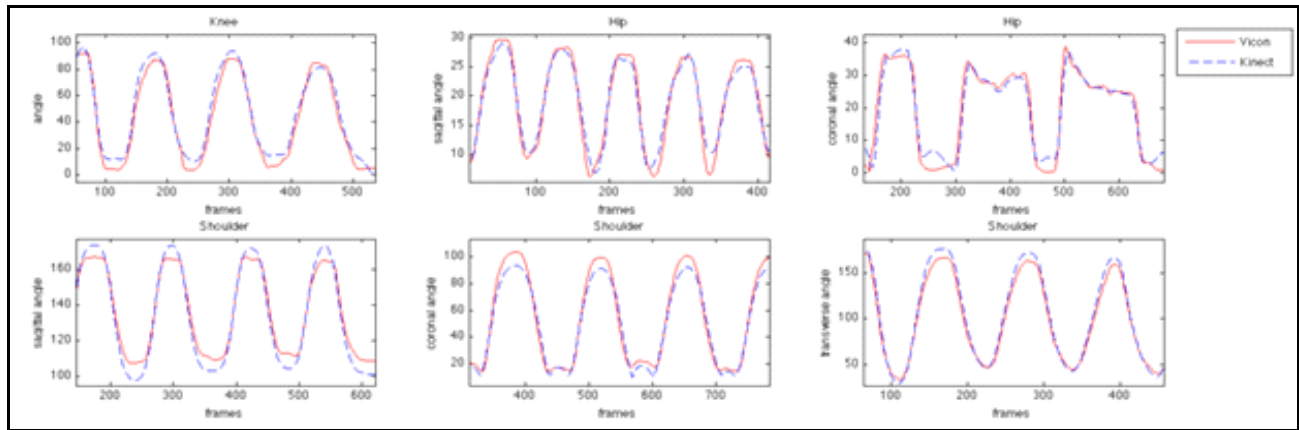


Figure 13 - Comparison of Kinect and Vicon captures

Reflective markers also capable of tracking human motions [11]. In order to take 3D model of the human motion, researchers have used 42 reflective markers with 9 cameras to track body the movements. In that research they have built the biomechanical modeling of the body positions using the data gathered from markers and cameras. The marker placement is as presented in Figure 20.



Figure 20 - Application of marker based sensor

Motion tracking devices as in Kinect since it is relatively a cost effective motion capturing device, introduces the possibility of changing paradigms based on complex and expensive technologies and devices in the biomechanical domain [8] [28]. A recent study has been carried out to measure the quality and the precision of the Kinect sensor against an optical motion capture.

It is also cited that although technologies as in inertial or electromagnetic sensors are currently used [39], the most common mechanism used at present is optical systems along with reflective

markers [8]. This is due to the limitations endowed in marker based technologies; a controlled environment is required in order to obtain high quality information, a considerable time is needed to place the markers and an experience personnel is also required in the process of placing markers properly in the human body as incorrect placement of trackers will result in corrupted and incorrect outputs. In this study [8] it is stated that Kinect can be used in the frame of physical rehabilitation.

Human musculoskeletal motions can be tracked using the Kinect in model-based and appearance-based approaches [27]. In model based approach, it provides a continuum of solutions which are costly and also depending on the wealth of visual information provided by a multi camera system. When it comes to appearance-based method, it is associated with much less computational cost and the complexity of hardware is very less. In a previous research [8], a novel model-based approach for 3D tracking hand articulations is used. This model minimizes the inconsistency between the 3D structure and appearance of hypothesized 3D hand model and the actual visual observation comes from the Kinect sensor.

A combination of usage of Inertial and Kinect sensors for applications on rehabilitation robotics and devices is been studied to identify the deficiencies in each system by evaluating human subject behavior in several movements [30] [25]. Human and patient movements followed by rehabilitation treatment cannot be tracked down by using optical motion devices as per the limitations discussed in [8]. Therefore usage of markerless sensors are proposed as an alternative. Precision of the Kinect sensor based information is less precise than the optical motion capture [8]. To overcome that issue, Kinect is combined with inertial sensor to obtain better visualization, system initialization and improved overall precision [30]. Data from both the sensors are integrated via Kalman Filter and is proposed to correct the estimate the inertial sensor by using joint angles obtained from the Kinect.

Two types of inertial sensors are used in the study; accelerometers and gyro meters. Gravity component measured by the accelerometer is concerned and is used to estimate the joint angles. Kinect provides preprocessed data directly to create the integration with Inertial such as 3D joint position of the human subject and 3D visualization. Reconstruction of joint positions is as per Primesense module [30]. To evaluate the sensor integration, following postures are used.

- Sit to stand
- Squat
- Shoulder abduction and adduction

In the experiment phase when the subject takes a particular task or position, angles have been computed. Then online calibration has been carried out to enable better visualization. Future work of this study focuses on extending the online calibration filter to include further sensor errors such as scaling, and evaluating integration of Kinect and portable sensors for motion capture system with more postures [30]. Initial state and covariance of each sensor is found to be problematic and Kinect initialize this integration filter (KF). Sensor reading errors are stated as another deficiency and to overcome that Kinect is used to perform online calibration for inertial sensor.

2.3. Study review of motion tracking in gait cycle applications

In recent studies human gait cycle has been used to denote different type of outcomes of an individual. Analyzing the human gait cycle is a new emerging trend in the research world for many applications such as human identification, neurological disease identification and fall detection of elderly people [35].

Individual human recognition by gait cycle has been performed [31] via Gait Energy Image (GEI) mechanism. GEI is a spatio-temporal gait representation for individual recognition by characterizing the human gait cycle properties which is represented in a single image while preserving temporal information. This representation saves both storage and computation time for recognition compared to binary silhouette [31].

In recent studies gait cycle parameters have been used to be predictive of future falls and adverse events in older people using Kinect [32] [33] [35]. Impairments in gait and balance causes falling of adults basically. Identification of these gait abnormalities is essential to early initiation of fall prevention strategy. By analyzing the stride time, stride symmetry, speed, age parameters of sample objects while they walk, previous researchers have found that accelerometers give accurate results of gait analysis of fallers and non-fallers [33]. They have placed accelerometers in head, trunk and the lower body to capture the gait cycle characteristics. Not only accelerometers but in another study [36]

micro sensors have been used to track the gait cycle and send the status of gait cycle to aid station real time at the falling moment. This system is very powerful to capture, analyze and communicate results to remote place real time. Kinect sensor with a computer deployed in an apartment was used in another study to capture the gait cycle of older adults in the apartment and make predictions on their health situation [36] [37].

Identification of neurological disorders of patients was conducted based on the support, Double support time percentage, Single support time percentage, Step-length, Step-time, step-width, Stride-length, Stride-time, and Swing-time characteristics of the gait cycle [21] [34] [46]. This research group was capable of identifying the gait variability of each neurologic patients for future prediction. By analyzing these characteristics, the certain disease was identified.

2.4. Study review of Kinect motion tracking device

Kinect, a markerless technology made its appearance in the videogame industry is used in a recent study which was carried out to study the precision in the joint angles computation against a professional optical motion capturing device. The sensor has an angular field of view of 57° horizontally and 43° vertically. Also the motorized pivot is capable of sloping the position of the sensor up to 27° either up or down. Human musculoskeletal motions can be tracked using the Kinect in model-based and appearance-based approaches [8]. In model based approach, it provides a continuum of solutions which are costly and also depending on the wealth of visual information provided by a multi camera system. When it comes to appearance-based method, it is associated with much less computational cost and the complexity of hardware is very less. The researches have obtained a guaranteed range of disparities to make validations on the used two devices regarding joint angles when the limbs are involved. Rehabtimals [8]; a framework which covers the physical rehabilitation cycle by making patients contribute themselves in a game series to track their progress is the ultimate outcome from this study to the biomechanical domain. Findings of this study are assistive to the proposed research in the means that we intend to use Kinect technology as well and the precision of the device is one of our concerns. By mounting a Kinect device and setting up an optical motion capture in the same motion capture laboratory, the comparison have been made. 32 cameras have been set up in the laboratory and 30 – 2000 frames are captured via these cameras per second and the capture volume is stated as 45 m^2 . In order to track the movements, several movements

are predefined as Knee flexion and extension, Hip flexion and extension on the sagittal plane, hip adduction and abduction on the coronal plane with knee extended, shoulder flexion and extension on the sagittal plane with elbow extended, shoulder adduction and abduction on the coronal plane with elbow extended, shoulder horizontal adduction and abduction on the transverse plane with elbow extended. The researchers have configured a calculation in order to calculate the joint positions of the markers and two markers are placed in each joint (front and back body element). Data captured from these markers are recorded in frame rate of 120 fps and OpenNI joint specification is used to capture Kinect motion data in a framerate of 30 fps.

When tracking the human motions using Kinect, it is possible to acquire images using the sensor with its accompanying depth map. Skin color of the human body section can be detected followed by depth segmentation and also this is used to capture the 3D image of particular body segment. In a previous research [30] human hand has been tracked using Kinect sensor. In order to model each hand pose they have used 27 parameters represented as vector. In order to quantify the inconsistency between hand hypotheses and the actual observation, this study has used graphics rendering techniques to compare skin and depth maps for a particular hand pose. A conversion of data obtained by the optical motion capture to align with the representation of Kinect motion data has been taken place in the data processing phase of the research and the captured movements are analysed to build a grouping of the same movement in both the systems. The two systems have exchanged the axes though the orientation. To make the appearance of the gathered data via the two systems, joint positions obtained from Kinect are estimated that captured from the optical markers by calculating the midpoint of the markers. Then rotational data has been computed with respect to knee, hip and shoulder rotations and the planes. The research is has been concluded by this comparison of joint rotational values. It is stated that Kinect, although not accurate and the precision is lower than the optical motion capture, can be used in the frame of physical rehabilitation and emphasizing the fact that it can be useful in this area.

Motion tracking devices as in Kinect since it is relatively a cost effective motion capturing device, introduces the possibility of changing paradigms based on complex and expensive technologies and devices in the biomechanical domain. A recent study [8] has been carried out to measure the quality and the precision of the Kinect sensor against an optical motion capture. In this study it is stated that Kinect, although not accurate and the precision is lower than the optical motion capture, can be used

in the frame of physical rehabilitation. A combination of usage of Inertial and Kinect sensors for applications on rehabilitation robotics and devices is been studied to identify the deficiencies in each system by evaluating human subject behavior in several movements [27]. Human (patient) movements followed by the rehabilitation treatments cannot be tracked down by using optical motion devices as per the limitations discussed in [8]. Therefore usage of markerless sensors are proposed as an alternative. Precision of the Kinect sensor based information is less precise than the optical motion capture. To overcome that issue, Kinect is combined with inertial sensor to obtain better visualization, system initialization and improved overall precision. Data from both the sensors are integrated via Kalman Filter and is proposed to correct the estimate the inertial sensor by using joint angles obtained from the Kinect.

Human hand has been tracked using Kinect motion tracking sensor before. In that research they have considered that hand model is consisted of a palm and five fingers. The palm is models as an elliptic cylinder and two ellipsoids for caps [12]. According to that model each finger is consisted of three cones and four spheres. These sphere and cylinder enabling a high degree of computational parallelism. Hand modeling process is given in the Figure 21.

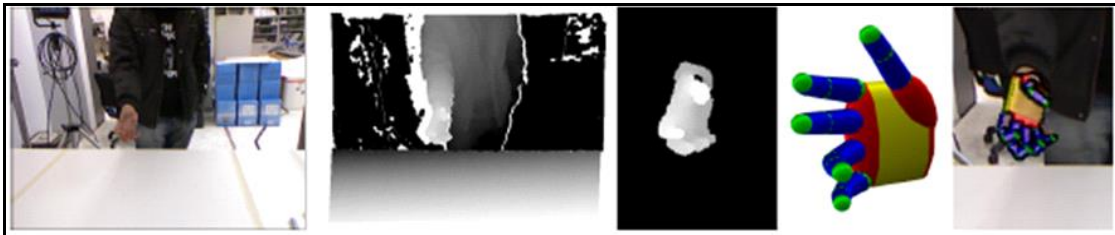


Figure 21 - Hand modelling process

Two types of inertial sensors are used in study [27] accelerometers and gyro meters. Gravity component measured by the accelerometer is concerned and is used to estimate the joint angles. Kinect provides preprocessed data directly to create the integration with Inertial such as 3D joint position of the human subject and 3D visualization. Reconstruction of joint positions is as per the Primesense module [27]. To evaluate the sensor integration, postures of sit to stand, squat, shoulder abduction and adduction are used. In the experiment phase when the subject takes a particular task and position angles have been computed. Then online calibration has been carried out to enable better visualization. Future work focuses on extending the online calibration filter to include further sensor errors such as scaling and evaluating integration of Kinect and portable sensors for motion capture system with more

postures. Initial state and covariance of each sensor is found to be problematic and Kinect initialize this integration filter (KF). Sensor reading errors are stated as another deficiency and to overcome that Kinect is used to perform online calibration for Inertial sensor.

In a recent research [45] Kinect is used for gait cycle recognition. The ultimate goal of this research is to use the Kinect for gait recognition and joint position identification. In another study [38] an automated system is developed using Kinect to derive the information of gait speed, step length and time, stride length and time and peak foot swing velocity by tracking the gait cycle. This research is conducted to make the clinical joint position identification process easier.

2.5. Generic gait cycle graphs in medical domain

In medical domain, standard gait cycle graphs for knee, hip and the ankle are defined [39]. The technique of defining the standard graph is not to be found in literature [39].

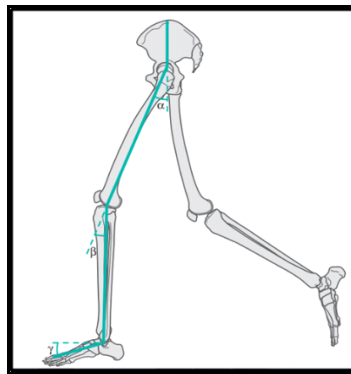


Figure 22 - Joints considered to generate generic gait cycle graphs in medical domain

Hip, knee and ankle joint angles are denoted by α , β and γ in Figure 22 which has been considered in the medical domain to generate the gait cycle graphs. Angles of the ankle joints are defined by the foot with respect to a line 90^0 to the tibia (lower limb born), with dorsiflexion defined as a positive angle and plantar flexion as a negative angle. According to this mathematical operation, the Figure 23 ankle gait cycle generic graph generates.

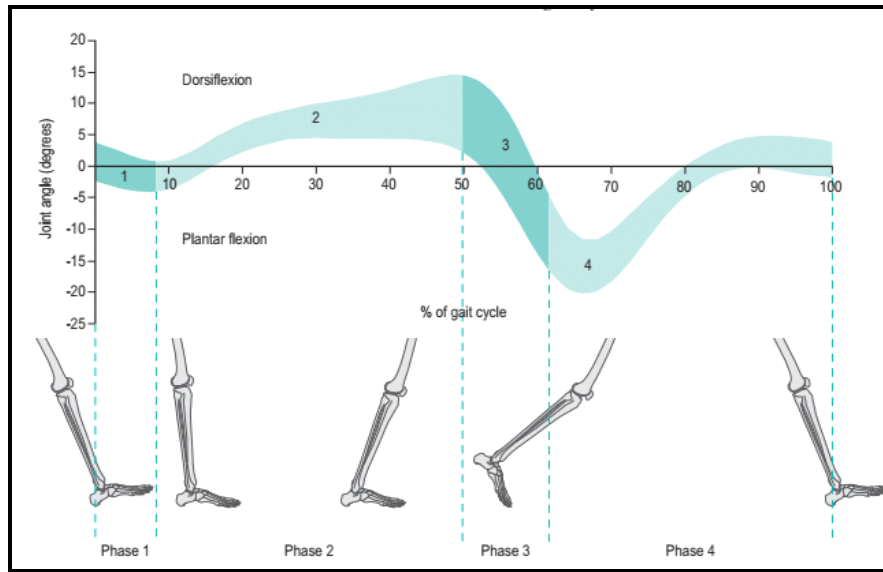


Figure 23 - Ankle gait cycle graph

The knee joint angle is defined by the long axis of the tibia with respect to the long axis of the femur, with full extension defined as zero degrees and movement into flexion being positive. The knee generic gait cycle generates in medical domain as follows in Figure 24.

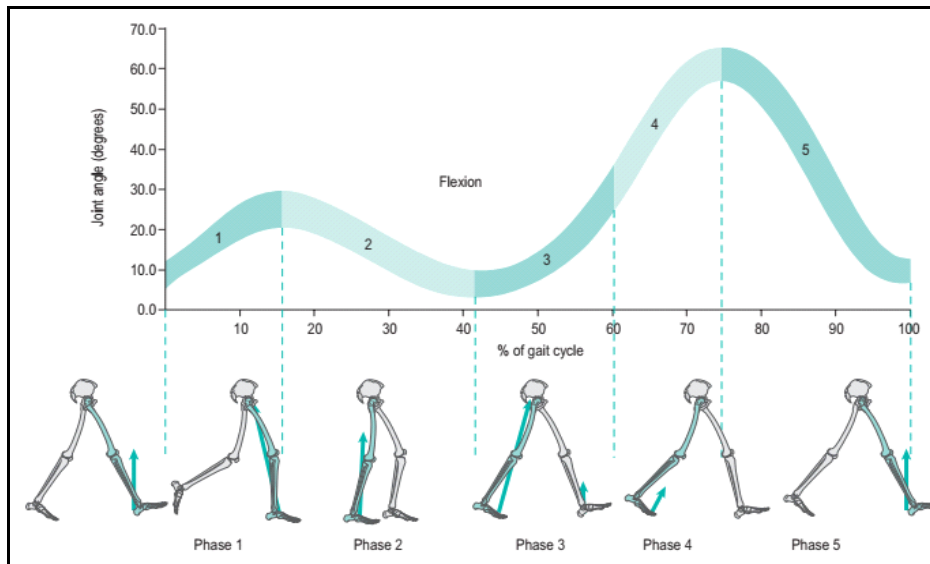


Figure 24 - Knee gait cycle graph

The hip joint angle is defined by the long axis of the femur with respect to the pelvis, with flexion defined as positive and extension negative. The hip generic gait cycle graph is as presented in Figure 25.

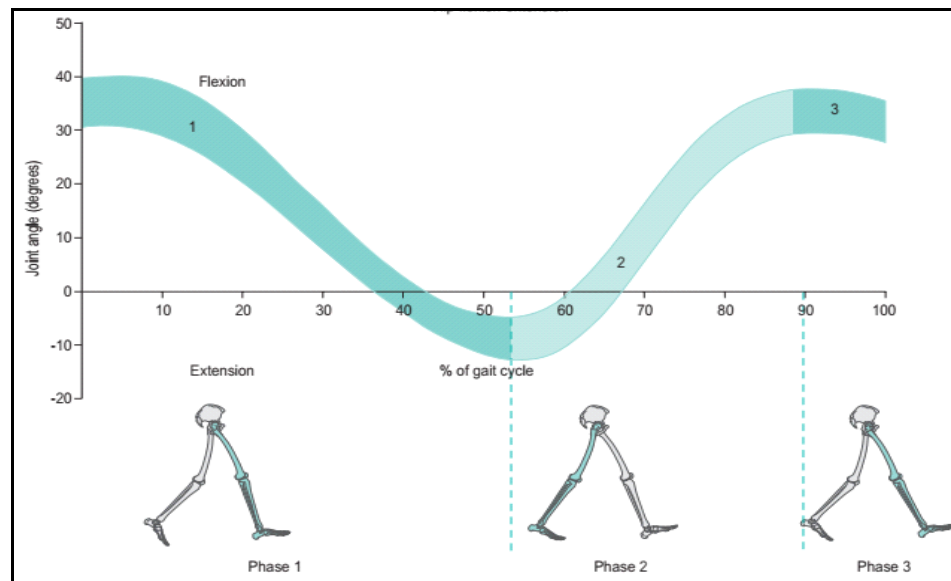


Figure 25 - Hip gait cycle graph

2.6. Summary

We carried out a comprehensive literature review in various aspects related to the current research. Firstly, researches carried out considering muscle imbalances was the concern and it can be concluded that muscle imbalance is a major problematic situation in sports and games as well as in the daily routine of an individual. We were also able to recognize that the rate of lower body injuries is higher than the upper body injuries.

A literature survey for the usage of motion tracking devices was also carried out and we were able to identify various usage of technology in human movement tracking. MYO armband, inertial sensor, MVN motion tracking sensor, Kinect and many other devices were used in previous studies and we identified the issues and limitations lie with these devices. Up to the point of the literature survey, we did not come across any study which were carried out to identify musculoskeletal imbalances using these sensors. We studied recent studies of tracking devices usage for fall detection, movement analysis, tracking rehabilitation treatments and many other similar applications. Gait cycle is another main concern of the current research and a study was carried out to understand the applications of the

gait cycle. We came across the fact that the human gait cycle is used in fields of human identification, neurological disease identification and fall detection.

A literature review for the Kinect motion tracking device was also carried out. We identified many past researches carried out with the Kinect in areas as in comparison with other sensors, Kinect in human movement analysis, Kinect in rehabilitations treatment tracking and in various other aspects. Followed by the literature review, we identified a current gap in identifying musculoskeletal imbalances and usage of motion tracking devices in physiotherapy. Therefore this research project can be presented as an attempt to bridge the identified gap.

Chapter 3

3. Design and methodology

3.1. Research design

In this research project, lower limb musculoskeletal system is considered in order to determine muscle imbalances. Three joint angles are considered in this case namely hip, ankle and knee joints. Angles between the three joints are calculated with the aid of position values captured by the Kinect. Considering the variation of these angles along the eight phases of the gait cycle, three graphs are drawn for a subject. Two types of graphs are introduced in this research: generic graphs and test sample graphs. In the evaluation phase, test sample graphs are compared with the generic gait cycle graphs. Availing the comparison, status of a subject's muscle imbalance is predicted. A qualitative evaluation is carried out under the supervision of domain specialists as to confirm the reliability and accuracy of the results produced by the proposed approach. Figure 26 summarizes the overall research architecture.

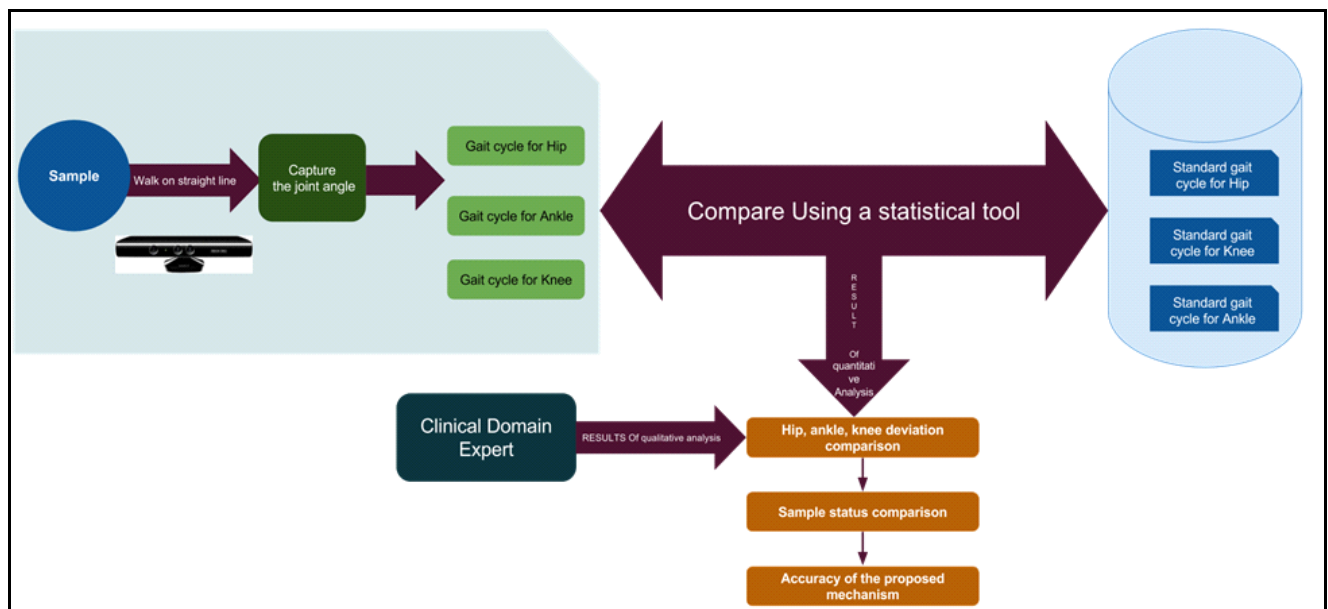


Figure 26 - Research design

3.1.1. Sampling mechanism

The sample of this research is mainly divided into two categories: control sample and test sample. The control sample was used to derive the generic hip, knee and ankle gait cycle graphs. The test sample was used to measure the status of a random person's musculoskeletal system against the defined generic gait cycle graphs. The two samples were consisted of both male and female subjects. The male sample included subjects who fell between the age range of 25 – 45 and the female sample included subjects who fell between the age range of 30 – 50 [42]. The BMI value of the subjects was defined to be a BMI value between the range of 18.5 – 23 which indicates the BMI value of a healthy person for both the genders [42]. Individuals having diseases which can affect the gait cycle have not been included in the sample of this research. The sample was selected under the supervision of domain experts. We provided written consents to the sample prior to their participation in the experiment. The consent for provided is attached in the Appendix section.

3.1.1.1. Sampling mechanism for healthy subjects

Healthy subjects participated in the research were further categorized into control and test samples. The control sample was used to derive the generic hip, knee and ankle graphs. The test sample was used to measure the status of a random person's musculoskeletal system against the defined generic gait cycle graphs. For the control sample, both male and female subjects were selected. The male control sample fell between the age range of 25 – 45. The female control sample fell between the age range of 30 - 50. Age categorization for sampling is due to the medical reason that the growth cycle of male gender is completed at the age of 25 and female skeletal growth completes at the age of 30 [31] [42]. After the age of 45, the musculoskeletal system of male gender begins to get depreciated. The female musculoskeletal system begins to get depreciated at the age of 50 [8]. The healthy population was checked for their skeletal system behavior by a domain expert prior considering their inclusion in the sample. The healthy sample did not contain any musculoskeletal imbalance as per the observations and comments made by the domain specialists. By analysing the gait cycle behavior of the control sample, it was ensured furthermore by the domain specialist that the sample's gait cycles can be taken as healthy. Control sample's BMI values were calculated and verified that they possess the BMI value of a healthy person. Step length of the sample was also considered and data was captured from subjects whose step size was between 5cm - 10cm which is the normal step length of a

healthy person [10]. The control sample was later used to define the generic minimum and maximum values for hip, knee and ankle variations along the gait cycle. For the test sample (healthy), a sample of five male subjects and five female subjects were drawn. The gait cycles of the test sample were compared against the control sample in order to determine the status of their musculoskeletal system.

Since getting information from every healthy individual in the population is impractical, infeasible and time consuming, a predefined sample set of 12 male subjects and 12 female subjects who aligned with our defined values were derived. This derivation was solely under the supervision of a domain expert. All the subjects provided the research group with a written consent and it was stated that this is a research falls under bioinformatics and personal information of the subject will not be disclosed. A template of the consent provided is attached in the Appendix section.

3.1.1.2. Sampling mechanism for imbalanced subjects

Imbalanced sample was considered as the second test sample of the research. As the imbalanced test sample for the survey, a sample of eight subjects of male gender was derived. The sample's age range varied from 25 – 45. The age categorization of sampling is due to the medically defined growth and depreciation limits of the human skeletal. The imbalanced test sample was derived from patients who suffer from musculoskeletal imbalances. The BMI values of the imbalanced test sample were calculated and ensured to be healthy. Step lengths of the imbalanced test sample were also measured and the only consideration was subjects who possessed a step size of 5cm - 10cm which was compatible with the step length defined for the average healthy sample. All the subjects were provided with and agreed to consent that this is a research falls under bioinformatics and personal information of the subject will not be disclosed. The consent for provided is attached in the Appendix section.

3.1.2. Data capturing via Kinect

Kinect motion tracking sensor was used for data collection purposes of the test sample in the study. Setup for data collection was defined in this research as a 3m straight line. Kinect was positioned to capture the straight line area and was able to cover all the phases of a subject's gait cycle. When a subject was walking along the predefined straight line in the laboratory environment, Kinect

was used to retrieve X, Y and Z coordinates of each joint of the lower limb musculoskeletal system of the subject as basic measurements where X; the horizontal axis coordinates of the laying object, Y; the vertical axis coordinates of the laying object and Z; distance between the object and the Kinect.

Skeleton tracking is one of the major components in this research project. Human skeleton is tracked and data is processed to determine the X, Y and Z position coordinates of the skeleton joints as shown in Figure 27. Kinect SDK is capable of tracking twenty joints of a human skeleton in a 3D space but only nine joints of lower human limb were required in the research for gait cycle analysis.

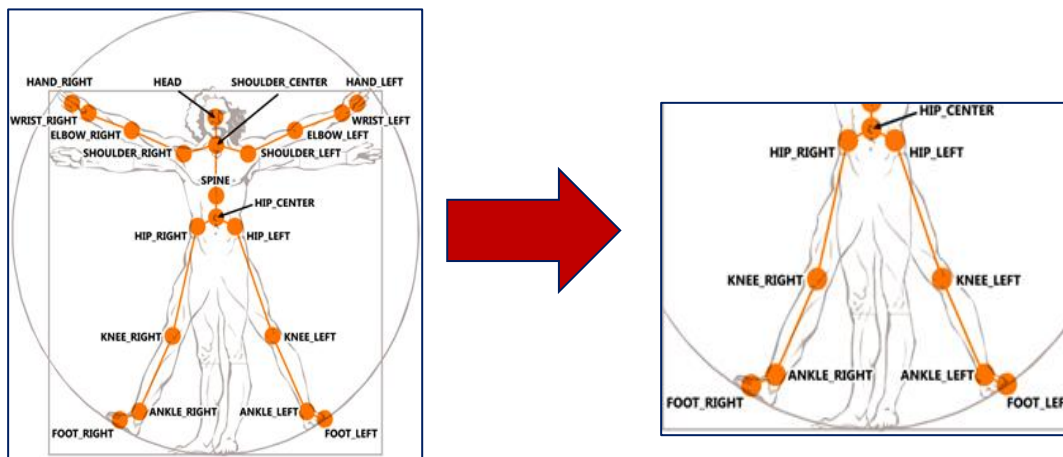


Figure 14 - Human joints captured by Kinect

3.1.3. Mathematical operation for joint angle calculation

In medical domain, goniometer is used to measure the joint angles of a patient. By the proposed approach, this measuring technique is automated by applying a mathematical operation. The angle calculation mechanisms for generic graph generation prevail in the medical domain and used in the proposed research study differ. The method of angle calculation for generic graph generation in medical domain is stated in the Background chapter. A divergent mechanism is proposed in this study taking the measuring technique of goniometer into consideration. This is due to the reason that primary angle measuring method used in clinical domain is obtaining joint angles directly from the goniometer.

Kinect V1 does not directly give the angle values of joints captured. In order to calculate the angles between joints (hip, knee and ankle) using the X, Y and Z coordinates captured via Kinect, a

mathematical operation was used. X, Y and Z coordinates of three related joints in a 3D space were considered to calculate the angle of a single joint. The three joints considered in this research. X, Y and Z coordinates of the three related joints in 3D space are utilized to calculate the angle of a particular joint given the joint is hip, knee or ankle. The Dot product function was used to calculate the angle between two vectors in 3D space in this mathematical operation.

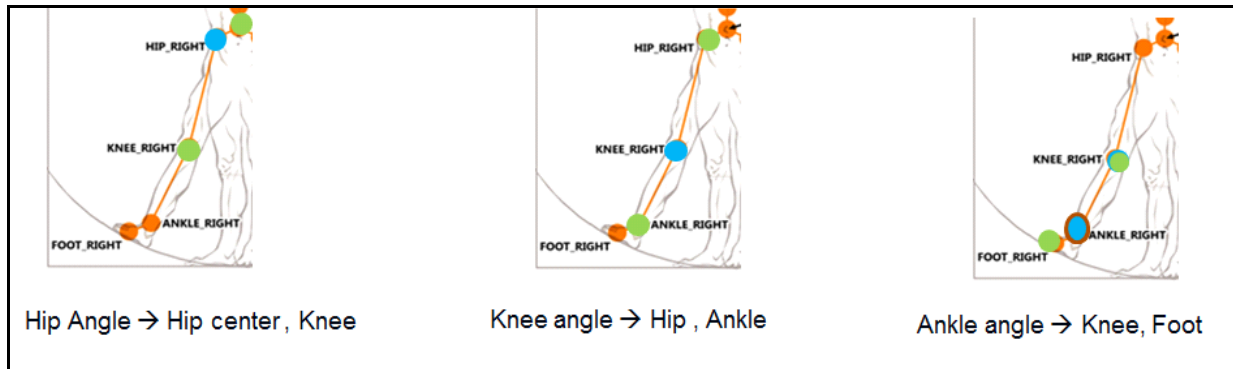


Figure 28 - Joint angle calculation in 3D space

Figure 28 shows the required joints in order to calculate the angles of the considered joints of this research study and how Kinect measures the joints in a 3D space. Blue color circle shows the particular joint we need to calculate the angle for and two green color circles show the other two positions which are required to calculate the particular joint angle. To calculate the angle of the middle joint, position coordinates of the joints which lie on each side of that joint is required. According to 1st picture of Figure 28, in calculating the hip angle, it considers hip center and the knee position with hip position in the 3D space. To calculate the knee angle, the model built considers the hip position and the ankle position in the 3D space. Using the same approach, to calculate the ankle angle, knee position and the foot position of the considerate leg is required.

The mathematical operation representing this process is as follows.

$$\text{Dot product } (\overrightarrow{PQ}, \overrightarrow{QR}) = \|\overrightarrow{PQ}\| \|\overrightarrow{QR}\| \cos\phi$$

This equation can be solved in two steps as follows when the X, Y, and Z coordinates are given.

Step 1

Join the three related joints considered and create two vectors in 3D space. If we consider the three joints are P, Q and R then two vectors are \overrightarrow{PQ} and \overrightarrow{QR}

X, Y and Z coordinates are as follows.

$$P = (x_1, y_1, z_1), Q = (x_2, y_2, z_2), R = (x_3, y_3, z_3)$$

$$\overrightarrow{PQ} = Q - P \rightarrow 1$$

$$\overrightarrow{QR} = R - Q \rightarrow 2$$

From 1

$$\overrightarrow{PQ} = ((x_2-x_1), (y_2-y_1), (z_2-z_1)) \rightarrow (X_1, Y_1, Z_1)$$

From 2

$$\overrightarrow{QR} = ((x_3-x_2), (y_3-y_2), (z_3-z_2)) \rightarrow (X_2, Y_2, Z_2)$$

$$\overrightarrow{PQ} \cdot \overrightarrow{QR} = (X_1) \cdot (X_2) + (Y_1) \cdot (Y_2) + (Z_1) \cdot (Z_2)$$

Step 2

Since $\overrightarrow{PQ} = (X_1, Y_1, Z_1)$ and $\overrightarrow{QR} = (X_2, Y_2, Z_2)$

$$\|\overrightarrow{PQ}\| = \sqrt{(X_1)^2 + (Y_1)^2 + (Z_1)^2}$$

$$\|\overrightarrow{QR}\| = \sqrt{(X_2)^2 + (Y_2)^2 + (Z_2)^2}$$

Thus,

$$\phi = \arccos \left(\frac{(X_1)(X_2) + (Y_1)(Y_2) + (Z_1)(Z_2)}{(\sqrt{(X_1)^2 + (Y_1)^2 + (Z_1)^2})(\sqrt{(X_2)^2 + (Y_2)^2 + (Z_2)^2})} \right)$$

3.1.4. .csv file generation

When a subject walks along the straight line defined, the Kinect sensor captures all the body joints and the application is developed to calculate and record the lower limb body joint angle values in each phase of the gait cycle of a subject using the mathematical operation defined. Hip, knee and the ankle angle values of both right and left side limbs of the subject in every 200ms is written to a .csv file and stored. In the initial data fed to the application, the number of gait cycles which needed to be captured should be given to the application. Number of .csv files generated is equal to the number of gait cycle value given in the initial data feed. These .csv files can then be used for further examination of the gait cycle of a subject.

3.1.5. Modelling the gait cycle graph

A gait cycle graph basically represents the movements of the human body when a subject walks. In the scope of this research study, how the joint angles of the lower limb musculoskeletal system change throughout a gait cycle is the consideration. A gait cycle graph can be drawn mainly in three different ways when it comes to the lower limb musculoskeletal system; graph for hip variation in gait, graph for knee variation in gait and graph for ankle variation in gait. Gait cycle graph represents the angle of a particular joint in each phase of the gait cycle. X axis denotes the percentage of the gait cycle as 10%, 20% ... 100% and Y axis denotes the angle of the particular joint in each phase of the gait cycle. The time taken to complete a gait cycle by a healthy person is around two seconds. Hence by the proposed application, it captures the joint angle values in each 200 millisecond. In order to generate a gait cycle graph, joint angles in each phase of the gait cycle were captured with the aid of the application. The gait cycle graph is then generated using the angle values in each stage of the gait cycle applying the values to the mathematical operation. Primarily, two main graph categories are considered: gait cycle graphs for initial and secondary step of a subject. Therefore, three separate graphs are generated for hip, knee and the ankle and they are further narrowed down to right hip, left hip, right knee, left knee, right ankle and left ankle.

3.1.5.1. Hip gait cycle graph

Hip gait cycle graph denotes how the hip joint angle is changed throughout the phases of the gait cycle. In this graph, x axis denotes percentage of the gait cycle completion and the y axis denotes the angle variations of the hip joint in each phase. Two separate hip gait cycle graphs for initial and secondary steps are generated.

3.1.5.2. Knee gait cycle graph

Knee gait cycle graph denotes how the knee joint angle is changed throughout the phases of the gait cycle. In this graph, x axis denotes percentage of the gait cycle completion and the y axis denotes the angle variations of the knee joint in each phase. Two separate knee gait cycle graphs for initial and secondary steps are generated.

3.1.5.3. Ankle gait cycle graph

Ankle gait cycle graph denotes how the ankle joint angle is changed throughout the phases of the gait cycle. In this graph, x axis denotes percentage of the gait cycle completion and the y axis denotes the angle variations of the ankle joint in each phase. Two separate ankle gait cycle graphs for initial and secondary steps are generated.

3.1.6. Generation of generic gait cycle graph

The control sample drawn was used to generate the generic hip, knee and ankle graphs. Hip, knee and ankle joint position values were captured using the Kinect. Angle measurements of the healthy sample were directly written into a .csv file for further analysis and by evaluating the data obtained, the generic graphs were generated. Separate graphs were generated for right hip, left hip, right knee, left knee, right ankle and left ankle. Data gathering was done three times (three gait cycles) for each individual to increase the data accuracy and the average value of these three values was taken. Microsoft Excel 2013 was used to perform the calculations and graph generations. Minimum and maximum threshold values were determined by analyzing the captured data. The same procedure was

followed to generate the male and female threshold values for hip, knee and ankle joint variations as well.

Order six polynomial graphs were generated for minimum and maximum data points derived. The reason to fit the curve to order six was, In the medical domain gait cycle graphs are drawn for the highest order and according to literature the maximum curve fitting is denoted by the highest R-squared value [41] [43] [44]. The highest R-squared value is generated for the curve drawn for the highest order and the lowest R-squared value is generated for the curve drawn for the lowest order. Hence the minimum and maximum generic graphs were generated as order six polynomial graphs.

For analysis purposes, two generic graphs for initial and secondary step sides of the skeletal were required. This is due to different position initiations of two limbs. One generic graph demonstrates how the hip, knee and ankle joint angles of a subject's initial step side varied and the second generic graph demonstrates how the hip, knee and ankle joint angle values varied in the secondary step side of a subject during a gait cycle.

The generic gait cycle graphs show the minimum joint angle values which can be taken by an average healthy person and the maximum joint angle values which can be taken by an average healthy person. Figure 29 summarizes the generic gait cycle graph generation process.

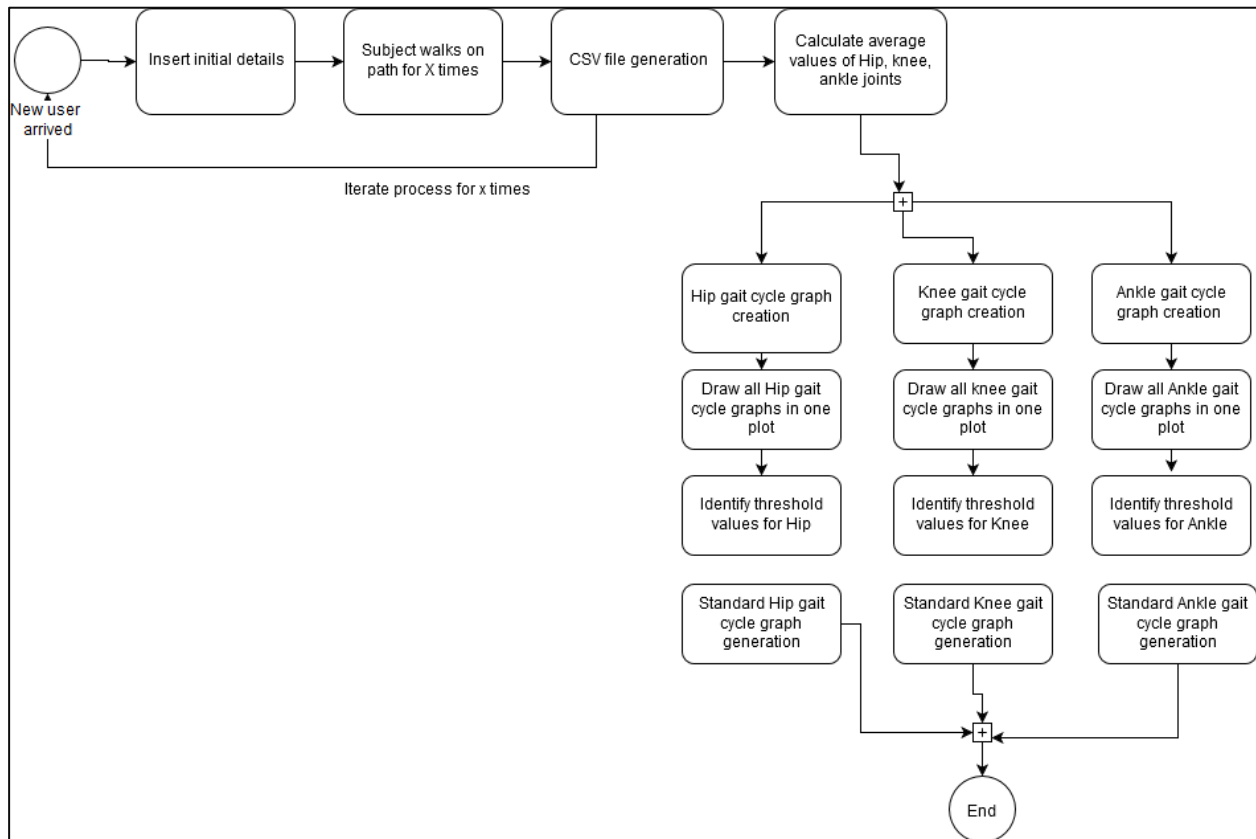


Figure 29 - Generic graph generation process

3.1.7. Comparison of graphs

Followed by gathering initial details of a test sample subject, particular number of gait cycles were tracked by the application. Number of gait cycles required to capture varied according to the given initial value for 'No. of gait cycles'. After the angle values are written to the .csv file, the average hip, knee and ankle gait cycle values of the subject was calculated by using Microsoft Excel 2013. Gait cycle graphs for both initial and secondary step sides are generated using the data included in the .csv file. The generated six graphs of the test subject were then compared with the generic gait cycle graphs separately in order to identify whether the subject is having an imbalance in his lower limb and if so where the imbalance is. The decision of which side limb should be compared (right or left) with the captured data is taken by considering the primary and secondary step side of the subject's initiative. If the subject's gait cycle lies beyond the minimum and maximum threshold values defined in the generic gait cycle graphs, the condition of the subject can be identified as imbalanced. If the gait cycle

of the subject lies in between the minimum and maximum threshold values defined in the generic gait cycle graphs, the status of the subject is identified as balanced. Comparison of graphs generated can be given in brief as represented in Figure 30.

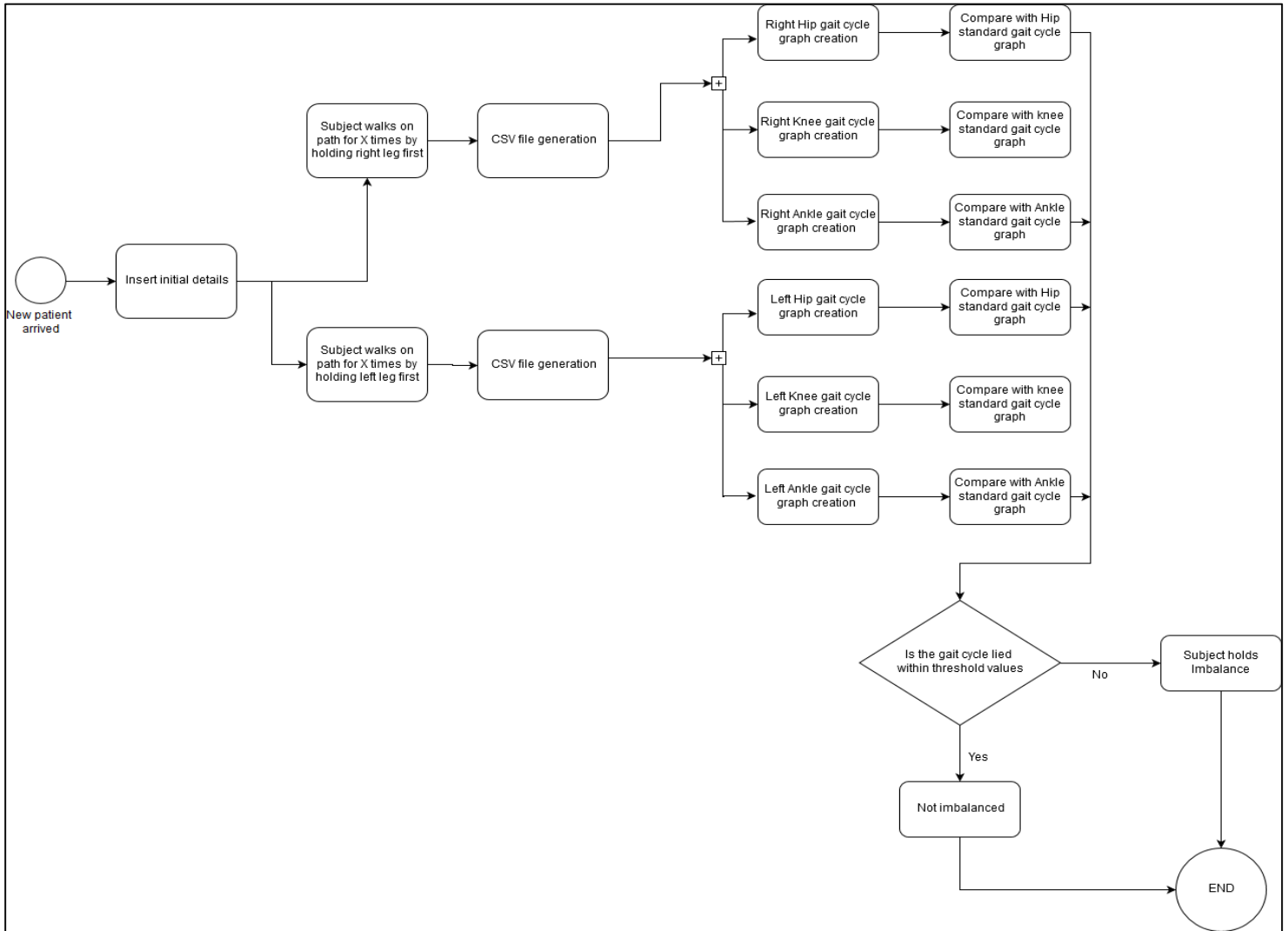


Figure 30 - Gait cycle comparison

3.2. Research methodology

3.2.1. Environmental setup

An indoor clinical environment where the physiotherapist operates was used to setup the Kinect sensor for data collection of the imbalanced test sample. Due to limitations of the field of view of the Kinect sensor, an area of 3m*2m as the experiment region. The sample was advised of loose lower limb clothing and to avoid the uncomfortable walking patterns and unnecessary capturing of data. The Kinect was set on a stand where its position is parallel to the floor and was able to operate on the maximum field of view of the sensor. Avoidance of occlusion areas and minimization of the shadow conditions of the environment was also concerned. Since Kinect requires a distance of 2 meters from the object to be captured, the distance between the subject and the Kinect was arranged to 2 meters. Figure 31 represents the environmental setup for the control and healthy test samples.



Figure 15 - Defined walkway

3.2.2. Data collection

Data collection of the research study was carried out in separate phases. First phase was performed in order to obtain data to define the generic hip, knee and ankle values. The second phase was carried out in order to experiment with the test sample against the defined generic. Samples of the research is categorized into three categories; control sample, healthy test sample and imbalanced test sample.

Data from the control sample was first captured via Kinect in the University of Colombo premises. The gait cycles of the control sample were observed by a domain expert and they were ensured that the gait cycles do not deviate from the medical explanations of the domain. Name, age, height, weight, gender and number of gait cycles were fed into the system for further purposes of the research. Followed by this procedure, a test walk was given for every subject in order to make the subject relaxed. The subject was then requested to walk on the straight line defined. Five gait cycles for each subject were captured. Information regarding the captured gait cycles and respective angles were written automatically into a spreadsheet for analysis purposes. Same procedure was applied to all the control sample subjects. The final outcome of this data gathering phase was defining generic minimum and maximum threshold values for right_hip, right_knee, right_ankle, left_hip, left_knee and left_ankle graphs for male and female genders separately.

Data collection for the imbalanced test sample was carried out again in two different approaches. Data collection for the imbalanced test sample was carried out in a clinical environment at Peradeniya General Hospital and was fully under the supervision of domain experts (Dr. Kalpani Mahindaratne, Dr. Deepthika Chandrasekara and fellow specialists). Kinect was used to gather data from the test sample along with the application developed. In the initial data fed, a subject's name, age, height, weight, gender and number of gait cycles to be captured were fed into the application. Followed by filling the initial details about the subject, test sample subjects were requested to walk along a 3m walkway used by the physiotherapists in the clinical environment. Three gait cycles from each test sample subject were captured. Time, left hip angle, left knee angle, left ankle angle, right hip angle, right knee angle and right ankle angle for one subject was included in the data captured throughout the time frame of the gait cycle. All the data obtained was stored in a .csv file defined individually for the subjects for analysis purposes. Figure 32 represents an imbalanced sample subject.



Figure 16 - Data collection of imbalanced test subject

The next approach of data collection was for the healthy test sample. Data collection for the healthy test sample was carried out in University of Colombo premises and the subjects were supervised by a domain experts. Kinect was used to gather data from the test sample along with the application developed. In the initial data fed, a subject's name, age, height, weight, gender and number of gait cycles to be captured were fed into the application. Followed by filling the initial details about the subject, test sample subjects were requested to walk along a 3m*2m area. Three gait cycles from each test sample subject were captured. Time, left hip angle, left knee angle, left ankle angle, right hip angle, right knee angle and right ankle angle for one subject was included in the data captured throughout the time frame of the gait cycle. All the data obtained was stored in a .csv file defined individually for the subjects for analysis purposes.

Following Table 2 contains a sample dataset for a healthy subject.

Subject identifier: Subject 2

Age: 36

Height: 189 cm

Weight: 81 kg

Gender: Male

Table 2 - Captured data of a healthy subject

Time (s)	hip left (degrees)	knee left (degrees)	ankle left (degrees)	hip right (degrees)	knee right (degrees)	ankle right (degrees)
1	129.8769882	170.8705849	105.3085851	150.9045388	172.9927312	150.9045388
2	123.183092	172.6895966	117.0050363	98.06423605	160.9560328	81.90457935
3	130.9762856	164.6738232	110.5197297	69.48340466	116.9029171	63.74576903
4	136.4781786	159.2415263	86.56861626	144.8625206	166.8869823	144.8625206
5	172.5867876	130.2674868	100.0474726	144.2189316	167.7968047	107.4777971
6	169.8546489	164.8694088	131.1533588	102.0676443	168.2671672	92.50310555
7	160.9692319	165.9329101	135.9789736	85.5750074	163.4025385	77.06561316
8	161.4515653	157.863246	27.47221539	111.3846188	140.8295844	132.7473654
9	156.6234736	157.5208623	106.286636	132.3223575	152.3418722	127.640873
10	140.7672297	139.6042177	82.98876507	145.3634272	155.16888	147.950242
11	125.3264698	146.8831218	103.1986684	111.1431969	161.1240333	107.245159
12	155.9523767	167.0234091	147.8982391	102.4212169	159.9297367	93.00029723
13	162.3126351	160.7912156	126.9418385	86.81539653	141.3964795	151.1739654

Following Table 3 contains a sample dataset for an imbalanced subject.

Subject identifier: Subject 11

Age: 24

Height: 151 cm

Weight: 54 kg

Gender: Male

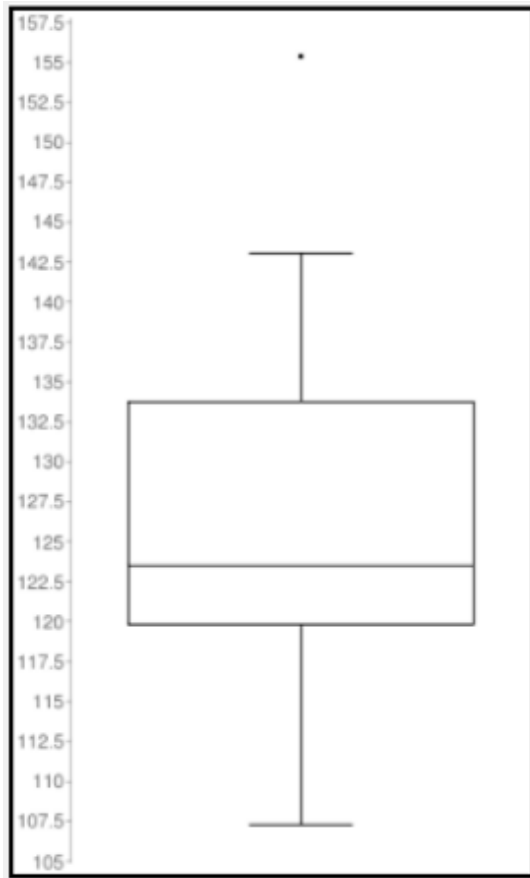
Table 3 - Captured data of an imbalanced subject

Time (s)	hip left (degrees)	knee left (degrees)	ankle left (degrees)	hip right (degrees)	knee right (degrees)	ankle right (degrees)
1	131.3139	171.5078	109.0341	156.4593	178.2937	156.4593
2	133.491	170.5699	155.7674	108.8961	177.8429	156.8465
3	134.2889	170.05	155.8491	110.1843	176.8718	110.0398
4	135.0485	170.0916	110.3168	110.254	176.0668	110.1613
5	136.3535	170.25	111.7115	109.7549	177.7311	109.349
6	136.968	170.9597	151.1697	110.8073	175.2257	110.8054
7	137.3127	171.4419	111.4104	111.4742	175.156	111.4742
8	138.5413	171.0376	110.9589	111.8106	174.7524	111.9195
9	138.5789	170.9098	112.3359	111.7219	173.8361	111.5591
10	138.4902	171.3816	112.1911	110.7543	175.024	110.7543

3.2.3. Data cleansing and preparation

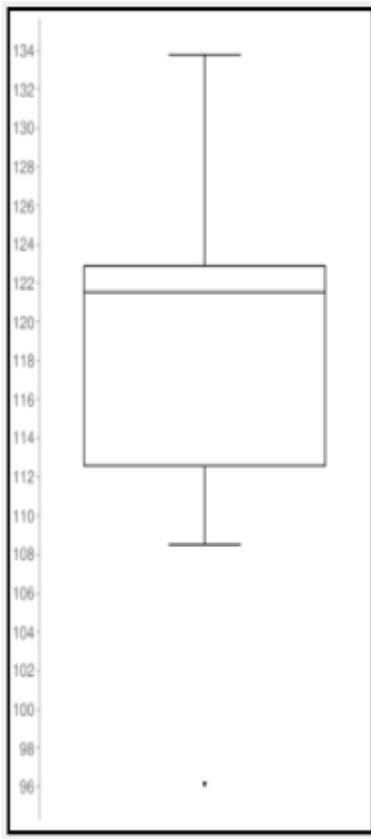
The importance of having error free, reliable data for statistical analysis was identified. All the data captured in the .csv files and spreadsheets were directly imported to a separate Excel file for the purpose of advanced analysis of raw data. Data preprocessing was carried out to ensure effectiveness and reliability of the final outcome of the research project.

All the data gathered from the control sample for generic graph generation was cleansed and prepared before defining the minimum and maximum threshold values. Box plot mechanism was used to remove the outliers in the data set by calculating median, minimum, maximum, first quartile, third quartile and interquartile range. For the defined ten data points, a box plot was graphed and therefore 60 box plots were graphed for male and 60 box plots were graphed for female subjects in the control sample. Four outliers were identified in the dataset. The outlier identification mechanism and the statistical values of the outliers are presented in Figure 33 – Figure 36.



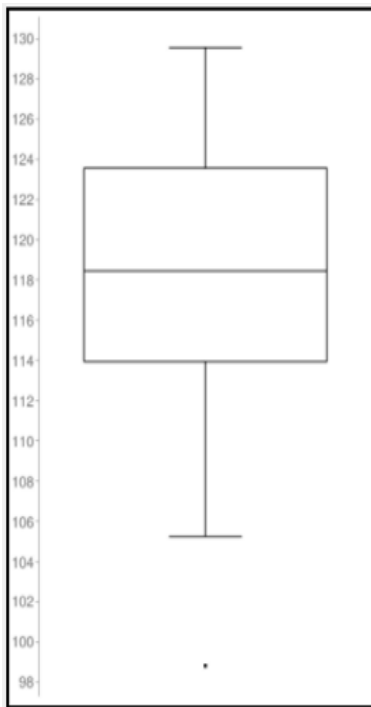
Median: 123.5070486
Minimum: 107.3026587
Maximum: 155.3569154
First quartile: 119.8560266
Third quartile: 133.7837682
Interquartile range: 13.9277416
Outlier: 155.3569154

Figure 17 - Boxplot outlier identification 1



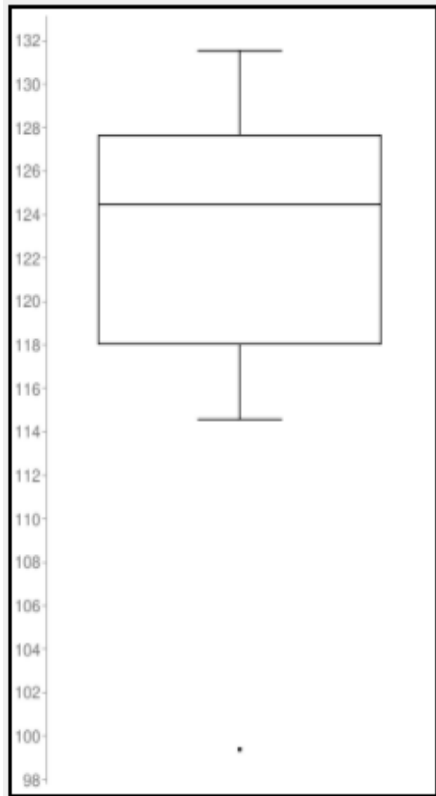
Median: 121.5117819
Minimum: 96.18044524
Maximum: 133.7725451
First quartile: 112.5985201
Third quartile: 122.8550101
Interquartile range: 10.25649
Outlier: 96.18044524

Figure 18 - Boxplot for outlier identification 2



Median: 118.4724568
Minimum: 98.83970714
Maximum: 129.5498567
First quartile: 113.9669475
Third quartile: 123.5446593
Interquartile range: 9.5777118
Outlier: 98.83970714

Figure 19 - Boxplot for outlier identification 3



Median: 124.4828924
Minimum: 99.40216144
Maximum: 131.5402366
First quartile: 118.0429659
Third quartile: 127.6764975
Interquartile range: 9.6335316
Outlier: 99.40216144

Figure 20 - Boxplot for outlier identification 4

Since some data gathered were incompatible with other captured data points (according to the boxplots), several data points captured for hip, knee and ankle angles of few subjects were neglected and removed. The reason for this type of data was later identified as the cutting edge of an individual's gait cycle.

Chapter 4

4. Implementation

4.1. Capturing human gesturing via Vitruvius library

In this research project, Vitruvius library is used to capture the human skeletal along with the usage of Kinect motion tracking sensor. This library contains some handy extension methods that helps to measure an angle using ‘Camera Space Points’. As described in the design chapter, joint angle is measured in a 3D space which needs three joints to calculate the angle; starting point, middle point and the end point. The main usage of this library in the research is its use in calculating the length of specified segments in the 3D space and the rotation in the X, Y and Z axis X, Y and Z being the horizontal axis coordinates of the laying object, the vertical axis coordinates of the laying object and the distance between the object and the Kinect in order.

Camera Space Point

A ‘Camera Space Point’ is a set of coordinates in the 3D space. It has X, Y, and Z coordinate values, all measured in meters. The X value represents the horizontal distance of the point, measured from the left side of the field-of-view. The Y value represents the vertical distance of the point, measured from the top of the field-of-view. The Z value represents the distance between the point and the sensor plane.

4.2. Obtaining joint positions via Vitruvius library

Following are the functions which are used in this research study in order to identify the hip, knee and ankle joint positions of the initial and secondary limbs of a subject.

```
//Obtaining positions

Joint hip_left = skeleton.Joints[JointType.HipLeft];
Joint knee_left = skeleton.Joints[JointType.KneeLeft];
Joint ankle_left = skeleton.Joints[JointType.AnkleLeft];
Joint foot_left = skeleton.Joints[JointType.FootLeft];

//Obtaining positions
```



```

Joint hip_right = skeleton.Joints[JointType.HipRight];
Joint ankle_right = skeleton.Joints[JointType.AnkleRight];
Joint knee_right = skeleton.Joints[JointType.KneeRight];
Joint foot_right = skeleton.Joints[JointType.FootRight];

```

As descriptively stated in the research design, to calculate the hip joint angle, at least three joints from each side of that particular joint is required to measure the hip angle. In first case, hip center, hip and knee positions are considered to obtain the hip joint angle. In second case hip, knee and ankle positions are considered to obtain the knee joint angle. In third case knee, ankle and foot positions are considered to obtain the ankle joint angle.

The calculation mechanism of the joint angles using the above mentioned joint positions is stated in the following section.

```

//calculating angles

Joint hip_center = skeleton.Joints[JointType.HipCenter];

rhip_angle = getAngle(hip_center, hip_right, knee_right);
rknee_angle = getAngle(hip_right, knee_right, ankle_right);
ranckle_angle = getAngle(knee_right, ankle_right, foot_right);

lhip_angle = getAngle(hip_center, hip_left, knee_left);
lknee_angle = getAngle(hip_left, knee_left, ankle_left);
lanckle_angle = getAngle(knee_left, ankle_left, foot_left);

```

In the scenario of calculating the right hip joint angle, the inbuilt method, ‘getAngle’ is used and three parameters are passed to this method namely hip_center, hip_right and knee-right. In the scenario of calculating the left hip joint angle, the ‘getAngle’ is used and three parameters; hip_center, hip_left and knee-left are passed to this method. In the scenario of calculating the left knee joint angle, the ‘getAngle’ is used and three parameters; hip_left, knee-left and ankle_left are passed to this method. In the scenario of calculating the right knee joint angle, the ‘getAngle’ is used and three parameters; hip_right, knee-right and ankle_right are passed to this method. In the scenario of calculating the left ankle joint angle, the ‘getAngle’ is used and three parameters; knee_left, ankle-left and foot_left are passed to this method. In the scenario of calculating the right ankle joint angle, the ‘getAngle’ is used and three parameters; knee_right, ankle-right and foot_right are passed to this method.

Following is the defined angle calculation mechanism using the dot product function with the captured joint position values.

```
//calculate angle
private double getAngle(Joint upper, Joint center, Joint lower)
{
    Vector3 pq = new Vector3(upper.Position.X - center.Position.X,
upper.Position.Y -center.Position.Y, upper.Position.Z - center.Position.Z);
    Vector3 qr = new Vector3(center.Position.X - lower.Position.X,
center.Position.Y -lower.Position.Y, center.Position.Z - lower.Position.Z);

    //normalize the vector so that both vectors are in same units
    pq.Normalize();
    qr.Normalize();

    double dotProduct = Vector3.DotProduct(pq, qr);
    double pq_magnitude = pq.Length;
    double qr_magnitude = qr.Length;
    double angle_rad = Math.Acos(dotProduct / (pq_magnitude *
qr_magnitude));

    double angle_degrees = angle_rad * 180 / Math.PI;

    return 180 - angle_degrees;
}

static int count = 0;
static int nextCount = 1;

static double lhip_angle = 0; List<double> lhip = new List<double>();
static double lknee_angle = 0; List<double> lknee = new List<double>();
static double lanckle_angle = 0; List<double> lanckle = new
List<double>();

static double rhip_angle = 0; List<double> rhip = new List<double>();
static double rknee_angle = 0; List<double> rknee = new List<double>();
static double ranckle_angle = 0; List<double> ranckle = new
List<double>();
```

The mathematical operation defined in the design chapter is used to calculate the joint angle value as represented in the following code base. Dot product value of two vectors in 3D space is measured to get the degree value of an angle. These joint angle values are then written to a .csv file for further analysis.

```
//get median
lhip_angle = lhip.ElementAt(lhip.Count/2);
lknee_angle = lknee.ElementAt(lknee.Count/2);
lanckle_angle = lanckle.ElementAt(lanckle.Count / 2);

rhip_angle = rhip.ElementAt(rhip.Count / 2);
```

```
rknee_angle = rknee.ElementAt(rknee.Count / 2);
rhip_angle = ranckle.ElementAt(ranckle.Count / 2);

//write line to csv file
writeLineToCSV();
```

Before the values are written into the .csv file, the median value of the angle of each joint is taken in order to increase the accuracy of captured data. This .csv file contains the angle values of hip, knee and ankle of both the limbs of a subject. Angle values for a joint are captured in every 200ms.

```
//create a new thread to run the timer
    new Thread(() =>
    {
        Thread.CurrentThread.IsBackground = true;

        //start timer
        System.Timers.Timer aTimer = new System.Timers.Timer();
        aTimer.Elapsed += new ElapsedEventHandler(OnTimedEvent);
        aTimer.Interval = 200; //200 millisecond count gap
        aTimer.Enabled = true;
    }).Start();
}
// When timer triggered
private void OnTimedEvent(object source, ElapsedEventArgs e)
{
    count++;
}

protected override void OnKeyDown(KeyEventArgs e)
{
    base.OnKeyDown(e);
    if (e.Key == Key.X && currentGait<=gaits)
    {
        count = 0;
        nextCount = 1;
        resetCSV();
    }else if(e.Key == Key.N && currentGait <= gaits)
```

If any disturbance occur during the gait analysis, it is possible to reset data in the .csv file by entering “X” key stroke and to proceed to the next gait cycle, “N” key stroke can be used.

4.3. Application interfaces

Below Figure 37 shows the initial interface of the application where the user has to fill the subject details which will be stored in a .csv file separately in a folder named after the given subject name along with the gait cycle angles of that subject. The gender of the subject should be taken in the initial

data fed in order to decide, against which generic gait cycle values should the captured data be compared with. The number of gait cycles can be selected and this is for the sole purpose of data integrity.

The screenshot shows a standard Windows-style dialog box titled "Input Window". It contains the following fields and controls:

- Name:** A text box containing "Buddhika Dahanayake".
- Age:** A text box containing "25".
- Weight (kg):** A text box containing "71".
- Height (cm):** A text box containing "172".
- Gender:** Two radio buttons, "Male" (which is selected) and "Female".
- No. of gait cycles:** A dropdown menu currently showing the value "3".
- OK:** A button at the bottom center of the dialog.

Figure 21 - Initial user interface of the application

Followed by the initial data fed to the system, the system proceeds to the next level of data capturing process via Kinect as shown in the interface Figure 38. In this step, subject has to walk along the straight line defined and the human skeleton of the subject is displayed in the view panel of the system interface while the hip, knee and the ankle angles of left and right sides of the subject's skeleton are displayed in the right side of the interface. Since the consideration in this research project is the gait cycle of the subject, side view of the human skeletal movements is the main observation for capturing data. Hence the subjects walk sideways of the Kinect sensor. Number of gait cycles completed by the subject and the count of .csv files are displayed in the bottom of the same interface. Options are given for the system user to reset the gait cycle values if disturbances occur and an option to start the next log of the gait cycle.

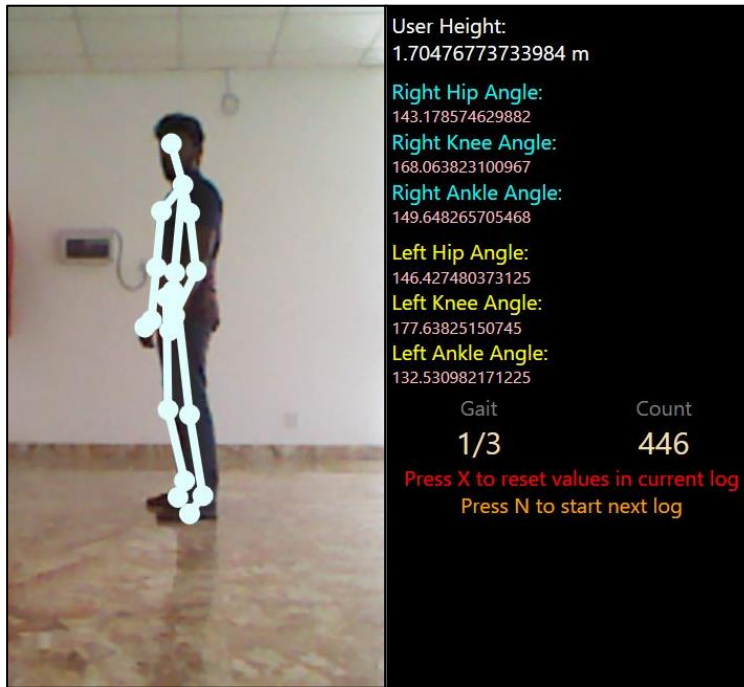


Figure 38 - Side view of the tracked user skeleton

Figure 39 shows the front view of the skeleton and hip, knee and ankle angle values of the right and left side limbs of the subject tracked via Kinect.

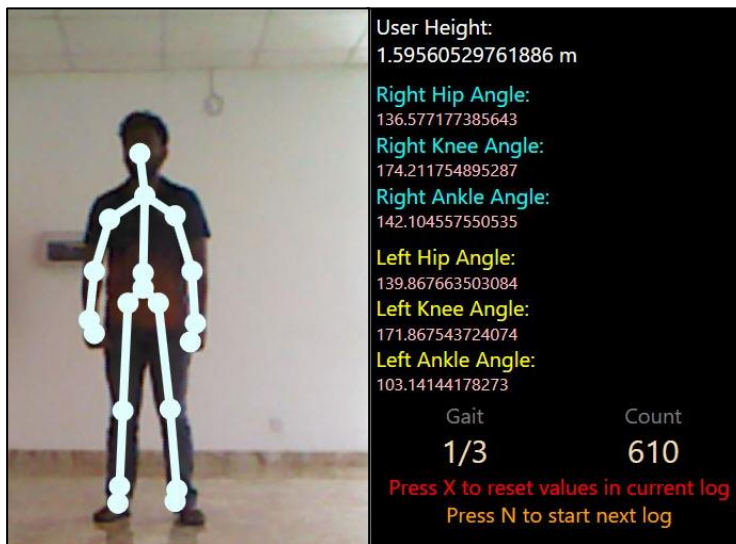


Figure 22 - Front view of the tracked user skeleton

Chapter 5

5. Evaluation and results

5.1. Evaluation

Evaluation of the research was conducted in two approaches; quantitative and qualitative. The quantitative measure was carried out by using the data captured from the system and the qualitative measure was conducted by physiotherapists in the domain to ensure the accuracy of the quantitative measure and the overall system.

The control sample was consisted of 24 healthy subjects. Among the sample, 12 subjects were female and healthy and 12 subjects were male and healthy. The control sample was used to generate the generic gait cycle graphs. The test sample of 18 subjects consisted of healthy and imbalanced subjects. Among the test sample subjects, eight subjects were imbalanced and 10 subjects were healthy. The age limits, BMI values and step lengths are as mentioned in the Design and methodology chapter. Following Table 4 represents the sample distribution precisely.

Table 4 - Gender distribution of the research sample

Control sample		Test sample	
Male	Female	Male	Female
12	12	13	5

5.1.1. Generic graph generation

Minimum and maximum threshold values for male and female generic gait cycles were generated by analyzing the gait cycle graphs of 12 healthy male subjects and 12 healthy female subjects. This section describes how the hip, knee and ankle generic gait cycle graphs were generated for both male and female genders.

Followed by attaining the minimum and maximum angle values that can be taken by a healthy subject during a gait cycle, statistical methods were practiced for the data set. Polynomial graphs were generated using sixth order to find the best representation of data.

In the medical domain, the gait cycle graphs are drawn for the highest order [41] and according to the domain of statistics, a graph which has the highest R-squared value includes the best fitted curve for data [43] [44]. Hence the generic polynomial graphs for hip, knee and ankle were drawn for the highest order.

5.1.2. Male generic graph generation

Generic minimum and maximum threshold values for knee, hip and ankle joints were derived by analyzing the gait cycle graphs of 12 male subjects who were identified as healthy by a domain specialist. The average value obtained from five gait cycles of each subject was used in the male generic graph. These graphs were generated for both initial and secondary steps taken by a subject's lower limb human skeleton joints. Therefore six generic graphs were derived and they correspond to the generic hip, knee and ankle joint angle value variation of a healthy male.

5.1.2.1. Male hip generic graph generation

By plotting all the average hip gait cycles of the control sample in one context, generic minimum and maximum threshold values were derived. Figure 40 shows the variations of hip gait cycles of the control sample subjects.

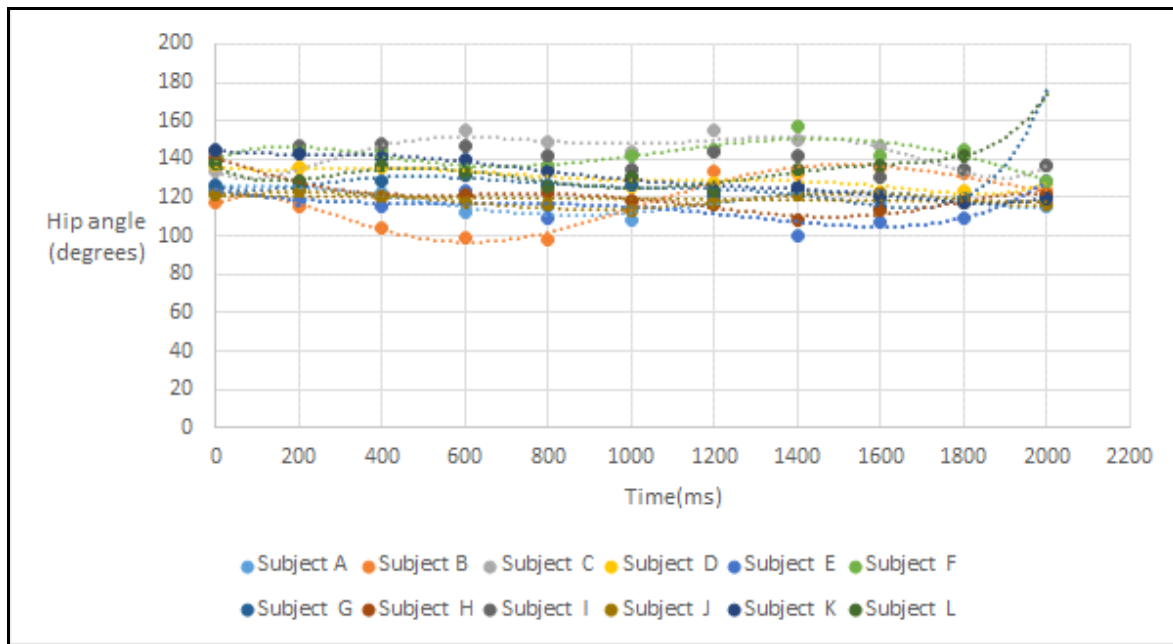


Figure 40 – Generation of generic gait cycle for male hip

By performing further analysis for the generic hip gait cycle graph of the male control sample, minimum and maximum threshold values were derived and a 6th order polynomial graph was generated as represented in Figure 41.

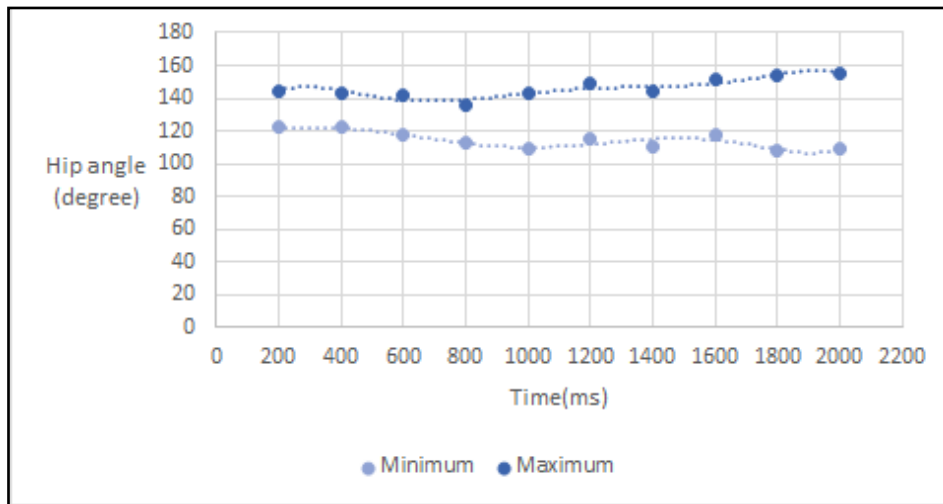


Figure 23 - Generic gait cycle for male hip (initial step)

Equation for the minimum male hip generic of the initial step is as follows.

$$y = 8E-17x^6 - 4E-13x^5 + 1E-09x^4 - 9E-07x^3 + 0.0004x^2 - 0.0771x + 127.43$$

The maximum R-Squared value that has been generated for the 6th order polynomial curve is 0.8412 which is an approximation to 1. Hence it can be concluded that this is the best fitted minimum threshold curve for the male hip generic graph (initial step).

Equation for the maximum male hip generic of the initial step is as follows.

$$y = -1E-16x^6 + 8E-13x^5 - 2E-09x^4 + 3E-06x^3 - 0.0017x^2 + 0.4757x + 98.128$$

The maximum R-Squared value that has been generated for 6th order polynomial curve is 0.8828 which is an approximation to 1. Hence it can be concluded that this is the best fitted maximum threshold curve for the male hip generic graph (initial step).

The same procedure was followed for the secondary step side of the subject and the minimum and maximum male hip generic was derived as represented in Figure 42.

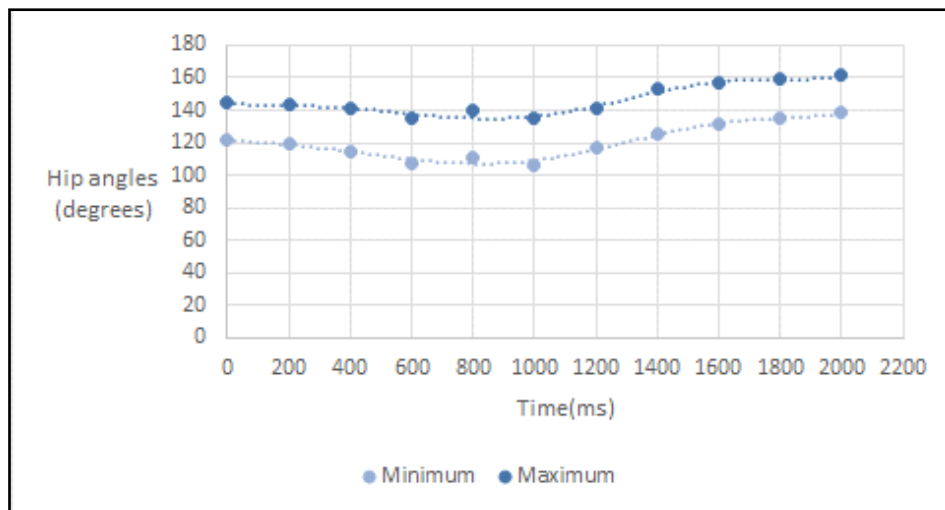


Figure 24 – Generic gait cycle for male hip (secondary step)

Equation for the minimum male hip generic of the initial step is as follows.

$$y = 3E-17x^6 - 2E-13x^5 + 4E-10x^4 - 3E-07x^3 + 8E-05x^2 - 0.0232x + 122.04$$

The maximum R-Squared value that has been generated for 6th order polynomial curve is 0.9699 which is an approximation to 1. Hence it can be concluded that this is the best fitted minimum threshold curve for the male hip generic graph (secondary step).

Equation for the maximum male hip generic of the initial step is as follows.

$$y = 5E-17x^6 - 3E-13x^5 + 6E-10x^4 - 5E-07x^3 + 0.0002x^2 - 0.0324x + 144.99$$

The maximum R-Squared value that has been generated for 6th order polynomial curve is 0.9625 which is an approximation to 1. Hence it can be concluded that this is the best fitted maximum threshold curve for the male hip generic graph (secondary step).

5.1.2.2. Male knee generic graph generation

By plotting all the average knee gait cycles of the control sample in one context, generic minimum and maximum threshold values were derived. Figure 43 shows the variations of knee gait cycles of the control sample subjects.

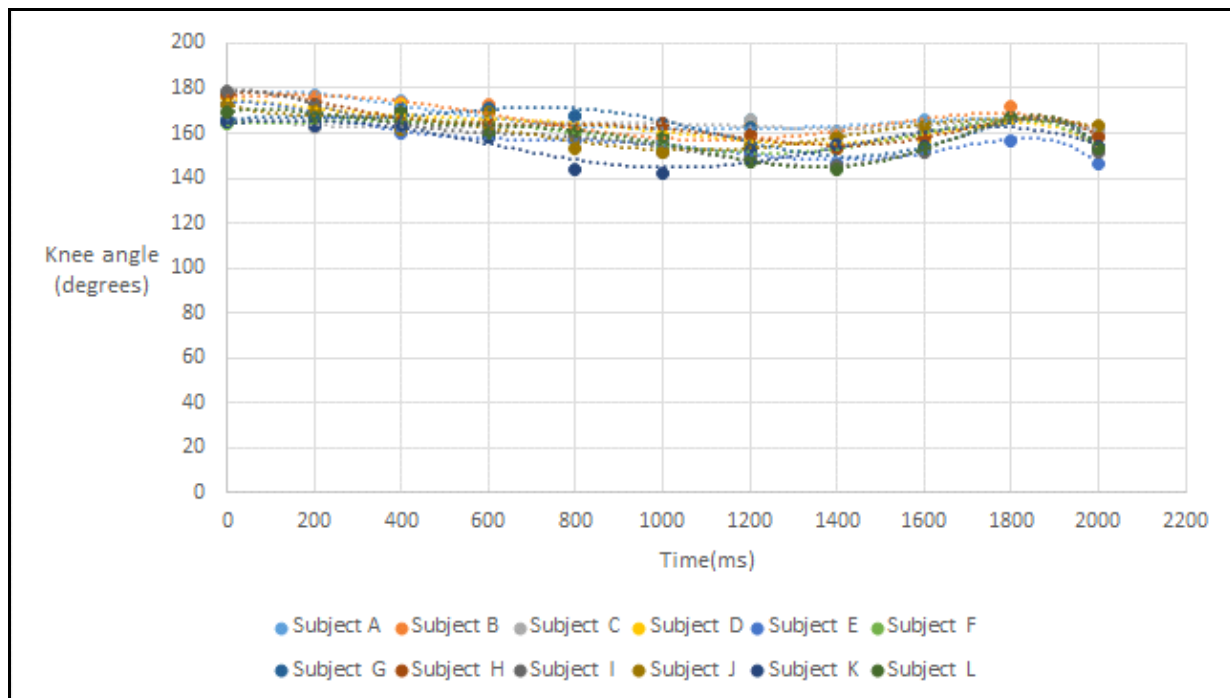


Figure 25 – Generation of generic gait cycle for male knee

By performing further analysis for the generic knee gait cycle graph of the male control sample, minimum and maximum threshold values were derived and a 6th order polynomial graph was generated as represented in Figure 44.

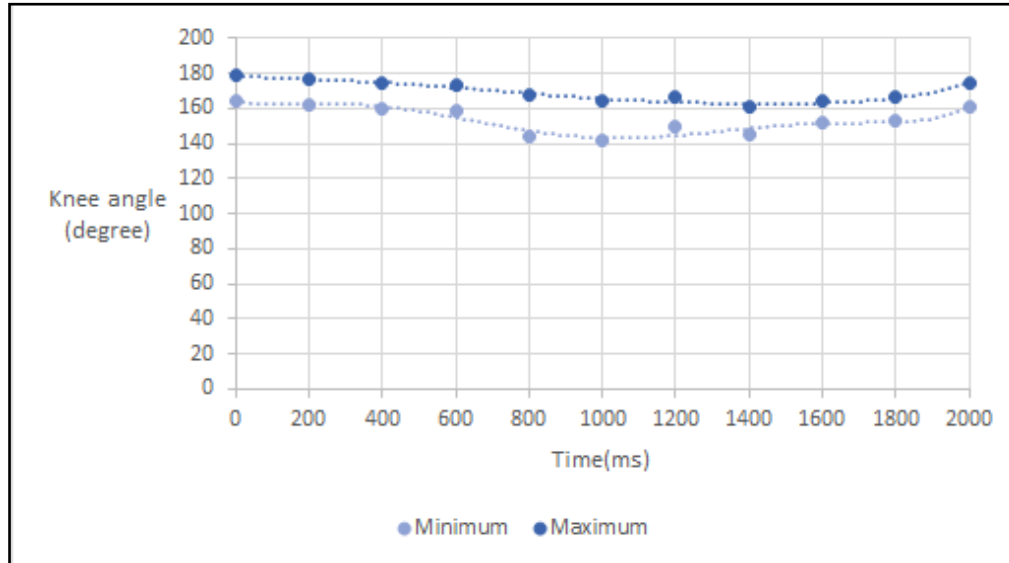


Figure 26 - Generic gait cycle for male knee (initial step)

Equation for the minimum male hip generic of the initial step is as follows.

$$y = 6E-17x^6 - 4E-13x^5 + 8E-10x^4 - 7E-07x^3 + 0.0002x^2 - 0.0315x + 164.2$$

The maximum R-Squared value that has been generated for 6th order polynomial curve is 0.9027 which is an approximation to 1. Hence it can be concluded that this is the best fitted minimum threshold curve for the male knee generic graph (initial step).

Equation for the maximum male hip generic of the initial step is as follows.

$$y = 1E-17x^6 - 6E-14x^5 + 1E-10x^4 - 1E-07x^3 + 5E-05x^2 - 0.015x + 178.83$$

The maximum R-Squared value that has been generated for 6th order polynomial curve is 0.9027 which is an approximation to 1. Hence it can be concluded that this is the best fitted maximum threshold curve for the male knee generic graph (initial step).

The same procedure was followed for the secondary step side of the subject and the minimum and maximum male knee generic was derived as represented in Figure 45.

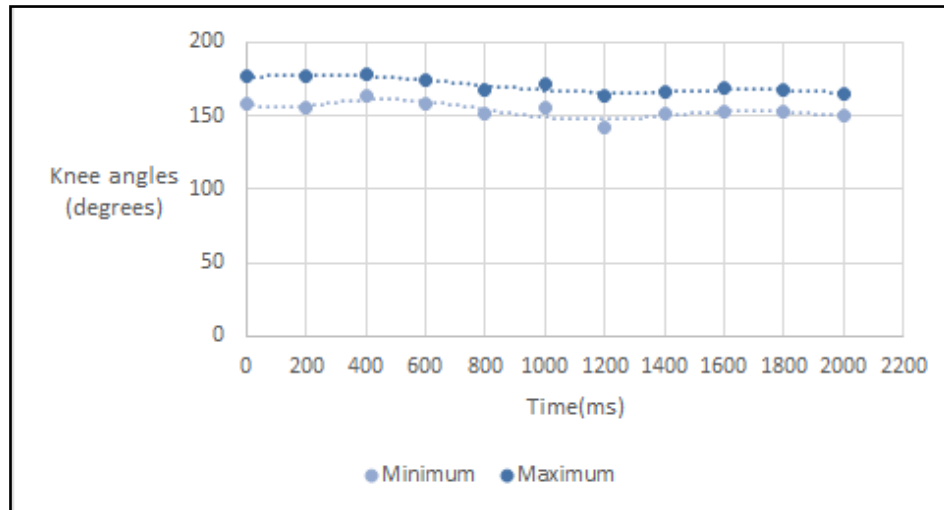


Figure 27 - Generic gait cycle for male knee (secondary step)

Equation for the minimum male hip generic of the initial step is as follows.

$$y = 6E-17x^6 - 4E-13x^5 + 9E-10x^4 - 1E-06x^3 + 0.0004x^2 - 0.0654x + 158.63$$

The maximum R-Squared value that has been generated for 6th order polynomial curve is 0.8874 which is an approximation to 1. Hence it can be concluded that this is the best fitted minimum threshold curve for the male knee generic graph (secondary step).

Equation for the maximum male hip generic of the initial step is as follows.

$$y = 1E-17x^6 - 7E-14x^5 + 2E-10x^4 - 2E-07x^3 + 4E-05x^2 - 0.001x + 177.03$$

The maximum R-Squared value that has been generated for 6th order polynomial curve is 0.8673 which is an approximation to 1. Hence it can be concluded that this is the best fitted maximum threshold curve for the male knee generic graph (secondary step).

5.1.2.3. Male ankle generic graph generation

By plotting all the average ankle gait cycles of the control sample in one context, generic minimum and maximum threshold values were derived. Figure 46 shows the variations of ankle gait cycles of the control sample subjects.

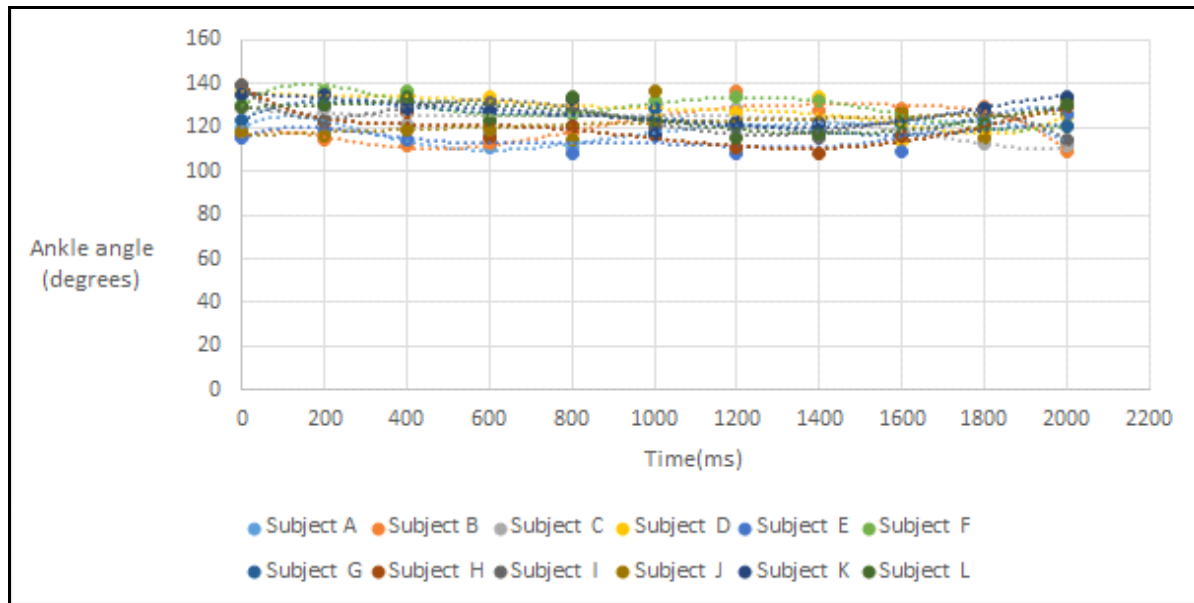


Figure 46 - Generation of generic gait cycle for male ankle

By performing further analysis for the generic ankle gait cycle graph of the male control sample, minimum and maximum threshold values were derived and a 6th order polynomial graph was generated as represented in Figure 47.

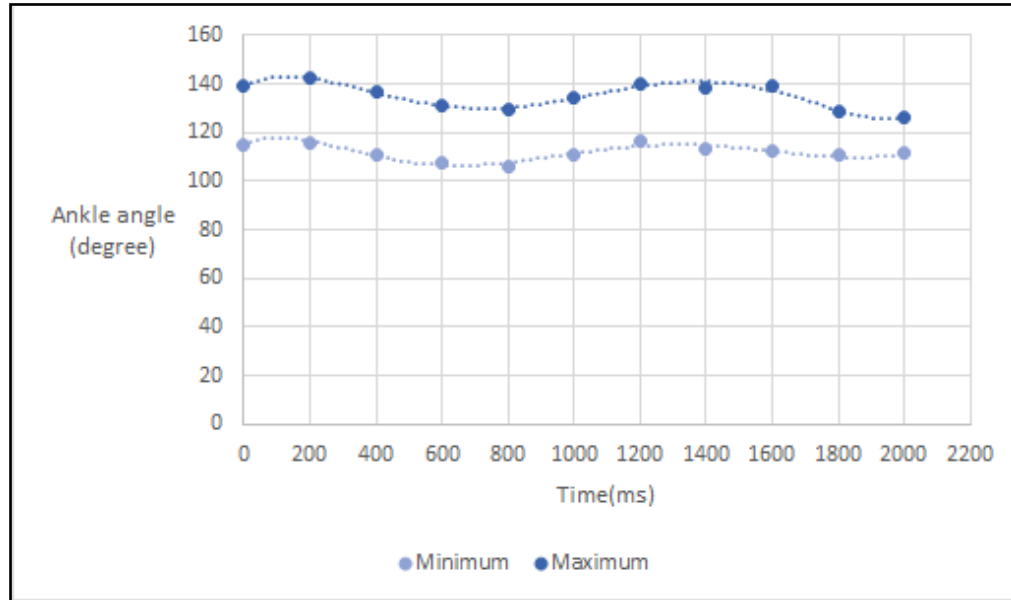


Figure 28 - Generic gait cycle for male ankle (initial step)

Equation for the minimum male hip generic of the initial step is as follows.

$$y = -2E-17x^6 + 2E-13x^5 - 5E-10x^4 + 7E-07x^3 - 0.0004x^2 + 0.0639x + 114.96$$

The maximum R-Squared value that has been generated for 6th order polynomial curve is 0.8979 which is an approximation to 1. Hence it can be concluded that this is the best fitted minimum threshold curve for the male hip generic graph (initial step).

Equation for the maximum male hip generic of the initial step is as follows.

$$y = 1E-17x^6 - 7E-15x^5 - 2E-10x^4 + 4E-07x^3 - 0.0003x^2 + 0.0606x + 139.38$$

The maximum R-Squared value that has been generated for 6th order polynomial curve is 0.9526 which is an approximation to 1. Hence it can be concluded that this is the best fitted maximum threshold curve for the male hip generic graph (initial step).

The same procedure was followed for the secondary step side of the subject and the minimum and maximum male ankle generic was derived as represented in Figure 48.

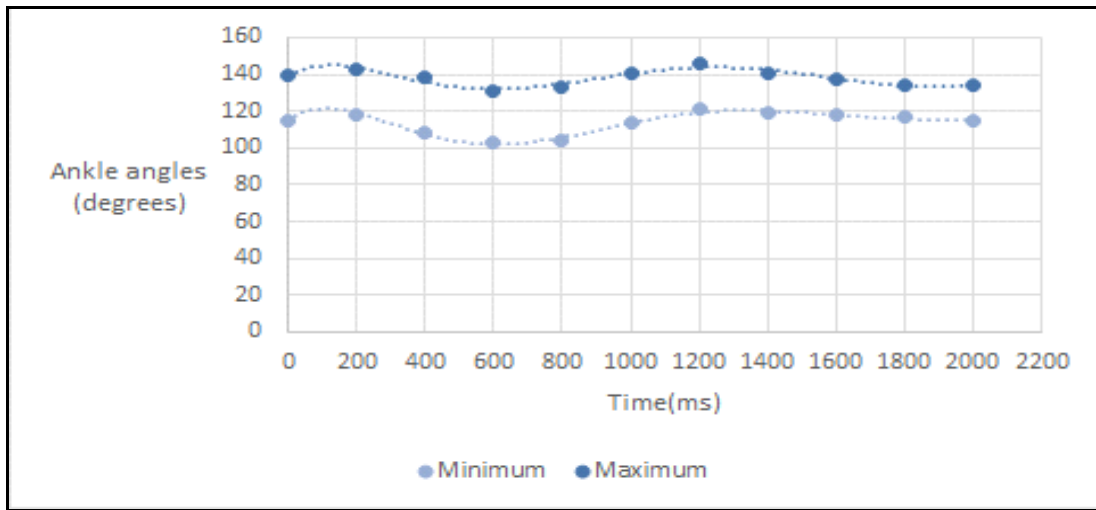


Figure 29 - Generic gait cycle for male ankle (secondary step)

Equation for the minimum male hip generic of the initial step is as follows.

$$y = -7E-17x^6 + 5E-13x^5 - 1E-09x^4 + 2E-06x^3 - 0.0008x^2 + 0.1322x + 114.92$$

The maximum R-Squared value that has been generated for 6th order polynomial curve is 0.9712 which is an approximation to 1. Hence it can be concluded that this is the best fitted minimum threshold curve for the male hip generic graph (secondary step).

Equation for the maximum male hip generic of the initial step is as follows.

$$y = -5E-17x^6 + 3E-13x^5 - 9E-10x^4 + 1E-06x^3 - 0.0006x^2 + 0.1109x + 139.09$$

The maximum R-Squared value that has been generated for 6th order polynomial curve is 0.8835 which is an approximation to 1. Hence it can be concluded that this is the best fitted maximum threshold curve for the male hip generic graph (secondary step).

5.1.3. Female generic graph generation

Generic minimum and maximum threshold values for knee, hip and ankle joints were derived by analyzing the gait cycle graphs of 12 healthy female subjects. The average value obtained from five gait cycles of each subject was used in the female generic graph. These graphs were generated for both initial and secondary steps taken by a subject's lower limb human skeleton joints. Therefore

six generic graphs were derived and they correspond to the generic hip, knee and ankle joint angle value variation of a healthy female.

5.1.3.1. Female hip generic graph generation

By plotting all the average hip gait cycles of the control sample in one context, generic minimum and maximum threshold values were derived. Figure 49 shows the variations of hip gait cycles of the control sample subjects.

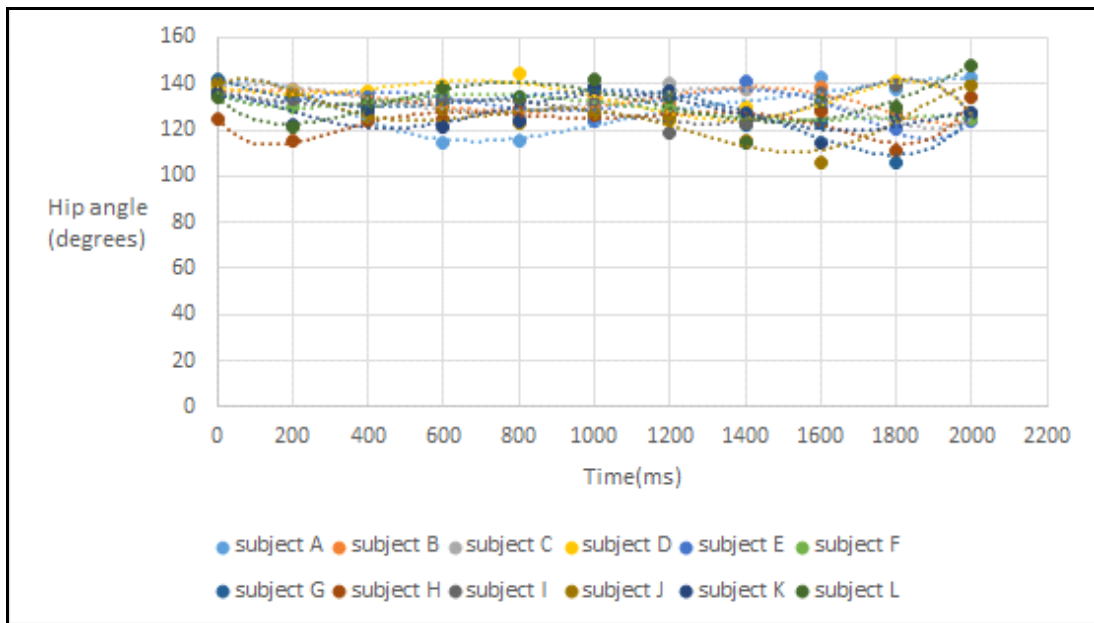


Figure 30 - Generation of generic gait cycle for female hip

By performing further analysis for the generic hip gait cycle graph of the female control sample, minimum and maximum threshold values were derived and a 6th order polynomial graph was generated as represented in Figure 50.

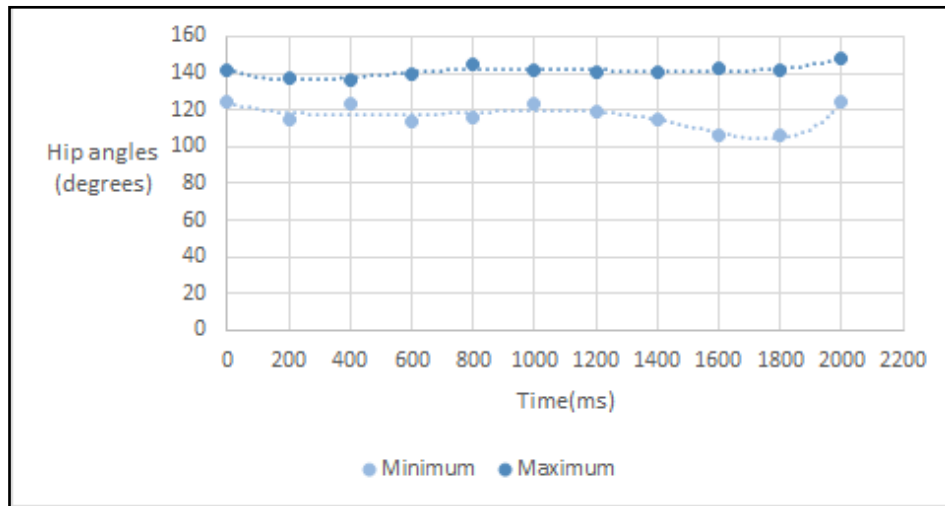


Figure 50 - Generic gait cycle for female hip (initial step)

Equation for the minimum male hip generic of the initial step is as follows.

$$y = 3E-17x^6 - 1E-13x^5 + 2E-10x^4 - 2E-07x^3 + 0.0001x^2 - 0.0443x + 123.8$$

The maximum R-Squared value that has been generated for 6th order polynomial curve is 0.8031 which is an approximation to 1. Hence it can be concluded that this is the best fitted minimum threshold curve for the female hip generic graph (initial step).

Equation for the maximum male hip generic of the initial step is as follows.

$$y = 1E-17x^6 - 7E-14x^5 + 2E-10x^4 - 3E-07x^3 + 0.0002x^2 - 0.0643x + 142.23$$

The maximum R-Squared value that has been generated for 6th order polynomial curve is 0.8421 which is an approximation to 1. Hence it can be concluded that this is the best fitted maximum threshold curve for the female hip generic graph (initial step).

The same procedure was followed for the secondary step side of the subject and the minimum and maximum female hip generic was derived as represented in Figure 51.

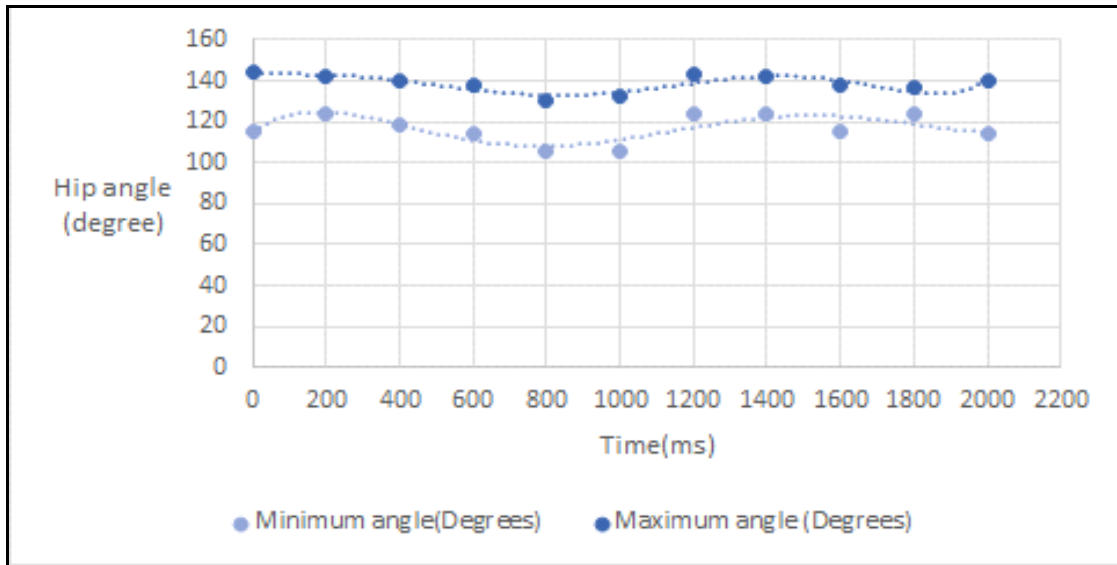


Figure 31 - Generic gait cycle for female hip (secondary step)

Equation for the minimum male hip generic of the initial step is as follows.

$$y = -2E-18x^6 + 7E-14x^5 - 3E-10x^4 + 6E-07x^3 - 0.0005x^2 + 0.1243x + 115.31$$

The maximum R-Squared value that has been generated for 6th order polynomial curve is 0.7083 which is an approximation to 1. Hence it can be concluded that this is the best fitted minimum threshold curve for the female hip generic graph (secondary step).

Equation for the maximum male hip generic of the initial step is as follows.

$$y = 6E-17x^6 - 3E-13x^5 + 5E-10x^4 - 4E-07x^3 + 1E-04x^2 - 0.0147x + 144.28$$

The maximum R-Squared value that has been generated for 6th order polynomial curve is 0.7533 which is an approximation to 1. Hence it can be concluded that this is the best fitted maximum threshold curve for the female hip generic graph (secondary step).

5.1.3.2. Female knee generic graph generation

By plotting all the average knee gait cycles of the control sample in one context, generic minimum and maximum threshold values were derived. Figure 52 shows the variations of knee gait cycles of the control sample subjects.

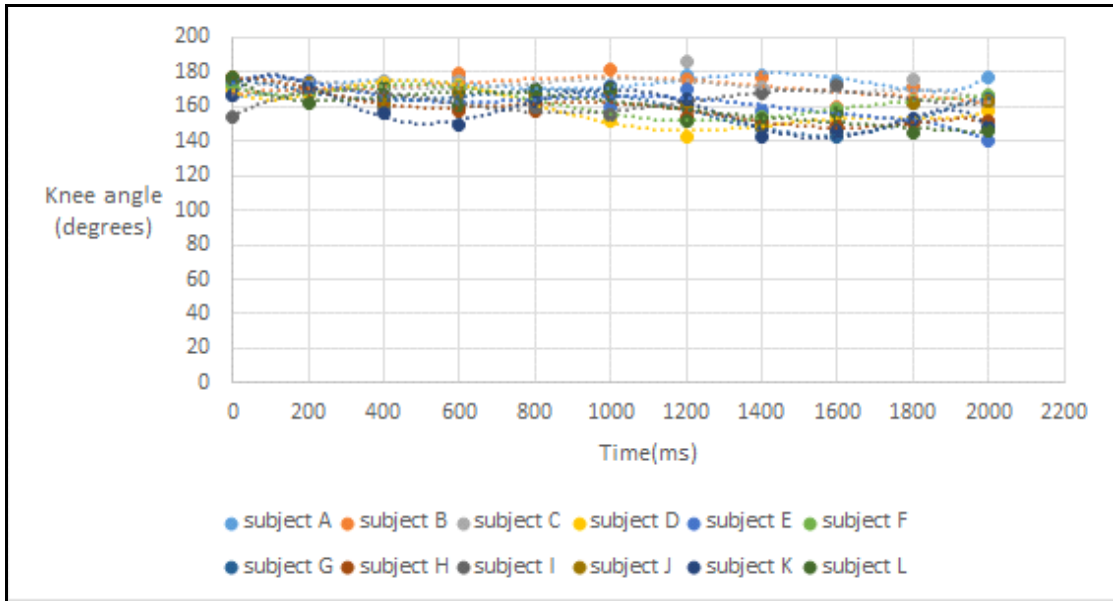


Figure 32 - Generation of generic gait cycle for female knee

By performing further analysis for the generic knee gait cycle graph of the female control sample, minimum and maximum threshold values were derived and a 6th order polynomial graph was generated as represented in Figure 53.

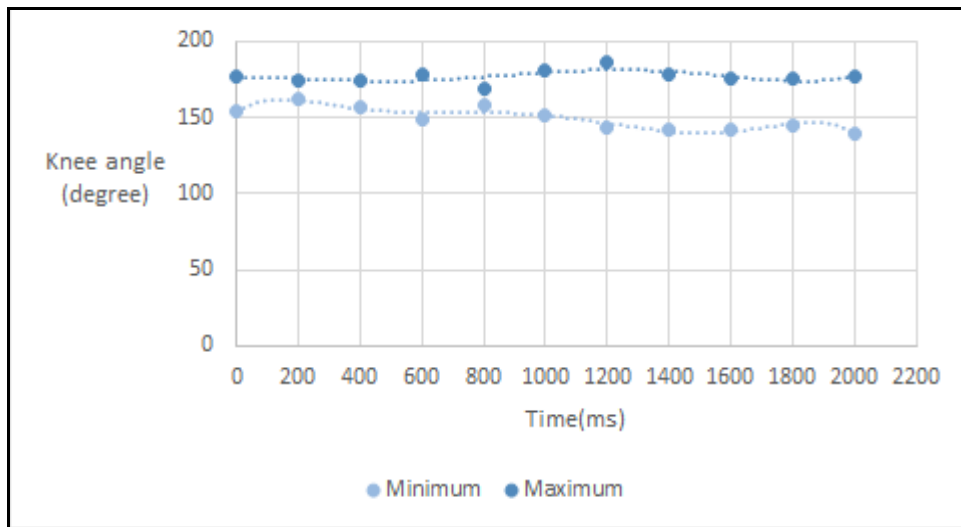


Figure 33 - Generic gait cycle for female knee (initial step)

Equation for the minimum male hip generic of the initial step is as follows.

$$y = -1E-16x^6 + 6E-13x^5 - 1E-09x^4 + 1E-06x^3 - 0.0007x^2 + 0.1325x + 153.83$$

The maximum R-Squared value that has been generated for 6th order polynomial curve is 0.9048

which is an approximation to 1. Hence it can be concluded that this is the best fitted minimum threshold curve for the female knee generic graph (initial step).

Equation for the maximum male hip generic of the initial step is as follows.

$$y = -2E-18x^6 + 4E-14x^5 - 1E-10x^4 + 2E-07x^3 - 9E-05x^2 + 0.0081x + 176.73$$

The maximum R-Squared value that has been generated for 6th order polynomial curve is 0.7521 which is an approximation to 1. Hence it can be concluded that this is the best fitted maximum threshold curve for the female knee generic graph (initial step).

The same procedure was followed for the secondary step side of the subject and the minimum and maximum female hip generic was derived as represented in Figure 54.

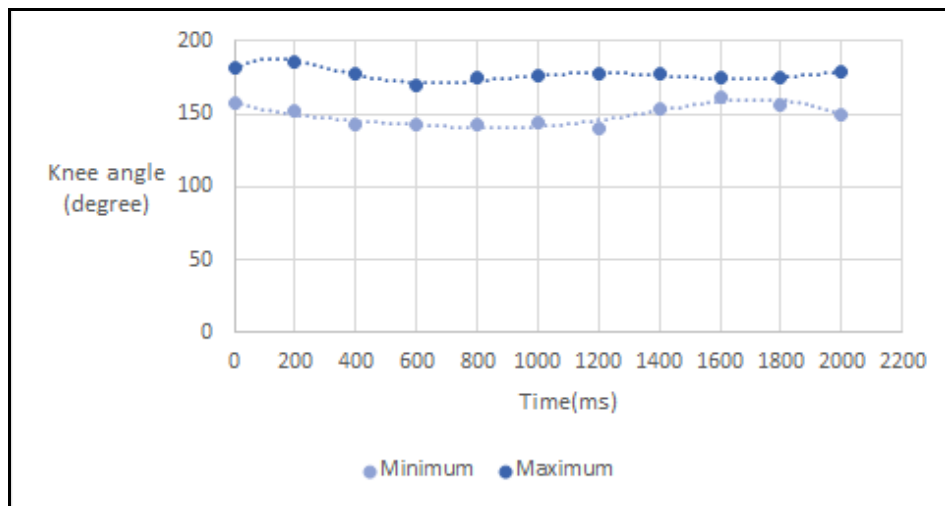


Figure 34 - Generic gait cycle for female knee (secondary step)

Equation for the minimum male hip generic of the initial step is as follows.

$$y = 1E-17x^6 - 1E-13x^5 + 2E-10x^4 - 3E-07x^3 + 0.0002x^2 - 0.0647x + 158.18$$

The maximum R-Squared value that has been generated for 6th order polynomial curve is 0.8607 which is an approximation to 1. Hence it can be concluded that this is the best fitted minimum threshold curve for the female knee generic graph (secondary step).

Equation for the maximum male hip generic of the initial step is as follows.

$$y = -6E-17x^6 + 4E-13x^5 - 1E-09x^4 + 1E-06x^3 - 0.0007x^2 + 0.1227x + 181.14$$

The maximum R-Squared value that has been generated for 6th order polynomial curve is 0.9301

which is an approximation to 1. Hence it can be concluded that this is the best fitted maximum threshold curve for the female knee generic graph (secondary step).

5.1.3.3. Female ankle generic graph generation

By plotting all the average ankle gait cycles of the control sample in one context, generic minimum and maximum threshold values were derived. Figure 55 shows the variations of ankle gait cycles of the control sample subjects.

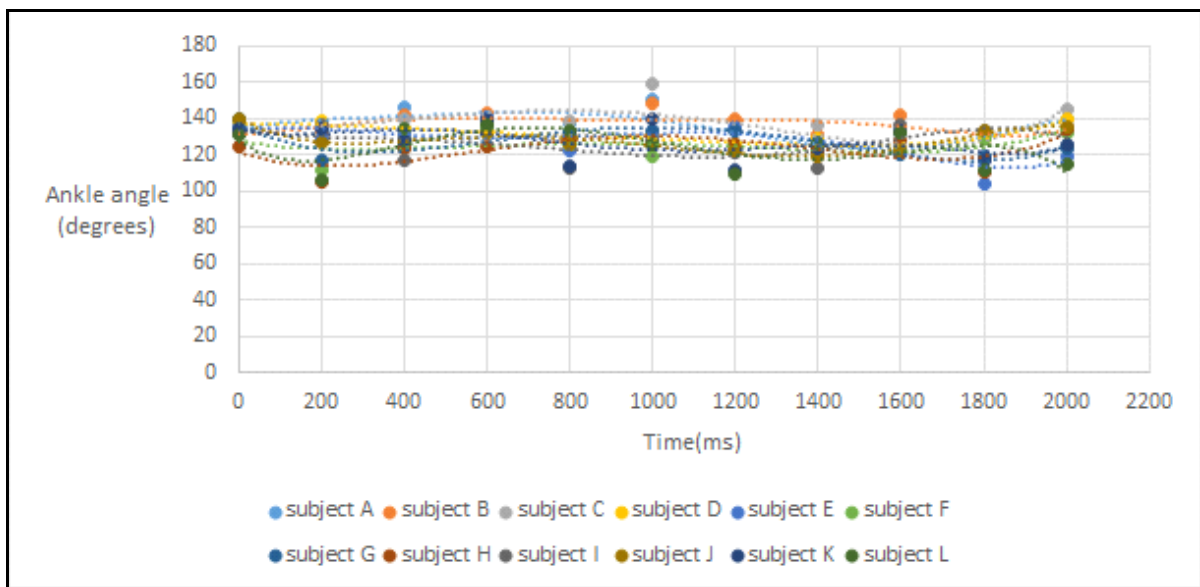


Figure 35 - Generation of generic gait cycle for female ankle

By performing further analysis for the generic ankle gait cycle graph of the female control sample, minimum and maximum threshold values were derived and a 6th order polynomial graph was generated as represented in Figure 56.

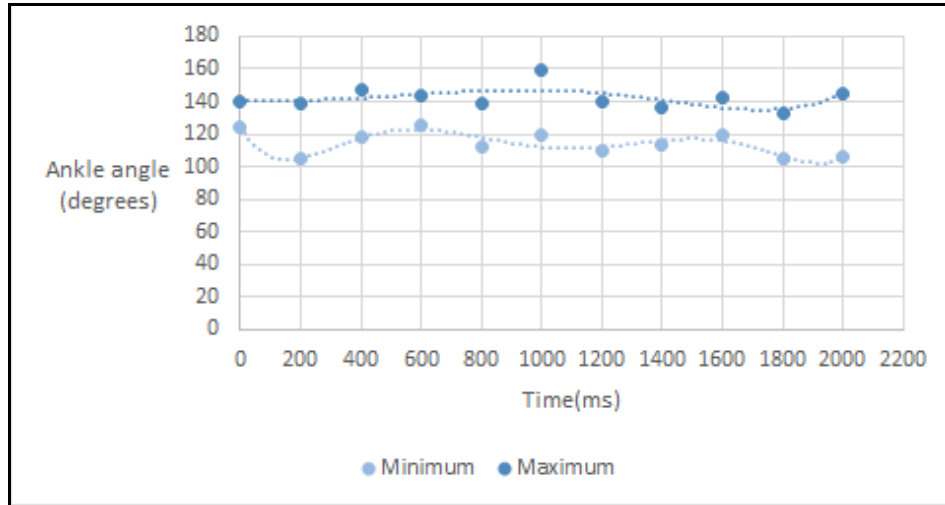


Figure 36 - Generic gait cycle for female ankle (initial step)

Equation for the minimum male hip generic of the initial step is as follows.

$$y = 2E-16x^6 - 1E-12x^5 + 3E-09x^4 - 3E-06x^3 + 0.0016x^2 - 0.3128x + 124.44$$

The maximum R-Squared value that has been generated for 6th order polynomial curve is 0.7808 which is an approximation to 1. Hence it can be concluded that this is the best fitted minimum threshold curve for the female ankle generic graph (initial step).

Equation for the maximum male hip generic of the initial step is as follows.

$$y = -4E-18x^6 + 4E-14x^5 - 1E-10x^4 + 1E-07x^3 - 3E-05x^2 + 0.0064x + 140$$

The maximum R-Squared value that has been generated for 6th order polynomial curve is 0.8068 which is an approximation to 1. Hence it can be concluded that this is the best fitted maximum threshold curve for the female ankle generic graph (initial step).

The same procedure was followed for the secondary step side of the subject and the minimum and maximum male ankle generic was derived as represented in Figure 57.

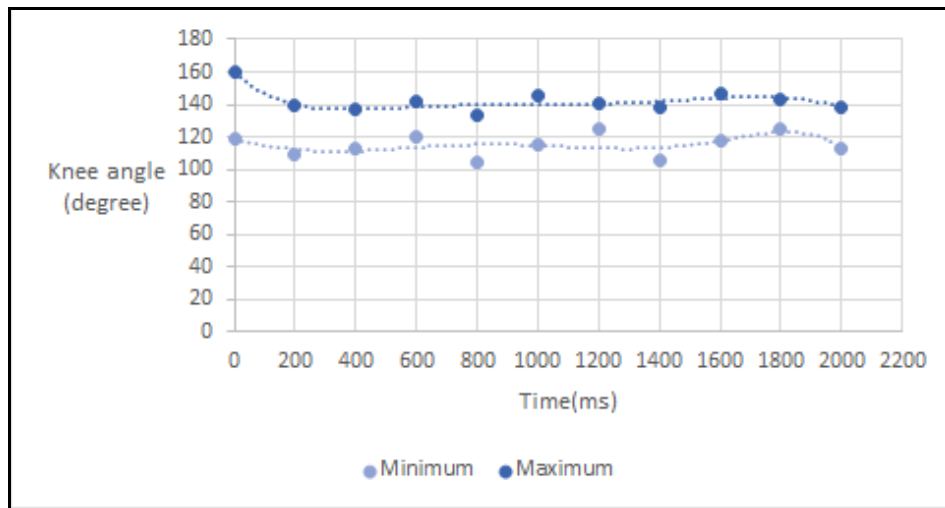


Figure 37 - Generic gait cycle for female ankle (secondary step)

Equation for the maximum male hip generic of the initial step is as follows.

$$y = -4E-17x^6 + 2E-13x^5 - 3E-10x^4 + 2E-07x^3 + 3E-05x^2 - 0.0412x + 118.44$$

The maximum R-Squared value that has been generated for 6th order polynomial curve is 0.7403 which is an approximation to 1. Hence it can be concluded that this is the best fitted minimum threshold curve for the female ankle generic graph (secondary step).

Equation for the maximum male hip generic of the initial step is as follows.

$$y = 1E-17x^6 - 1E-13x^5 + 4E-10x^4 - 6E-07x^3 + 0.0005x^2 - 0.1733x + 159.77$$

The maximum R-Squared value that has been generated for 6th order polynomial curve is 0.8844 which is an approximation to 1. Hence it can be concluded that this is the best fitted maximum threshold curve for the female ankle generic graph (secondary step).

5.2. Quantitative evaluation

5.2.1. Data evaluation of healthy subjects

Followed by performing a graph comparison for the test sample of the study, a quantitative conclusion was derived. 18 subjects were used in this research as the test sample. 10 subjects were identified as balanced (healthy) by the proposed mechanism. The status of the subject and the position of imbalance were identified by evaluating the data points of the joint angles as described in the Design

and methodology chapter. If the gait cycle of the test subject does not lie in between the minimum and maximum threshold values defined, the subject is considered as an imbalanced subject.

There are three techniques to measure the deviation of the test sample graphs from the two generic graphs. In statistics there are several methods to calculate error propagation and ‘averages’ is one of them. In the average method, root mean square and relative error is used to calculate the error in a graph. Among the three methods, root mean square (RMS) measure was used in this research to calculate the quantitative measure of the imbalance of a subject. The imbalance is quantified relative to the minimum and maximum threshold values defined. If the average error method is used and a negative value is identified in the curve, it effects the final outcome of the error value. Quantitative deviation relative to minimum and maximum threshold values can be measured using RMS method without an opening for such errors. RMS method is more suitable for this research since it needs to calculate the error only for the data points that lie out of the defined boundary values.

The root mean square is calculated using the following equation.

$$\sqrt{\frac{1}{n} \left\{ \frac{[(A1 - A')^2 + (A1 - A'')^2]}{2} + \frac{[(A2 - A2')^2 + (A2 - A2'')^2]}{2} \dots \frac{[(An - A2')^2 + (An - A2'')^2]}{2} \right\}}$$

A1, A2, ... An - Test subject angle values

A1', A2', An' - Minimum threshold value of the particular joint

A1'', A2'', An'' - Maximum threshold value of the particular joint

n - Number of joints that are out of threshold values

The average squared value of each point relative to minimum and maximum threshold values are summed and the mean value for all the error values is taken. The square root of the error value is then calculated and measured as the quantitative error value.

By comparing with minimum and maximum generics, the healthy sample could satisfy the constraint defined by their motion of data points along the gait cycle lying in between the defined values. This results show the evaluation of 10 subjects, both male and female who were selected under

the supervision of physiotherapists. According to the results of quantitative evaluation of the test sample, 11 subjects were identified as healthy subjects (one imbalanced subject was identified as healthy). The following graphs (Figure 58 – Figure 60) were drawn using Microsoft excel 2013 version to perform a comparison between the six generic graphs (hip_right, knee_right, ankle_right, hip_left, knee_left and ankle_left) and the six graphs generated for a subject using the captured joint position values. Sample hip, knee and ankle gait cycle graphs compared with the minimum and maximum thresholds of joints for both male and female healthy subjects are represented below from Figure 58 – Figure 60.

Figure 58 represents the hip gait cycle graph for Subject 2. The hip gait cycle lies in between the defined minimum and maximum generic values. Therefore subject 2 can be defined as a subject whose hip is balanced.

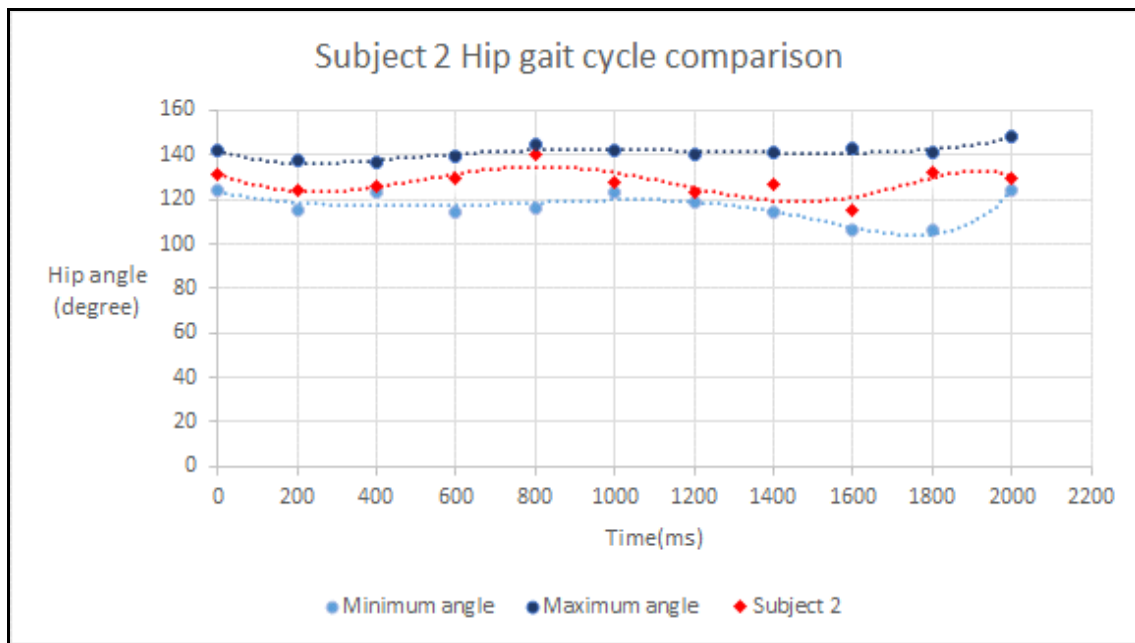


Figure 38 - Hip gait cycle graph of subject 2

Figure 59 represents the knee gait cycle graph for Subject 2. The knee gait cycle lies in between the defined minimum and maximum generic values. Therefore subject 2 can be defined as a subject whose knee is balanced.

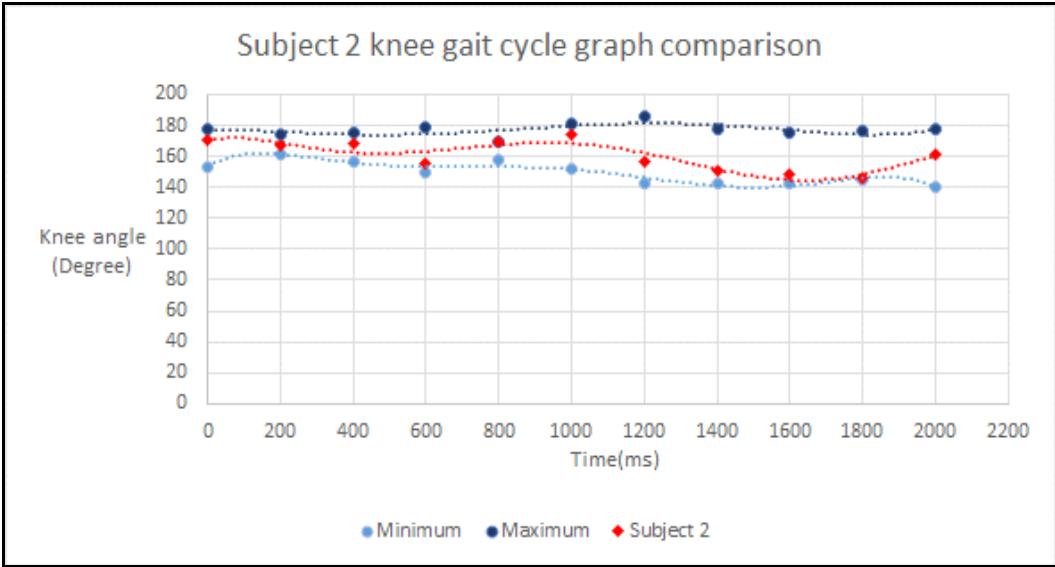


Figure 39 - Knee gait cycle graph of subject 2

Figure 60 represents the ankle gait cycle graph for Subject 2. The ankle gait cycle lies in between the defined minimum and maximum generic values. Therefore subject 2 can be defined as a subject whose ankle is balanced.

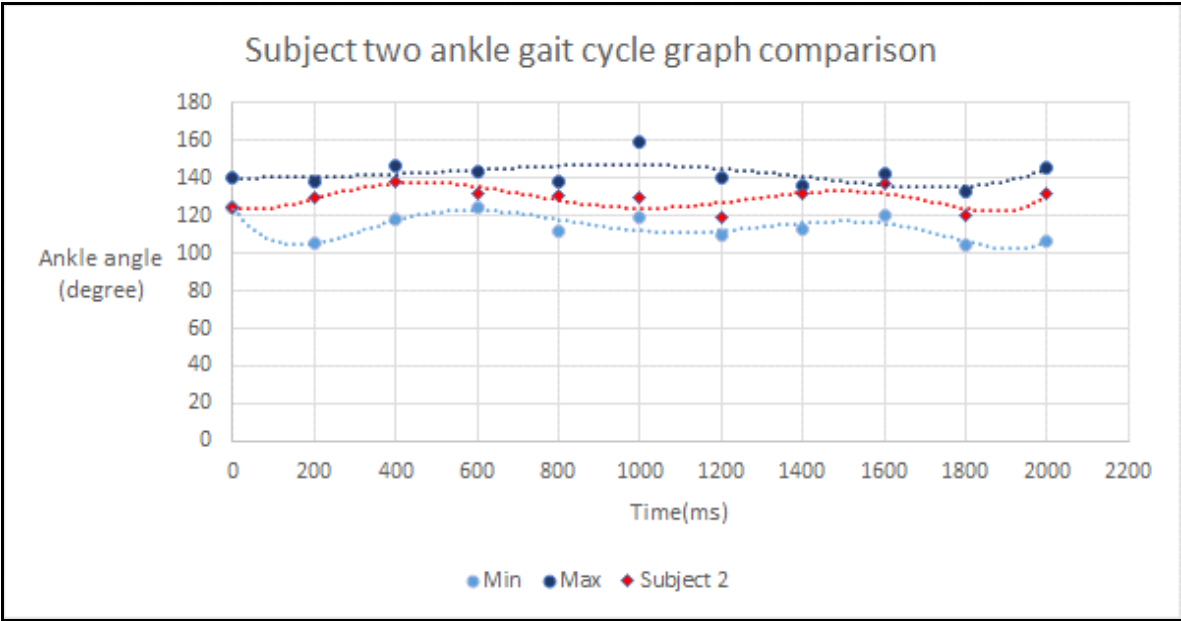


Figure 60 - Ankle gait cycle graph of subject 2

Considering all three gait cycle graphs of Subject 2, a conclusion can be derived as Subject 2 is a balanced person (taking lower limb as the only consideration).

5.2.2. Data evaluation of imbalanced subjects

By comparing with minimum and maximum generics, the imbalanced sample could not satisfy the constraint defined. Constraints were violated by surpassing and varying from the generic minimum and maximum threshold values defined for the joints. Evaluation was done using Microsoft excel 2013 by performing a comparison between the six generic graphs (hip_right, knee_right, ankle_right, hip_left, knee_left and ankle_left) and the six graphs generated for the gait cycles of a subject.

For each imbalanced gait cycle graph the RMS value was calculated in quantitative evaluation to give a numeric identification for the status of the skeletal system of a subject. This value can be used to define the severity of the imbalance of a subject. The evaluation results can be concluded under three main categories; results of hip imbalance, results of knee imbalance and results of ankle imbalance.

5.2.2.1. Hip gait cycle graph of imbalanced subjects

Figure 61 shows the imbalanced hip gait cycle graph of Subject 10 for the initial step side. Subject 10 was considered as a hip imbalanced individual since the subject's hip gait cycle graph lies beyond the threshold minimum value and the shape of the graph differs from the generic hip gait cycle graph. The Root Mean Square value of this graph is 21.6469.

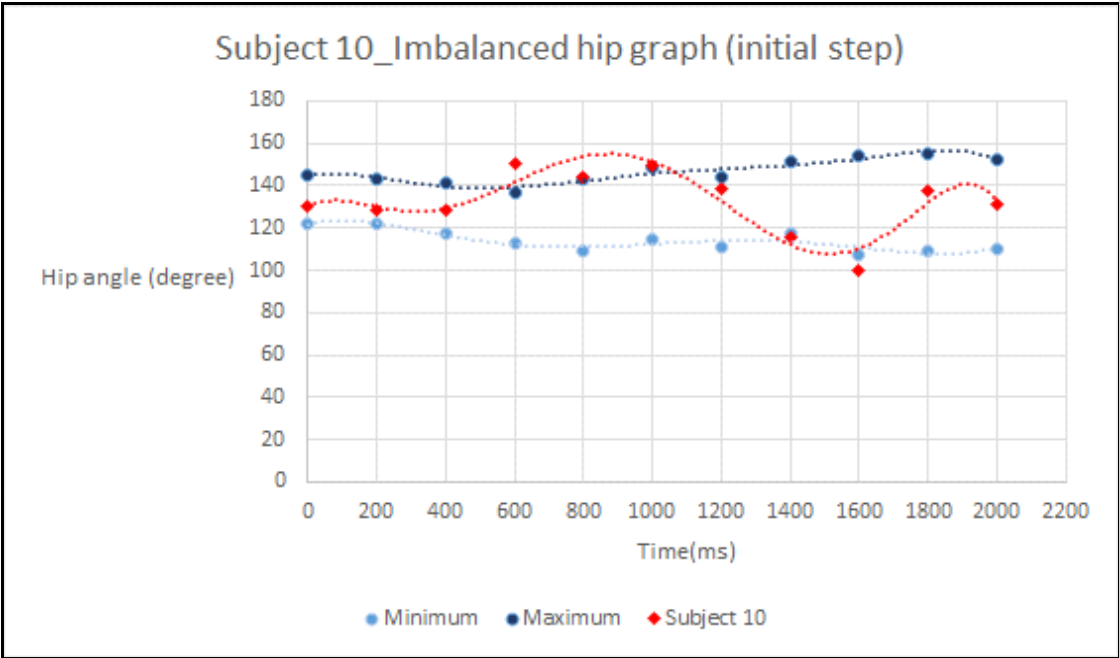


Figure 40 - Imbalanced hip graph of subject 10 (initial step)

The same subject holds an imbalance in the other side of the hip as shown in Figure 62. This hip gait cycle graph also lies beyond maximum threshold of hip generic and it can be concluded that Subject 10 holds an imbalance in both the hips. The RMS value of this graph is 14.090395.

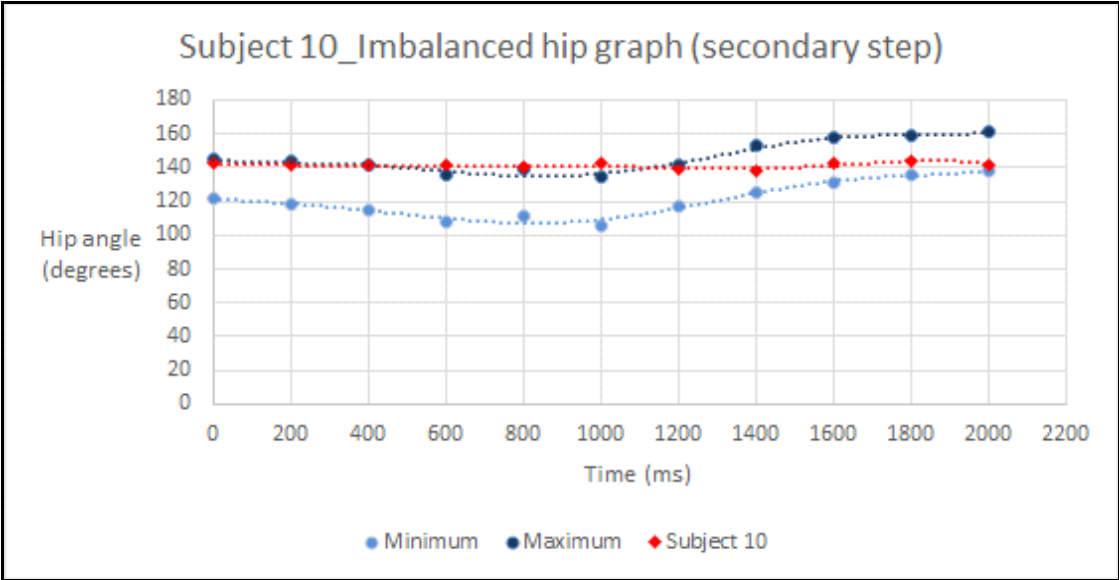


Figure 41 - Imbalanced hip graph of subject 10 (secondary step)

As shown in Figure 63, hip gait cycle graph of Subject 14 is deviated from the generic graph and its first five phases lie beyond the minimum threshold value. The RMS error is 15.53615.

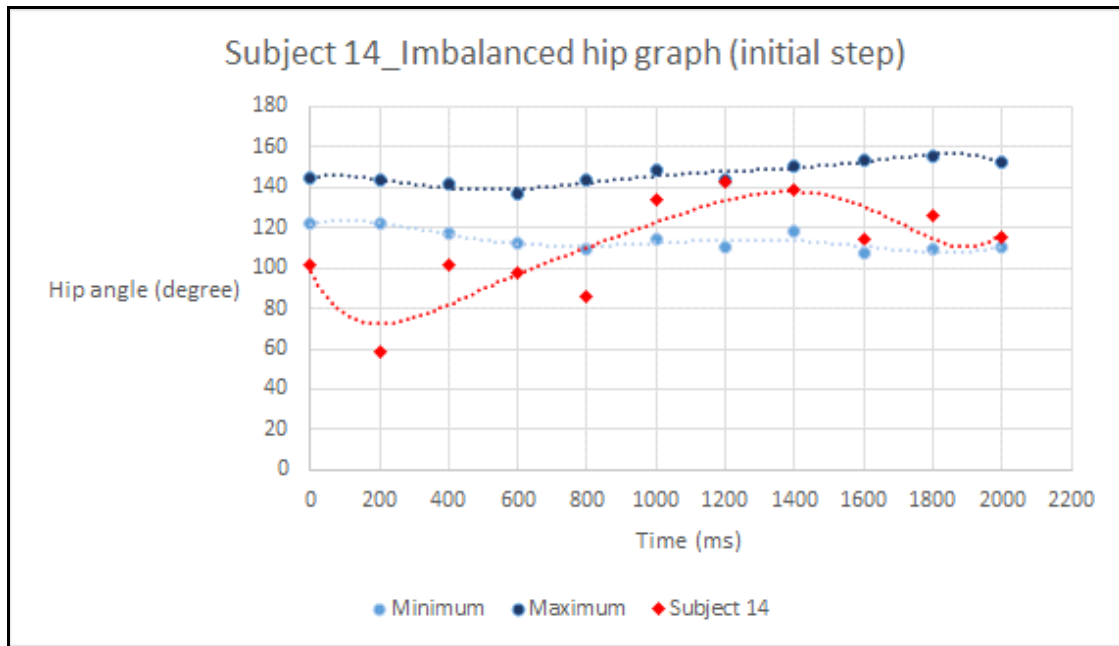


Figure 42 - Imbalanced hip graph of subject 14 (initial step)

The hip gait cycle graph of secondary step side of Subject 14 lies beyond the maximum threshold values as shown in Figure 64. The RMS value for the graph is 25.4224 hence it can be concluded that Subject 14 has an imbalance in both the hip joints.

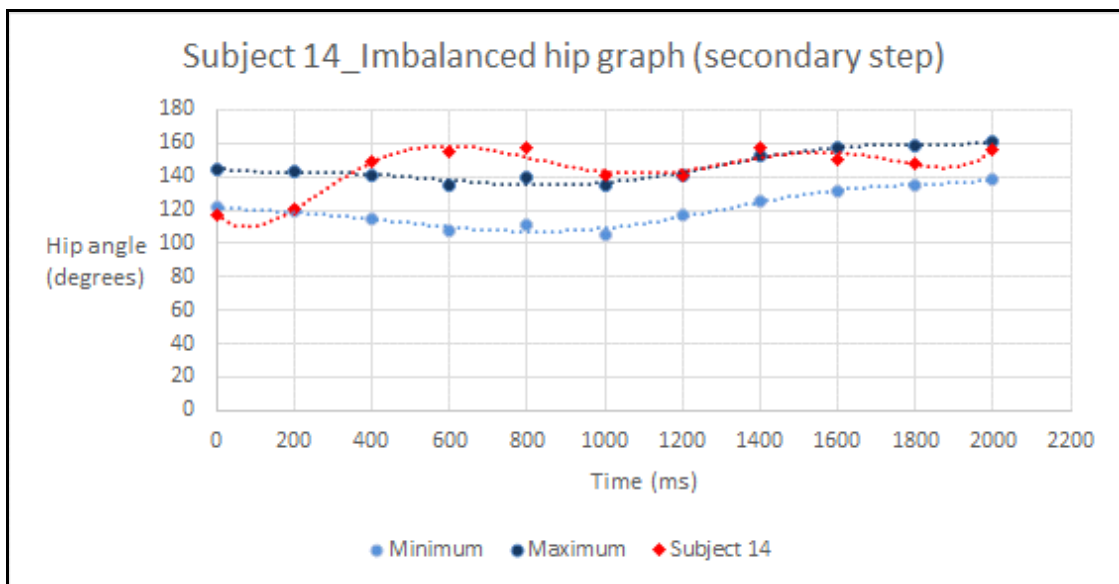


Figure 43 - Imbalanced hip graph of subject 14 (secondary step)

The hip gait cycle graph of Subject 15 lies beyond the maximum hip generic graph as shown in Figure 65. The RMS value of the hip gait cycle of Subject 15 is 28.3384 hence it can be concluded that Subject 15 has an imbalance in the hip.

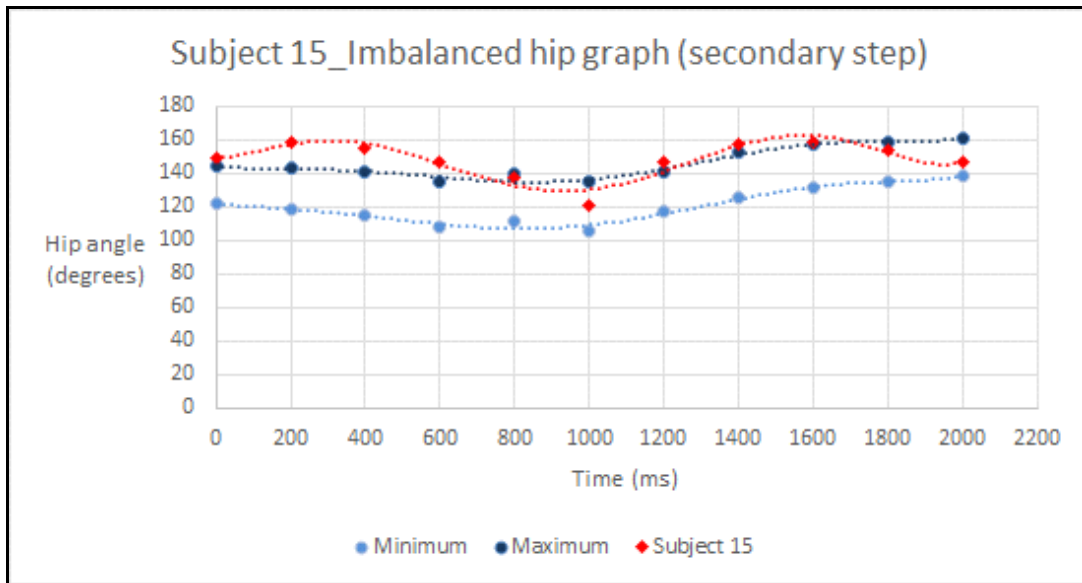


Figure 44 - Imbalanced hip graph of subject 15 (secondary step)

As shown in Figure 66, hip gait cycle of Subject 18 lies beyond the maximum threshold value and it can be concluded that Subject 18 holds an imbalance in the hip. The RMS error is 15.676.

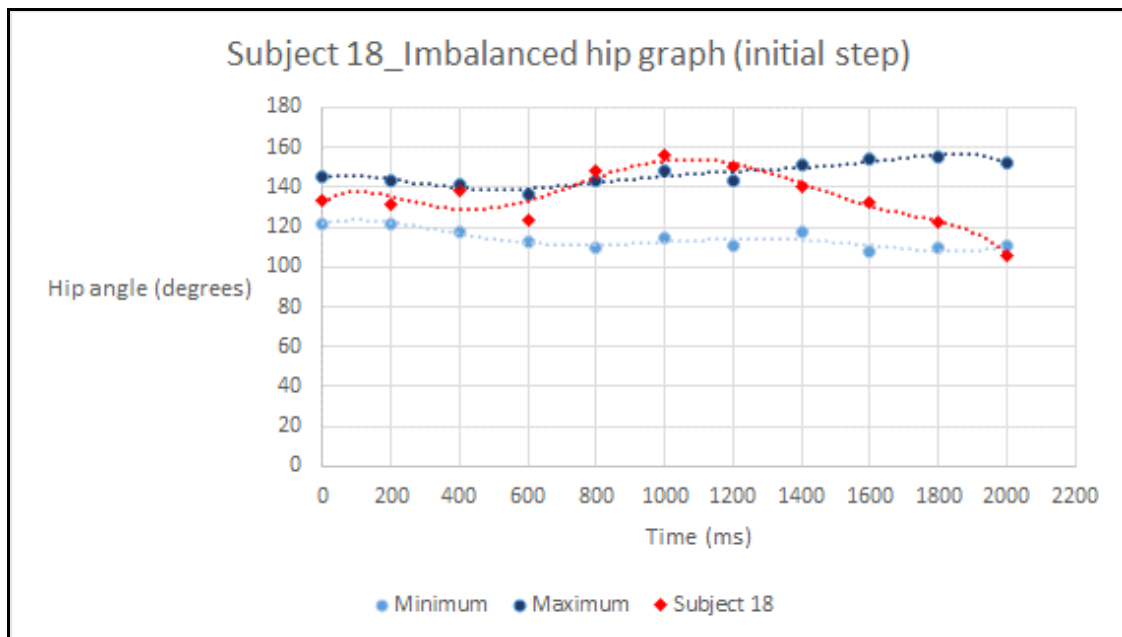


Figure 45 - Imbalanced hip graph of subject 18 (initial step)

5.2.2.2. Knee gait cycle graph of imbalanced subjects

Figure 67 shows the imbalanced knee gait cycle graph of Subject 14 for the secondary step side. Subject 14 was considered as a knee imbalanced individual since the subject's knee gait cycle graph lies lower than the minimum threshold value and the shape of the graph differs from the generic knee gait cycle graph. The Root Mean Square value of this graph is 19.36628.

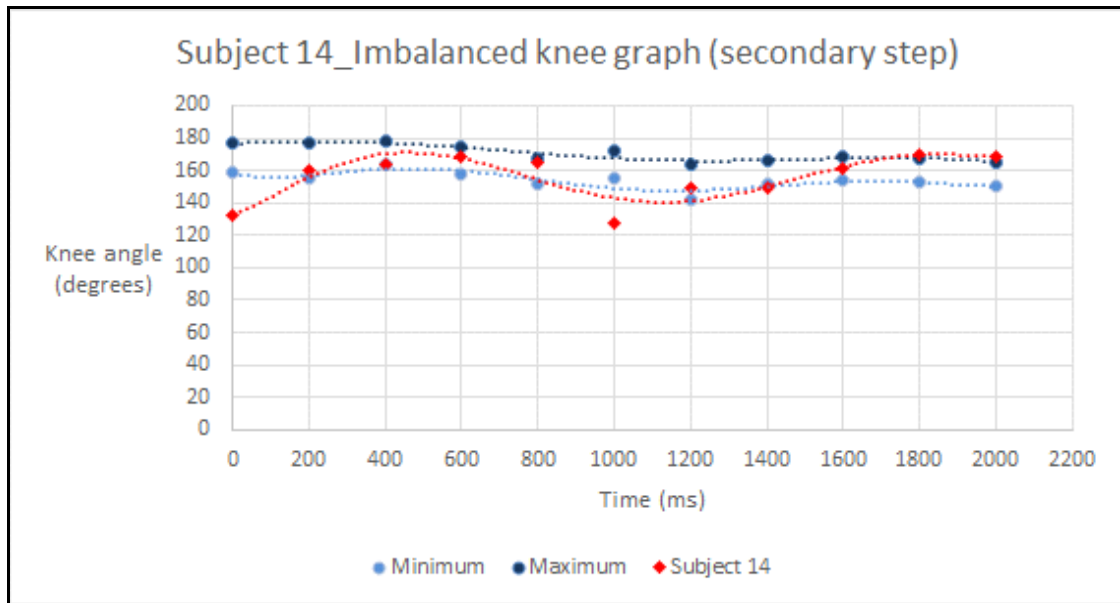


Figure 46 - Imbalanced knee graph of subject 14 (secondary step)

Figure 68 shows the imbalanced knee gait cycle graph of Subject 17 for the secondary step side. Subject 17 was considered as knee imbalanced individual since the subject's knee gait cycle graph lies outside the minimum and maximum threshold values and the shape of the graph differs from the generic knee gait cycle graph. The Root Mean Square value of this graph is 7.60127.

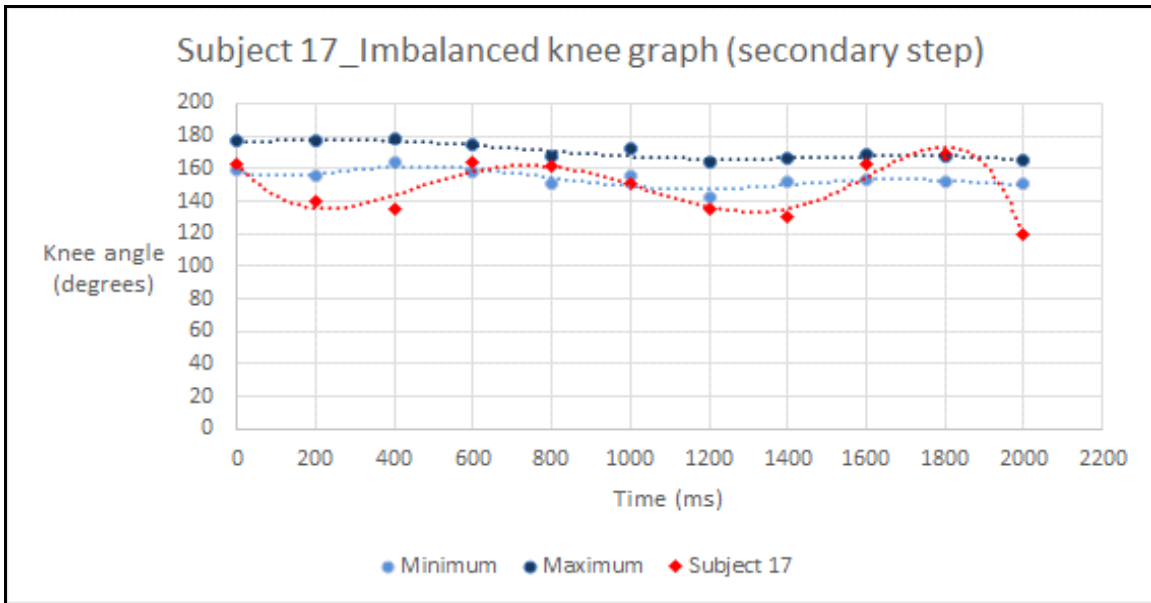


Figure 47 - Imbalanced knee graph of subject 17 (secondary step)

Figure 69 shows the imbalanced knee gait cycle graph of Subject 18 for the initial step side. Subject 17 was considered as knee imbalanced individual since the subject’s knee gait cycle graph lies outside the minimum and maximum threshold values and the shape of the graph differs from the generic knee gait cycle graph. The Root Mean Square value of this graph is 11.6308.

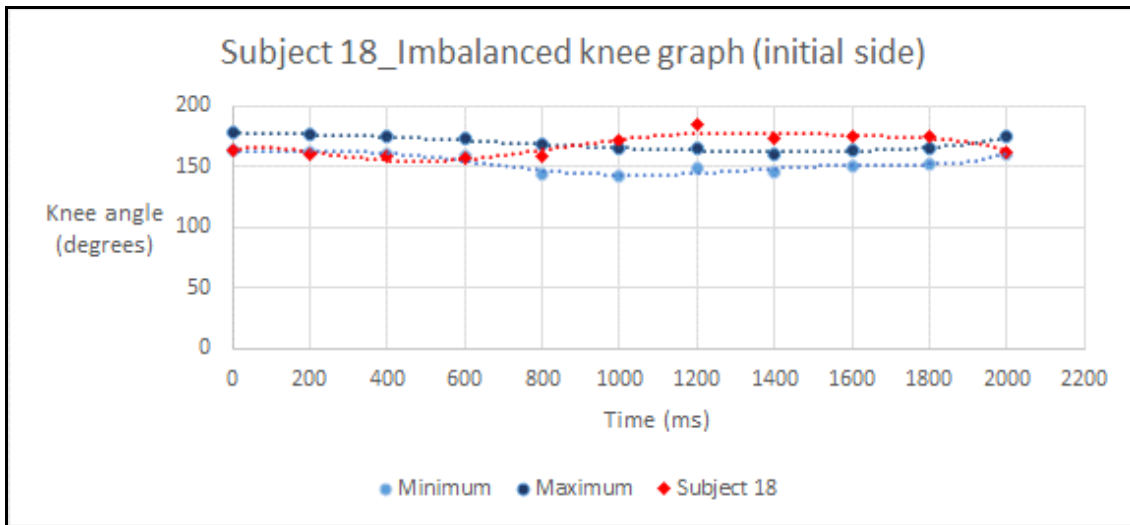


Figure 48 - Imbalanced knee graph of subject 18 (initial step)

5.2.2.3. Ankle gait cycle graph of imbalanced subjects

Figure 70 shows the imbalanced ankle gait cycle graph of Subject 11 for the initial step side. Subject 11 was considered as ankle imbalanced individual since the subject's ankle gait cycle graph lies outside the minimum and maximum threshold values and the shape of the graph differs from the generic ankle gait cycle graph. The Root Mean Square value of this graph is 14.3059.

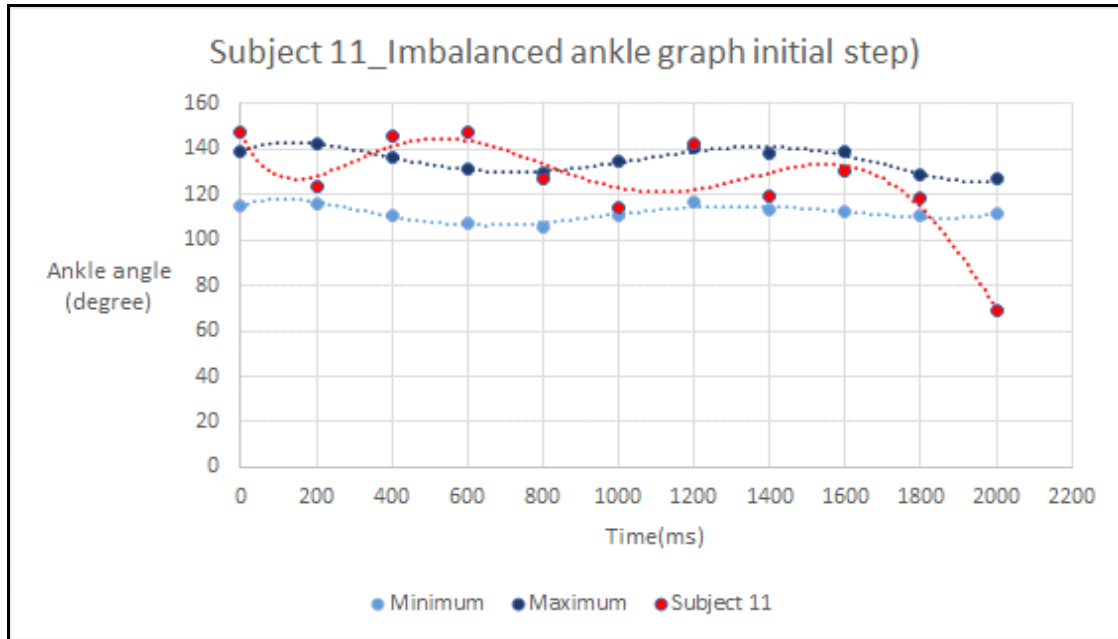


Figure 70 - Imbalanced ankle graph of subject 11 (initial step)

Figure 71 shows the imbalanced ankle gait cycle graph of Subject 11 for the secondary step side. Subject 11 was considered as ankle imbalanced individual since the subject's ankle gait cycle graph lies outside the minimum and maximum threshold values and the shape of the graph differs from the generic ankle gait cycle graph. The Root Mean Square value of this graph is 19.2894.

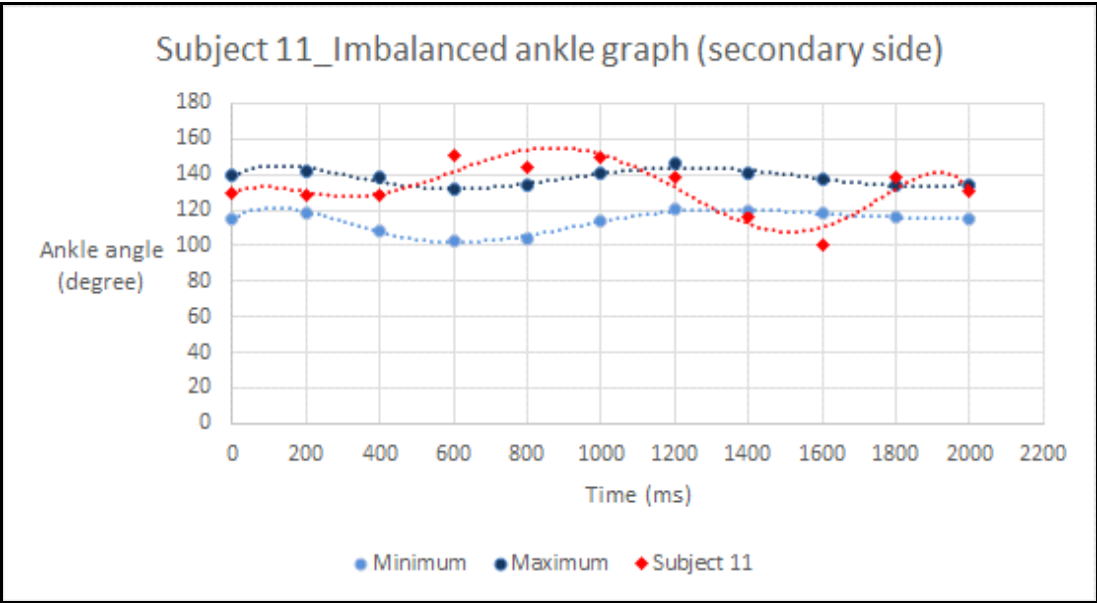


Figure 49 - Imbalanced ankle graph of subject 11 (secondary step)

Figure 72 shows the imbalanced ankle gait cycle graph of Subject 12 for the initial step side. Subject 12 was considered as ankle imbalanced individual since the subject’s ankle gait cycle graph lies far from the minimum threshold values. The Root Mean Square value of this graph is 47.69296.

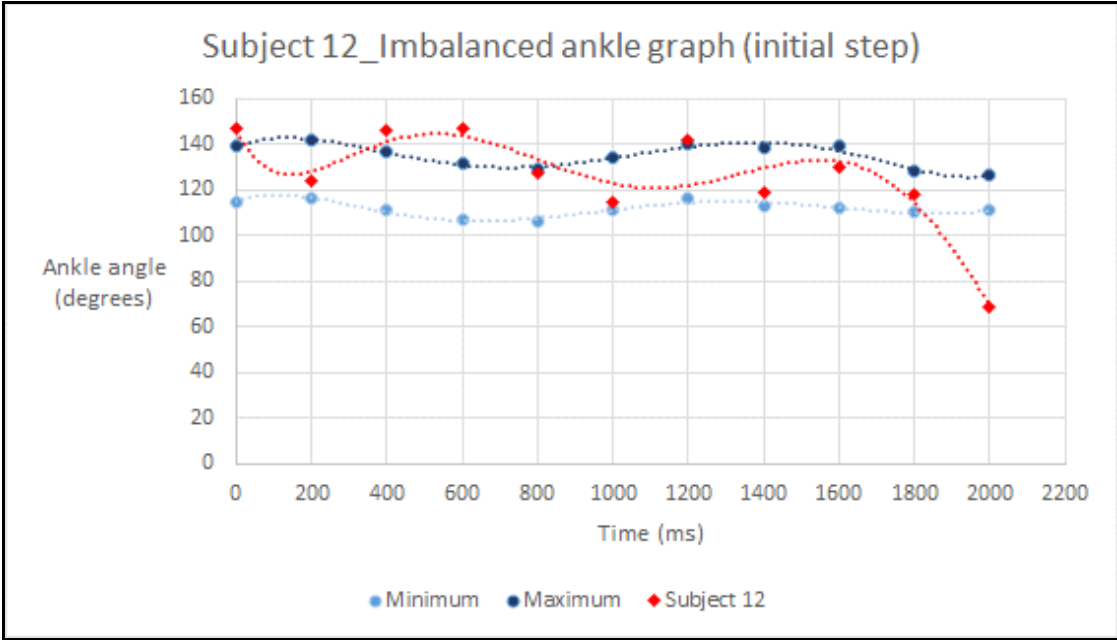


Figure 50 - Imbalanced ankle graph of subject 12 (initial step)

Figure 73 shows the imbalanced ankle gait cycle graph of Subject 12 for the secondary step side. Subject 12 was considered as ankle imbalanced individual since the subject's ankle gait cycle graph lies outside the minimum and maximum threshold values and the shape of the graph differs from the generic ankle gait cycle graph. The Root Mean Square value of this graph is 19.627.

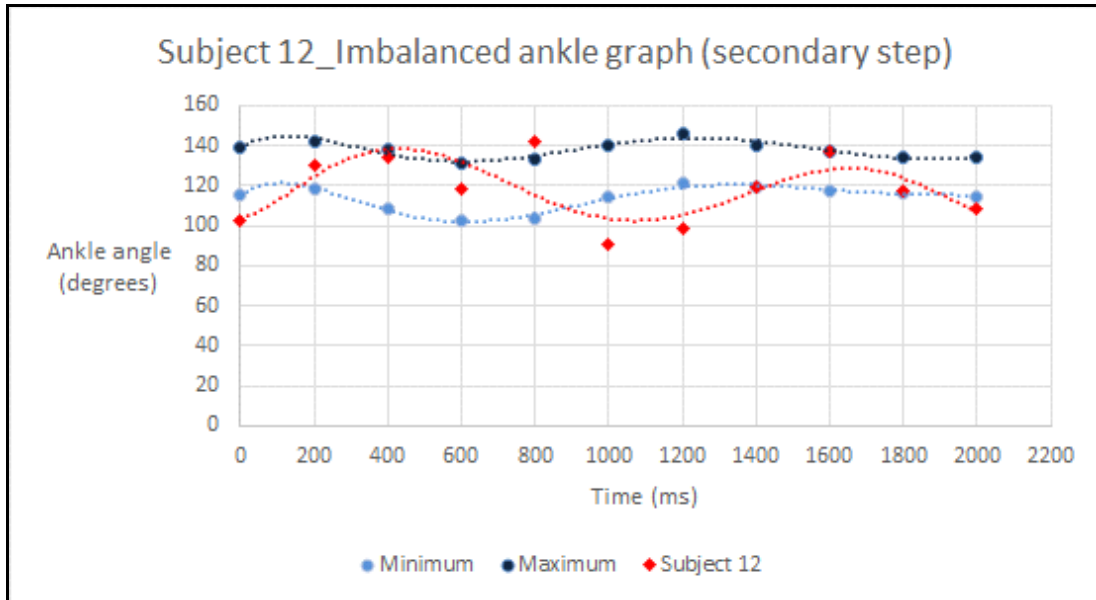


Figure 51 - Imbalanced ankle graph of subject 11 (secondary step)

Figure 74 shows the imbalanced ankle gait cycle graph of Subject 14 for the initial step side. Subject 14 was considered as ankle imbalanced individual although the ankle cycle takes the shape of the generic cycle since the subject's ankle gait cycle graph lies outside the minimum and maximum threshold values. The Root Mean Square value of this graph is 16.8527.

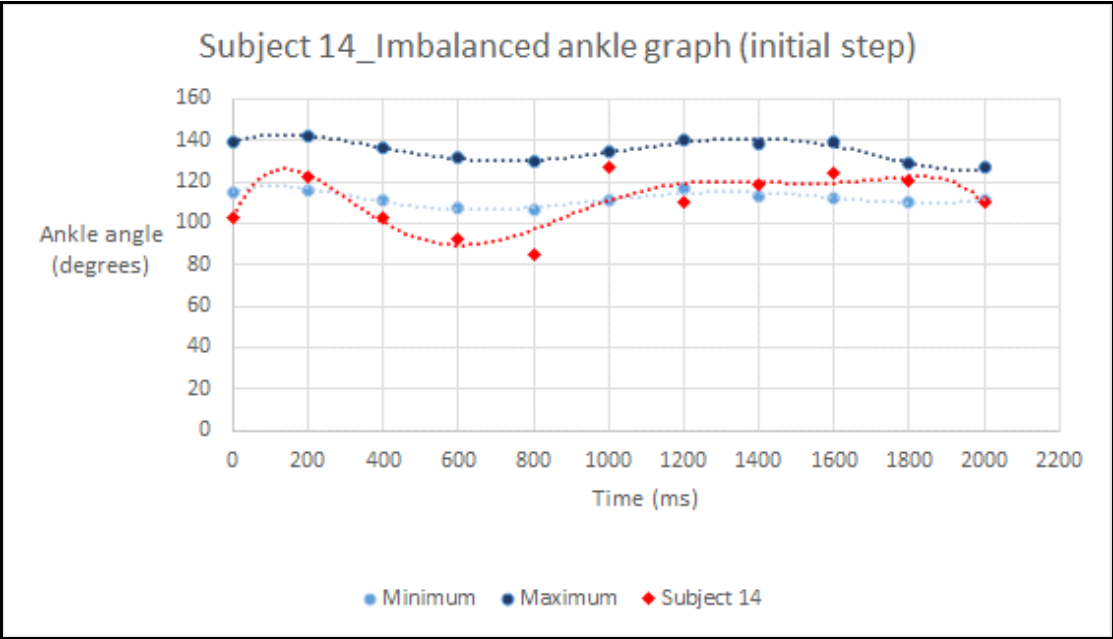


Figure 52 - Imbalanced ankle graph of subject 14 (initial step)

Figure 75 shows the imbalanced ankle gait cycle graph of Subject 14 for the initial step side. Subject 14 was considered as ankle imbalanced individual since the subject’s ankle gait cycle graph lies outside the minimum threshold values and the shape of the graph differs from the generic ankle gait cycle graph. The Root Mean Square value of this graph is 33.12737.

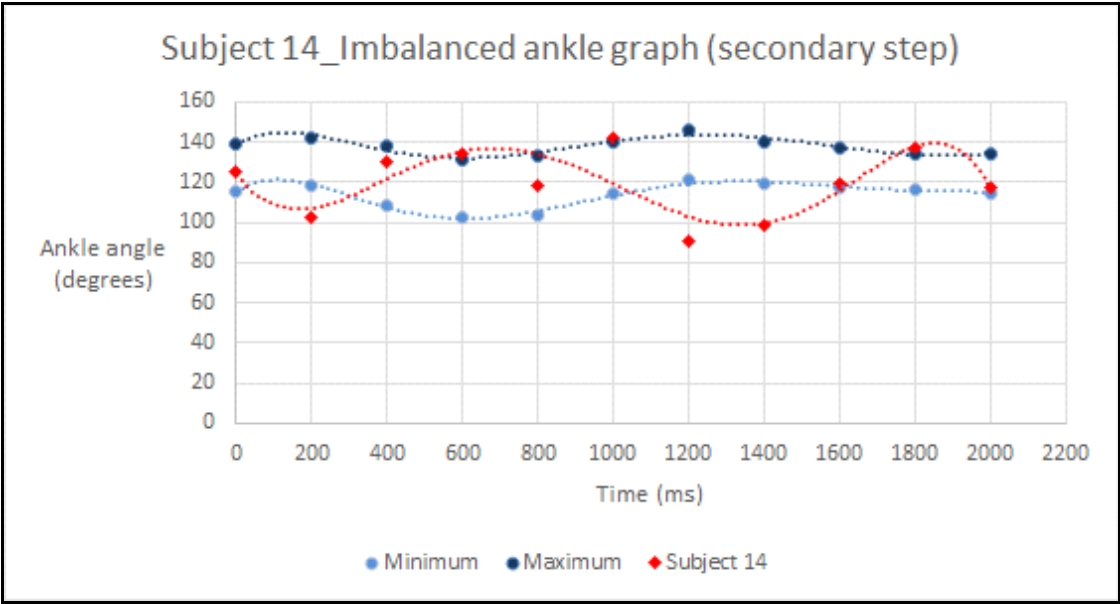


Figure 53 - Imbalanced ankle graph of subject 14 (secondary step)

Figure 76 shows the imbalanced ankle gait cycle graph of Subject 15 for the initial step side. Subject 15 was considered as ankle imbalanced individual since the subject's ankle gait cycle surpasses the maximum threshold values and the shape of the graph differs from the generic ankle gait cycle graph. The Root Mean Square value of this graph is 19.8541.

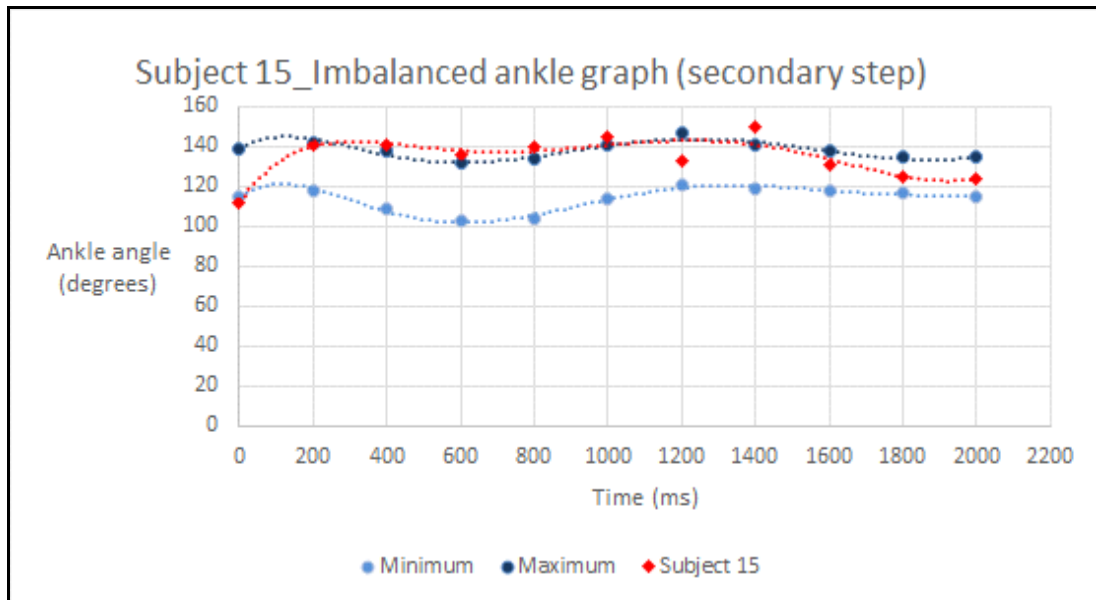


Figure 54 - Imbalanced ankle graph of subject 15 (secondary step)

Following Table 5 includes a brief of the results of the quantitative evaluation carried out. The test sample was consisted of five healthy female subjects, five healthy male subjects and eight imbalanced male subjects and the quantitative results obtained can be stated as follows.

Table 5 - Quantitative evaluation results

Subject identifier	Gender	Quantitative evaluation result
Subject 1	Female	Balanced
Subject 2	Female	Balanced
Subject 3	Female	Balanced
Subject 4	Female	Balanced
Subject 5	Female	Balanced
Subject 6	Male	Balanced
Subject 7	Male	Balanced
Subject 8	Male	Balanced
Subject 9	Male	Balanced
Subject 10	Male	Imbalance in hip and ankle
Subject 11	Male	Imbalance in ankle
Subject 12	Male	Imbalance in ankle
Subject 13	Male	Balanced
Subject 14	Male	Imbalance in hip, knee and ankle
Subject 15	Male	Imbalance in hip and ankle
Subject 16	Male	Balanced
Subject 17	Male	Imbalance in knee
Subject 18	Male	Imbalance in hip and knee

5.3. Qualitative evaluation

In order to increase the accuracy of the proposed mechanism, a qualitative analysis for the same sample was performed by conducting clinical analysis for the test sample with the aid of a domain specialist. In order to perform the qualitative evaluation, a gait cycle analysis was conducted for the same test sample and obtained the results. The qualitative evaluation process also conducted using the same imbalance analysis mechanism; gait analysis. While the subject was walking along the defined straight line, the gait cycle of the individual was visually observed and analyzed by the domain expert and a conclusion was given regarding the individual's status of the lower limb musculoskeletal system. This evaluation is highly dependent on the experience and the knowledge hold by the domain expert. Validity, reliability and accuracy of the research procedure followed can be also evaluated by the obtained outcomes. The qualitative evaluation was carried out by performing the steps mentioned in Figure 77.

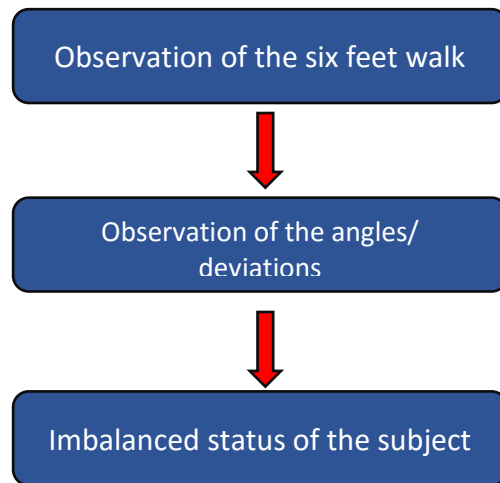


Figure 55 - Qualitative Evaluation Process

Following Table 6 includes a brief of the results of the qualitative evaluation carried out. The test sample was consisted of five healthy female subjects, five healthy male subjects and eight imbalanced male subjects and the results obtained by the qualitative analysis is as follows.

Table 6 - Qualitative evaluation results

Subject identifier	Gender	Qualitative evaluation result
Subject 1	Female	Balanced
Subject 2	Female	Balanced
Subject 3	Female	Balanced
Subject 4	Female	Balanced
Subject 5	Female	Balanced
Subject 6	Male	Balanced
Subject 7	Male	Balanced
Subject 8	Male	Balanced
Subject 9	Male	Balanced
Subject 10	Male	Imbalance in hip and knee
Subject 11	Male	Imbalance in ankle
Subject 12	Male	Imbalance in ankle
Subject 13	Male	Imbalance in knee
Subject 14	Male	Imbalance in hip, knee and ankle
Subject 15	Male	Imbalance in hip and ankle
Subject 16	Male	Balanced
Subject 17	Male	Imbalance in knee
Subject 18	Male	Imbalance in hip and knee

5.4. Comparison of evaluation methods

A final comparison between quantitative and qualitative methods was conducted to differentiate between the two techniques. Following Table 7 describes in brief the final comparison carried out for the quantitative method against the qualitative method (domain expert's conclusion). The results include the analysis of five healthy female subject, five healthy male subjects and eight imbalanced male subjects. Among this test sample, 10 healthy individuals were correctly identified as healthy. Among the imbalanced eight subjects, only seven subjects were identified as healthy. One imbalanced subject was identified as healthy by the quantitative method. The quantified value for the imbalanced joint and the imbalanced joint position is mentioned in the table. The methodology of deriving the quantified value in the following Table 7 is mentioned in the Evaluation and results chapter.

Table 7 - Qualitative and quantitative result comparison

Subject Identifier	Quantitative evaluation						Qualitative evaluation
	Hip evaluation		Knee evaluation		Ankle evaluation		
	Initial hip	Secondary hip	Initial knee	Secondary knee	Initial ankle	Secondary ankle	
Subject 1	Balanced	Balanced	Balanced	Balanced	Balanced	Balanced	Balanced
Subject 2	Balanced	Balanced	Balanced	Balanced	Balanced	Balanced	Balanced
Subject 3	Balanced	Balanced	Balanced	Balanced	Balanced	Balanced	Balanced
Subject 4	Balanced	Balanced	Balanced	Balanced	Balanced	Balanced	Balanced
Subject 5	Balanced	Balanced	Balanced	Balanced	Balanced	Balanced	Balanced
Subject 6	Balanced	Balanced	Balanced	Balanced	Balanced	Balanced	Balanced
Subject 7	Balanced	Balanced	Balanced	Balanced	Balanced	Balanced	Balanced
Subject 8	Balanced	Balanced	Balanced	Balanced	Balanced	Balanced	Balanced
Subject 9	Balanced	Balanced	Balanced	Balanced	Balanced	Balanced	Balanced
Subject 10	Balanced	Imbalanced RMS - 24.090395	Balanced	Balanced	Imbalanced RMS - 21.6469	Balanced	Secondary Hip and initial ankle Imbalance
Subject 11	Balanced	Balanced	Balanced	Balanced	Imbalanced RMS - 14.3059	Imbalanced RMS - 19.2894	Initial Ankle Imbalance
Subject 12	Balanced	Balanced	Balanced	Balanced	Imbalanced RMS - 47.69296	Imbalanced RMS - 19.627	Both Ankle Imbalance
Subject 13	Balanced	Balanced	Balanced	Balanced	Balanced	Balanced	Initial Knee Imbalance
Subject 14	Imbalanced RMS - 15.536 154	Imbalanced RMS - 25.42246	Balanced	Imbalanced RMS - 19.36628 2	Imbalanced RMS - 16.8527	Imbalanced RMS - 33.12737	Imbalance in all six joints

Subject 15	Balanced	Imbalanced RMS - 28.3384	Balanced	Balanced	Balanced	Imbalanced RMS - 19.8541	Secondary Hip and secondary ankle Imbalance
Subject 16	Balanced	Balanced	Balanced	Balanced	Balanced	Balanced	Balanced
Subject 17	Balanced	Balanced	Balanced	Imbalanced RMS - 17.601273	Balanced	Balanced	Secondary Knee Imbalance
Subject 18	Imbalanced RMS - 24.09039	Balanced	Imbalanced RMS - 21.64694	Balanced	Balanced	Balanced	Initial Hip and initial knee Imbalance

5.5. Confusion matrix

A confusion matrix was derived considering the results of the study. Both quantitative and qualitative evaluations are considered in deriving the matrix and the outcome is given in percentages. The confusion matrix of the study carried out is as follows.

Table 8 - Confusion matrix for the results obtained

		Prediction (System)	
		Positive (Imbalanced)	Negative (Healthy)
Actual (Domain Expert)	Positive (Imbalanced)	TP = 7	FN = 2
	Negative (Healthy)	FP = 0	TN = 10

True positives (TP) – The cases in which the system predicted that the subjects have an imbalance and the domain expert confirm that they actually have an imbalance.

True negatives (TN) – The cases in which the system predicted that the subjects do not have an imbalance and the domain expert confirm that they are healthy.

False positives (FP) – The cases in which the system predicted that the subjects have an imbalance and the domain expert confirm that they actually do not hold any imbalances.

False negatives (FN) – The cases in which the system predicted that the subjects do not have an imbalance and the domain expert confirm that they actually do not an imbalance.

$$\begin{aligned}\text{Accuracy (The correctness of the classifier)} &= (\text{TP}+\text{TN}) / \text{Total} \\ &= (7+10) / 18 \\ &= 94.4\%\end{aligned}$$

$$\begin{aligned}\text{Misclassification rate} &= (\text{FP}+\text{FN}) / \text{Total} \\ &= (0+2) / 18 \\ &= 11.11\%\end{aligned}$$

$$\begin{aligned}\text{True positive rate} &= \text{TP} / (\text{FN} + \text{TP}) \\ &= 7 / (2+7) \\ &= 77.77\%\end{aligned}$$

$$\begin{aligned}\text{False positive rate} &= \text{FP} / (\text{TN}+\text{FP}) \\ &= 0/ (10+0) \\ &= 0\%\end{aligned}$$

According to the results of quantitative and qualitative analysis, the accuracy of the proposed system is 94.4% which is a higher accuracy rate. Hence we can prove that this mechanism is a better solution to identify musculoskeletal imbalances in the lower body. Also the sensitivity and the specificity of the methodology denoted higher value depicting that this system is capable of predicting imbalances accurately.

Chapter 6

6. Discussion and conclusion

The intention of this chapter is to present the reader with our elucidations and opinions on the achieved results throughout the different phases of the research. This section includes a critical discussion of the method carried out, its limitations and accuracy aspects of the concept behind the proposed method.

Cost of diagnose, severity of the imbalance and time constraints were identified as the issues in the current mechanisms as mentioned in section 1. The research was conducted to find a solution for these issues in the medical muscle imbalance identification mechanisms. Taking these into consideration the fact that a novel approach should be implemented in the field of physiotherapy to track the behavior of musculoskeletal system and musculoskeletal imbalances was identified. We came up with an ICT based solution for imbalance identification. Main hypothesis of the research was derived as,

Musculoskeletal imbalances of the human body can be identified by joint angle values captured by Kinect.

In order to address this hypothesis, we followed a systematic approach. The research approach included the following steps stated in Figure 78.

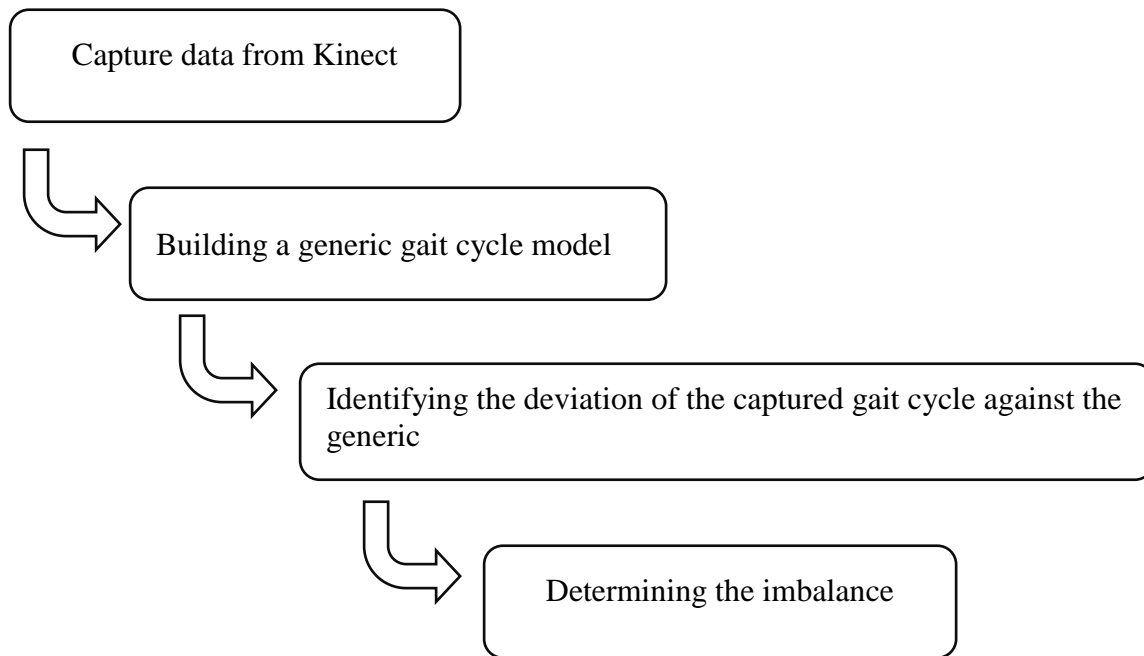


Figure 78- Systematic approach followed in the research

The main two research problems were identification of gait cycle pattern of average healthy person and identification of the deviation of the gait cycle pattern of an imbalanced person from gait cycle pattern of a healthy person. These research questions were addressed in this research project under following limitations and constraints.

The generic healthy gait cycle graphs for left and right hip, left and right knee and left and right ankle were defined for a limited age range. Individuals from the male gender fall between the age range of 25-45 can use the proposed mechanism to identify musculoskeletal imbalances in the lower body. Individuals from the female gender fall between the age range of 30-50 also can use the proposed mechanism to identify musculoskeletal imbalances in the lower body. Other individuals whose age ranges surpass and fall under the defined limits are unable to understand their musculoskeletal imbalances using the proposed method.

The method suggested by this research study can only be applied to the identification of lower body muscle imbalances taking hip, knee and ankle imbalances as the consideration. Upper body muscle imbalances are unable to identify by following this methodology. Since gait cycle was the examination technique, any other subject movement techniques will not be able to use to derive conclusions with regard to the status of the muscle imbalance of a subject.

Under the mentioned constraints, joint angle values were captured from a healthy sample by the Kinect in order to build the generic healthy gait cycle graphs for hip, knee and ankle joints. An application was developed for this purpose and left and right hip position values, left and right knee position values and left and right ankle position values were captured and stored via this application. A mathematical operation was applied to calculate the joint angle by using the position values captured by Kinect. Followed by data capturing, the generic healthy gait cycles for hip, knee and ankle joint variations were be modelled. By modelling the generic healthy gait cycle graphs, minimum and maximum threshold values were derived as limitations. Then the application developed was used along with the generic healthy gait cycles defined to capture and analyze the gait cycles of the imbalanced sample. To analyze data and calculate the deviation between the generic healthy and patient's gait cycles, Root Mean Square method was used. From the quantified value obtained, we came to a conclusion whether a subject is imbalanced or healthy according to the method followed.

Two evaluation mechanisms were used to evaluate the results of the study. A quantitative evaluation was carried out by the data obtained via Kinect. A qualitative evaluation was carried out using the knowledge of domain experts. The procedure of carrying out the two evaluation mechanisms is as mentioned in sections 5.2 and 5.3. As per both quantitative and qualitative analysis, a conclusion was derived with regard to the sample obtained. The sample of this research contained 18 male and female subjects. In the qualitative analysis, the imbalanced and healthy male sample and healthy female sample were correctly defined with and under the supervision of domain specialists. The male sample was consisted with 13 male subjects. The 13 male subjects included eight imbalanced subjects and five healthy subjects. For the evaluation carried out, the accuracy of the proposed operating method was 94.4%. The misclassification rate of the proposed mechanism according to the test sample results was 11.11%. The method of calculating the accuracy and misclassification is mentioned in section 5.5.

In the qualitative evaluation, it was stated that eight subjects were imbalanced with the position of the imbalance. The five male and female subjects used were stated as healthy in the qualitative evaluation. Eight imbalanced subjects were stated as imbalanced with the correct imbalanced joint.

In the quantitative evaluation, the results slightly differed from the domain experts' opinions. The five healthy female subjects were identified from the quantitative evaluation method correctly as healthy and the five healthy male subjects were also identified by the quantitative method as healthy. One imbalanced subject was identified by the quantitative method as balanced. In the qualitative method the subject's knee was identified as the imbalanced position. The reason for this misidentification can be explained as the less number of gait cycles obtained and analysed from the subject. By performing thorough testing using a larger data sample of the subject, this error rate can be decreased to lower value. Figure 79 contains the knee gait cycle graph of the subject.

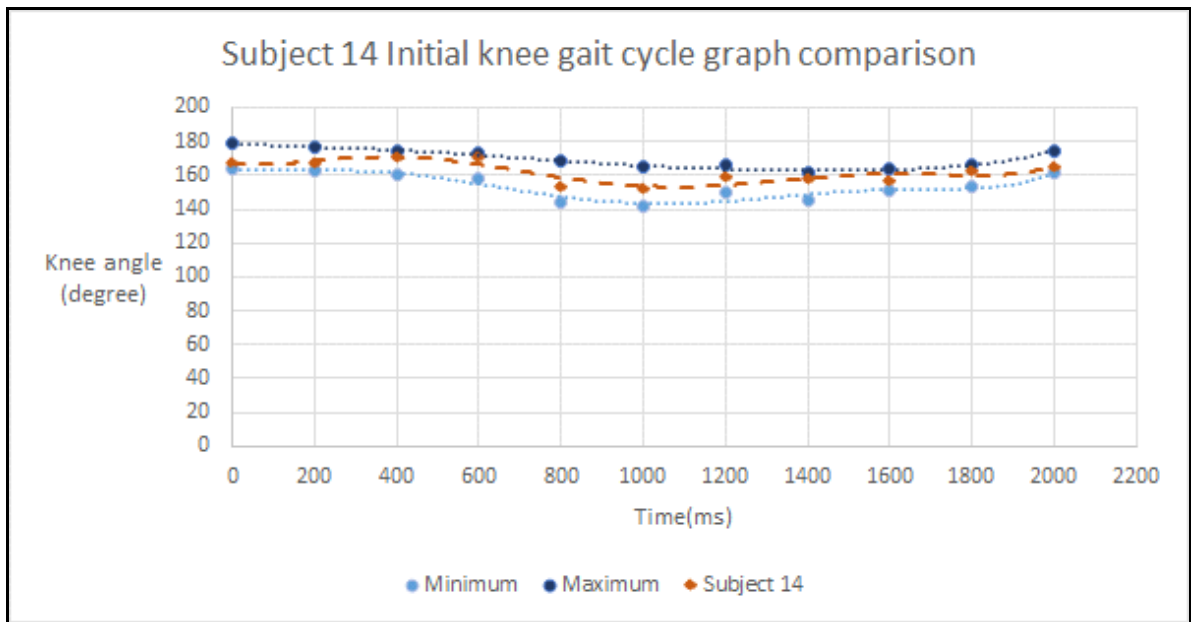


Figure 56 - Knee gait cycle graph of subject 14 (initial step)

Another subject who was identified as having imbalances in all the six joints was identified by the quantitative method as a subject having imbalances in five joints. By performing thorough evaluation of the data of the subject, this error rate can be decreased to lower value. The initial knee joint imbalance was not identified by the quantitative evaluation method. Reason for this classification can be stated as the pathology of the knee imbalance of the subject. Figure 80 contains the initial knee gait cycle graph of that subject.

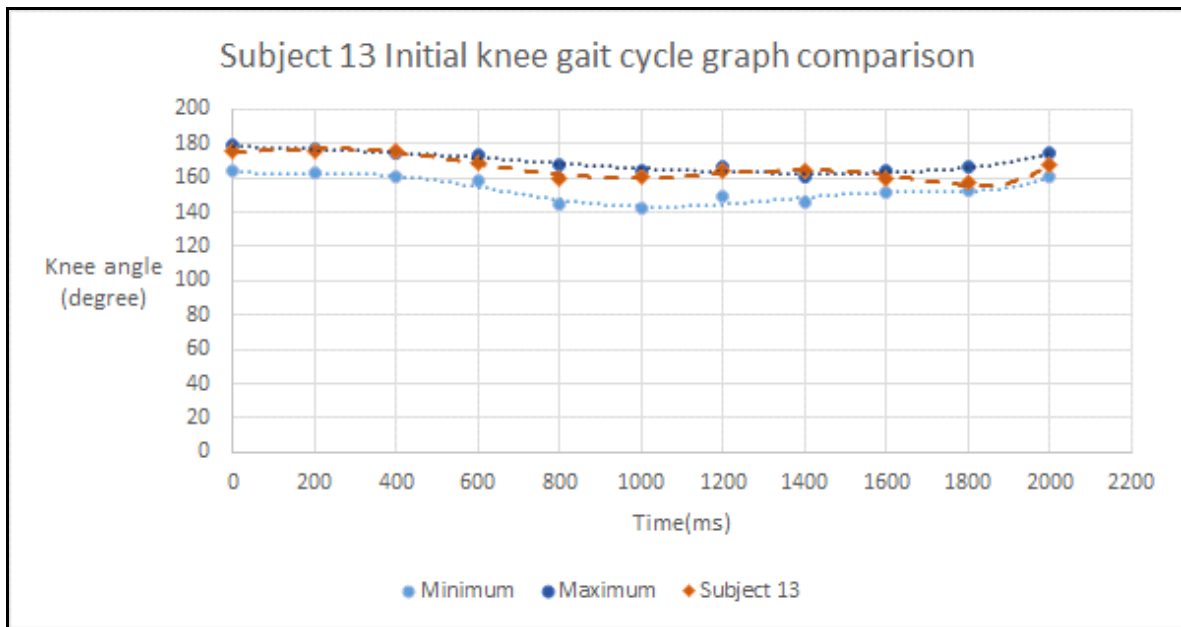


Figure 80 - Knee gait cycle graph of subject 13 (initial step)

By considering the above errors of the proposed technique, misclassification rate of the study was calculated as 11.11%, True Positive rate of the study was calculated as 77.77% and False Positive rate of the proposed study was calculated as 0%. With the aid of the confusion matrix, specificity, sensitivity and accuracy of the proposed methodology was defined as in section 5.5. The numerical results of the quantitative method denoted an accuracy level of 94.4%. We can come to a conclusion from observing the specificity, sensitivity and accuracy parameters that the proposed methodology has produced a satisfactory and a reliable output related to the imbalance status of an individual.

6.1. Contribution

The problem mentioned in earlier stages was adequately addressed and throughout the process, following research contributions were successfully brought about.

- By the time of the current study, gait cycle is used in the global context for human fall detection and human identification applications as mentioned in section 2.5. A similar musculoskeletal imbalance identification mechanism has not been introduced in the local and global contexts using the gait cycle analysis prior to the proposed method. Therefore the current study has initiated a novel approach to address the problems mentioned in section 1.

- Minimum and maximum joint angle values of a healthy individual are mathematically defined by the current study. The mathematical procedure followed to obtain the minimum and maximum values is stated in section 3.1.7.
- In the clinical domain, musculoskeletal system imbalances are not quantified. The proposed research includes a technique to quantify the imbalance of an individual by using the using Root Mean Square value. The derivation of the quantified value is mentioned in section 5.2.
- One research paper was published by the European Centre for Research Training and Development UK in the European Journal of Computer Science and Information Technology - Vol.5, No.6, pp.1-10, December 2017.
- One research paper was accepted by the International Journal of Information and Computation Technology and is processed to be published.

Chapter 7

7. Future directions

The main aim of this research project was to measure the ability of joint position values captured via Kinect sensor by analysing human gait cycle in predicting musculoskeletal imbalances. The only consideration was male gender but the generic gait cycle values for the female hip, knee and ankle were also defined.

The human lower body was the considered area for identifying musculoskeletal imbalances by analysing gait cycle graphs in this research. This was due to the medical fact that the relationship between human lower body joints are higher than the relationship between human upper body joints hence if this methodology cannot be applied for the lower body, it cannot be applied to the upper body as well. With this research study, we have proven that the proposed methodology can be used for lower body muscle imbalance identification. Extending the analysis for human upper body by analysing the upper body joints namely spine, shoulders, elbow and wrists will be another future direction of this study. A methodology to analyse the upper body muscle imbalances can be performed in future research studies since the gait cycle analysis technique used in this study can only be applied to the lower limb joints.

There are many newer technological devices and sensors which are also accurate than Kinect in the current market. By using other sensors as in MYO armband and inertial sensors, one can redo this research project to maximize the accuracy level and minimize the error rate identified and evaluate the usage of the sensor and the validity of captured data in the proposed method.

Other than gait analysis there exist many other muscle imbalance identification methods in the clinical domain as mentioned in the Background chapter. Application of Information Technology to posture analysis, movement analysis, joint range of motion analysis and muscle length analysis can be defined as another branch identified in extending this type of research projects. Imbalance identification mechanism can be developed using any of these methods and compare the accuracy with the proposed mechanism.

Another future direction we identified was developing a mobile application or a web based application for the proposed mechanism. The definition of ‘self-identification’ of muscle imbalances mentioned in this research can be highly reached by such approaches and will be able to cater the needs of clinical and physical fitness domains as a supporting device.

In this study we have considered the Root Mean Square (RMS) method to obtain the error value for each imbalanced gait cycle of an individual. Other error calculation mechanism can be used to level up or down the accuracy of the suggested procedure. The RMS value can be further analysed to define the severity of the pathology of the imbalance by carrying out a separate research.

Bibliography

- [1] J. Perry, S. K. and J. Davids, "Gait Analysis: Normal and Pathological Function", 2017.
- [2] P. Page, C. Frank and R. Lardner, *Assessment and treatment of muscle imbalance. Champaign [etc.]: Human kinetics, 2010.*
- [3] T. Grace, E. Sweetser, M. Nelson, L. Ydens and B. Skipper, "Isokinetic muscle imbalance and knee-joint injuries. A prospective blind study.", *The Journal of Bone & Joint Surgery*, vol. 66, no. 5, pp. 734-740.
- [4] S. NADLER, G. MALANGA, L. BARTOLI, J. FEINBERG, M. PRYBICIEN and M. DEPRINCE, "Hip muscle imbalance and low back pain in athletes: influence of core strengthening", *Medicine & Science in Sports & Exercise*, vol. 34, no. 1, pp. 9-16, 2002.
- [5] Frank, Lardner and Page, "The assessment and treatment of muscular imbalance," *The Janda Approach Hardback, Human Kinetics, Champlain, IL USA*
- [6] S. Nadler, G. Malanga, J. Feinberg, M. Prybicien, T. Stitik and M. DePrince, "Relationship Between Hip Muscle Imbalance and Occurrence of Low Back Pain in Collegiate Athletes", *American Journal of Physical Medicine & Rehabilitation*, vol. 80, no. 8, pp. 572-577, 2001.
- [7] Kenyon, Karen, Kenyon and Jonathan. *The Physiotherapist's Pocket Book - Essential Facts At Your Fingertips. 2nd ed. Kundli (Haryana): Rajkamal Electric Press, 2017. Print.*
- [8] A. Fernandez, A. Susin and X. Lligadas, *Biomechanical Validation of Upper-body and Lower-body Joint Movements of Kinect Motion Capture Data for Rehabilitation Treatments, 2012.*
- [9] KNAPIK, JOSEPH J. et al. *Preseason strength and flexibility imbalances associated with athletic injuries in female collegiate athletes (1991): n. pag. Print.*
- [10] *Muscle Imbalance, Part 1: A Common, Often Undetected Cause Of Aches, Pains And Disability. - Dr. Phil Maffetone". Dr. Phil Maffetone. N.p., 2017.*
- [11] Wan, Bingjun and Gongbing Shan. "Biomechanical Modeling As A Practical Tool For Predicting Injury Risk Related To Repetitive Muscle Lengthening During Learning And Training Of Human Complex Motor Skills". (2016): n. pag. Print
- [12] M. Weerasinghe, "Computer Aid Assessment of Muscular Imbalance for Preventing Overuse Injuries in Athletes", 2016.
- [13] K. Sweeting, *Gait and Posture Assessment in General Public, 1st ed. 2007, pp. 398-405.*
- [14] K. Kirtley, *Clinical Gait Analysis: Theory and Practice. ELSEVIER, 2006.*
- [15] Muro-de-la-Herran, Alvaro and Begonya Garcia-Zapirain. *Gait Analysis Methods: An Overview of Wearable and Non-Wearable Systems, Highlighting Clinical Applications (2014): n. pag. Print.*

- [16]B. Jiang, F. Zhao and X. Liu, "Observation-oriented silhouette-aware fast full body tracking with Kinect", *Journal of Manufacturing Systems*, vol. 33, no. 1, pp. 209-217, 2014.
- [17]J. Loudon, S. Bell and J. Johnston, *The clinical orthopedic assessment guide*. Champaign, Ill.: Human Kinetics, 2008.
- [18]L. QUESADA and A. LEÓN, "UNSUPERVISED MARKERLESS 3-DOF MOTION TRACKING IN REAL TIME USING A SINGLE LOW-BUDGET CAMERA", *International Journal of Neural Systems*, vol. 22, no. 05, p. 1250019, 2012.
- [19]Mahindaratne, Kalpani. *Clinical Method Of Identify Human Body Imbalance*. 2017. in person.
- [20]S. K. and M. M., *Gait and posture - assessment in general practice*. 2017.
- [21]C. Groner, "Diabetes and altered gait: The role of neuropathy | Lower Extremity Review Magazine", *Lermagazine.com*, 2017.
- [22]A. Fasano and B. Bloem, "Gait Disorders", *CONTINUUM: Lifelong Learning in Neurology*, vol. 19, pp. 1344-1382, 2013.
- [23]D. Roetenberg, H. Luinge and P. Slycke, "Xsens MVN: Full 6DOF Human Motion Tracking Using Miniature Inertial Sensors", *XSENS TECHNOLOGIES*, 2003
- [24]M. Hägglund, M. Waldén and J. Ekstrand, "Risk factors for lower extremity muscle injury in professional soccer: the UEFA Injury Study.", 2012.
- [25]A. Bo, M. Hayashibe and P. Poignet, "Joint angle estimation in rehabilitation with inertial sensors and its integration with Kinect", *2011 Annual International Conference of the IEEE Engineering in Medicine and Biology Society*, 2011.
- [26]N. MILLER, O. JENKINS and M. KALLMANN, "MOTION CAPTURE FROM INERTIAL SENSING FOR UNTETHERED HUMANOID TELEOPERATION", 2004.
- [27]I. Oikonomidis and N. Kyriazis, "Efficient Model-based 3D Tracking of Hand Articulations using Kinect", 2017.
- [28]Springer, Shmuel, and Galit Yogev Seligmann. "Validity Of The Kinect For Gait Assessment: A Focused Review." *semanticscholar* (2016): n. pag. Web. 18 July 2017
- [29]A. Atrsaei, H. Salarieh and A. Alasty, "Human Arm Motion Tracking by Orientation-Based Fusion of Inertial Sensors and Kinect Using Unscented Kalman Filter", 2017
- [30]A. Bo, M. Hayashibe and P. Poignet, "Joint angle estimation in rehabilitation with inertial sensors and its integration with Kinect", *2011 Annual International Conference of the IEEE Engineering in Medicine and Biology Society*, 2011.

- [31] Han, J. and Bhanu, B. (2006). *Individual Recognition Using Gait Energy Image*. *IEEE*, 28(2)
- [32] "Gait Analysis in Neurological Disease", *Smart patients*, 2016 33 Stone, E. and Skubic, M. (2013). *Unobtrusive, Continuous, In-Home Gait Measurement Using the Microsoft Kinect*. *IEEE*, 60(10)
- [33] K. Culhane, "Accelerometers in rehabilitation medicine for older adults", *Age and Ageing*, vol. 34, no. 6, pp. 556-560, 2005. 36C.
- [34] E. Rodriguez, P. Chagas, P. Silva, R. Kirkwood and M. Mancini, "Impact of leg length and body mass on the stride length and gait speed of infants with normal motor development: A longitudinal study", *Brazilian Journal of Physical Therapy*, vol. 17, no. 2, pp. 163-169, 2013.
- [35] C. Lin, H. Hsu, Y. Lay, C. Chiu and C. Chao, "Wearable device for real-time monitoring of human falls", *Measurement*, vol. 40, no. 9-10, pp. 831-840, 2007.
- [36] Stone, E. and Skubic, M. (2013). *Unobtrusive, Continuous, In-Home Gait Measurement Using the Microsoft Kinect*. *IEEE*, 60(10)
- [37] M. Daher, A. Diab and M. Mohamad Ali Khalil, "Elder Tracking and Fall Detection System Using Smart Tiles", *IEEE*, vol. 17, no. 2, 2016.
- [38] Clark, R.A.; Bower, K.J.; Mentiplay, B.F.; Paterson, K.; Pua, Y.-H. "Concurrent validity of the Microsoft Kinect for assessment of spatiotemporal gait variables " vol 46, pp. 2722–2725 2013
- [39] Richards, A. Chohan and R. Erande, *Tidy's physiotherapy*.
- [40] J. Loudon, S. Bell and J. Johnston, *The clinical orthopedic assessment guide*. Champaign, Ill.: Human Kinetics, 2008.
- [41] Mostakhdemin, M., Sadegh, I. and Syahrom, A. (2015). *Multi-axial Fatigue of Trabecular Bone with Respect to Normal Walking*. Springer.
- [42] J. Røislien, Ø. Skare, M. Gustavsen, N. Broch, L. Rennie and A. Opheim, "Simultaneous estimation of effects of gender, age and walking speed on kinematic gait data", *Gait & Posture*, vol. 30, no. 4, pp. 441-445, 2009
- [43] Mostakhdemin, M., Sadegh, I. and Syahrom, A. (2015). *Multi-axial Fatigue of Trabecular Bone with Respect to Normal Walking*. Springer.
- [44] R. Olshen, E. Biden, M. Wyatt and D. Sutherland, "Gait Analysis and the Bootstrap", *The Annals of Statistics*, vol. 17, no. 4, pp. 1419-1440, 1989.
- [45] Preis, J., Kessel, M., Werner, M. and Linnhoff-Popien, C. (2012). *Gait recognition with Kinect*. ResearchGate
- [46] M. Y, S. J, A. R, H. ME and S. JJI, "Gait variability in people with neurological disorders: A systematic review and meta-analysis", 2016.

[47]Kumar, P. and Clark, M. (n.d.). *Kumar and Clark's Clinical Medicine. 1st ed.*

[48]S. Brozman and R. Manske, *Clinical Orthopaedic Rehabilitation, 3rd ed. 2011.*

[49]D. Magee, *Orthopedic Physical Assessment, 5th ed. 2006.*

[50]M. Benocci, L. Rocchi and E. Farella, "A wireless system for gait and posture analysis based on pressure insoles and Inertial Measurement Units", 2009. Web. 23 Mar. 2017

Appendices

Appendix 01 - Consent form for the research sample

CONSENT FORM

Title of Research Project: A Novel Approach to Identify Imbalances of the Lower Limb Musculoskeletal System via Gait analysis using Kinect

Requirements: Patient's angular movements, medical records and private information will be gathered in fulfilling the research requirements.

Name of the Researchers:

C. Paranamana | Undergraduate, University of Colombo School of Computing (Registration No: 2013/IS/034)

T. R. K. Hiranthi | Undergraduate, University of Colombo School of Computing (Registration No: 2013/IS/021)

Patient Identification Number for this trial:

Please tick the boxes appropriately

1. I confirm that I have read and understand the study information given in the consent form for the above study. I have had the opportunity to consider the information, ask questions and have had these answered satisfactorily.
2. I understand that my participation is voluntary and that I am free to withdraw at any time without giving any reason, without my medical care or legal rights being affected.
3. I understand that relevant sections of my medical notes and data collected during the study, may be looked at by individuals from UCSC and from regulatory authorities when it is relevant to my taking part in this research. I give permission for these individuals to have access to my records.



4. I agree to take part in the above study.

Name of the participant

Date

Signature

Appendix 02 - Generic ankle gait cycle graph (2nd order)

R^2 for minimum = 0.1733

R^2 for maximum = 0.0612

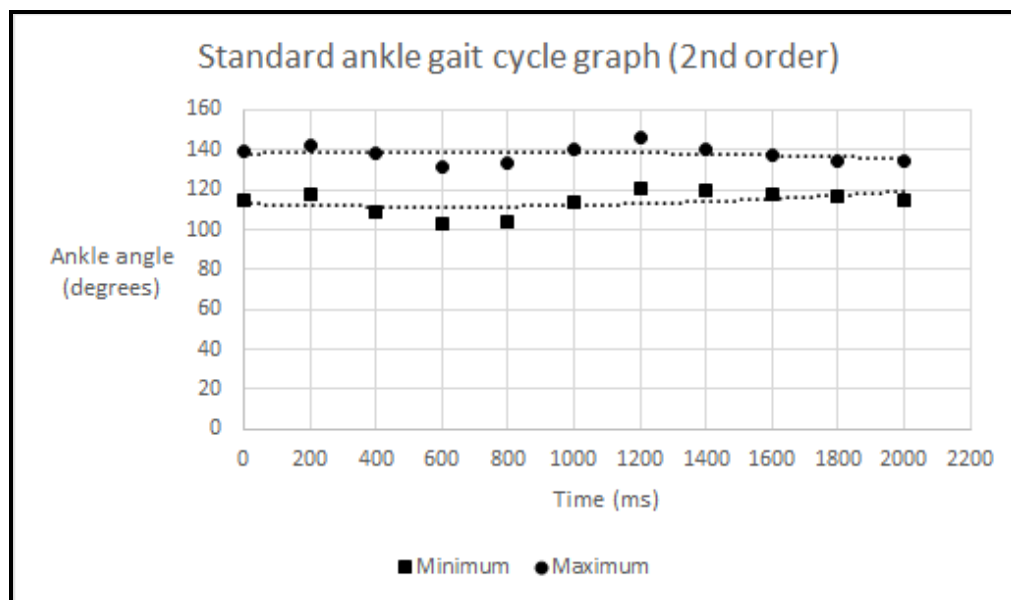


Figure 57 - Generic ankle gait cycle graph (2nd order)

Appendix 03 - Generic ankle gait cycle graph (3rd order)

R^2 for minimum = 0.5889

R^2 for maximum = 0.329

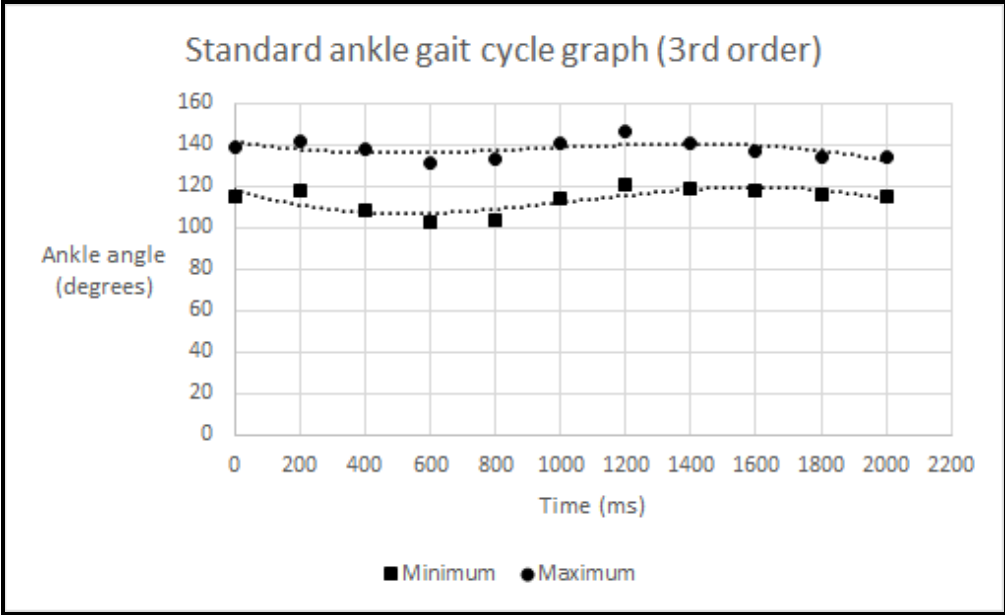


Figure 82- Generic ankle gait cycle graph (3rd order)

Appendix 04 - Generic ankle gait cycle graph (4th order)

R^2 for minimum = 0.5947

R^2 for maximum = 0.3354

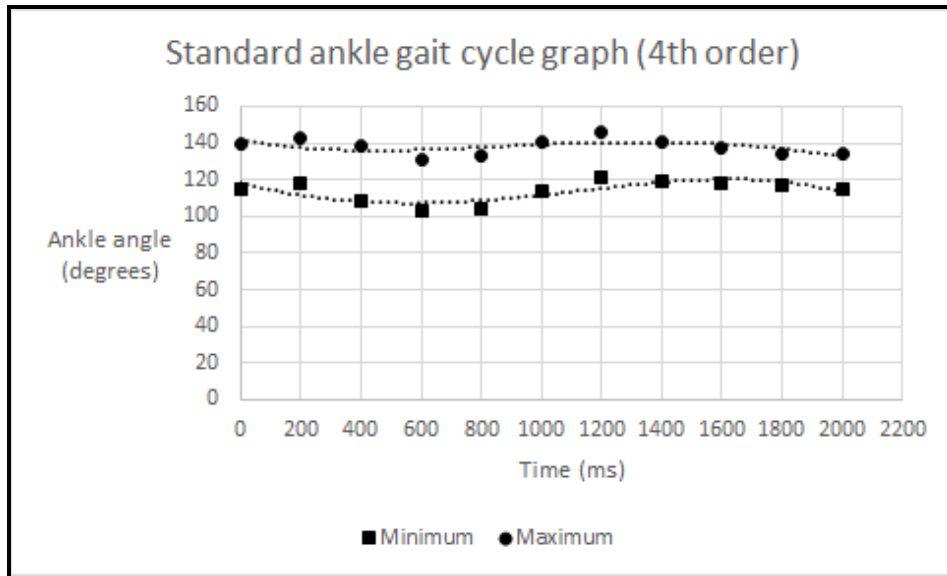


Figure 58 - Generic ankle gait cycle graph (4th order)

Appendix 05 - Generic ankle gait cycle graph (5th order)

R^2 for minimum = 0.8198

R^2 for maximum = 0.9052

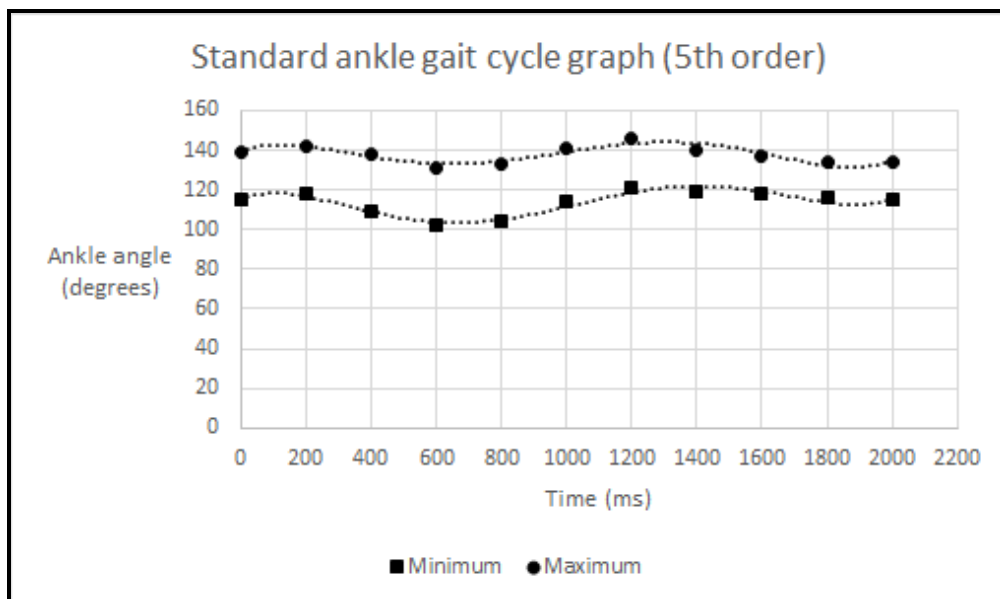


Figure 84 - Generic ankle gait cycle graph (5th order)

Appendix 06 - Imbalanced sample subject



Figure 59 - Imbalanced sample subject a

Appendix 07 - Imbalanced sample subject



Figure 60 - Imbalanced sample subject b

Appendix 08 - Imbalanced sample subject



Figure 61 - Imbalanced sample subject c